DISS. ETH NO. 30150

Resilience Analysis of Interdependent Critical Infrastructure Systems Using an Iterative Optimization-based Simulation Framework

A thesis submitted to attain the degree of

DOCTOR OF SCIENCES
(Dr. sc. ETH Zurich)

presented by

HAMED HAFEZNIA

MSc in Energy Systems Engineering, University of Tehran &
MSc in Civil Engineering, The Johns Hopkins University – Baltimore, MD

born on 10.08.1990

accepted on the recommendation of

Prof. Dr. Bozidar Stojadinovic	examiner
Prof. Dr. Bryan T. Adey	co-examiner
Prof. Dr. Edmond Lo Yat-Man	co-examiner
Prof. Dr. Srijith Balakrishnan	co-examiner

2024

Abstract

Critical Infrastructure Systems facilitate the functioning of urban communities. A prolonged lack of infrastructure services in an urban community is likely when infrastructure systems are exposed to an extreme event. The reasons for such a post-disaster situation in urban communities are insufficient resilience of individual infrastructure systems and cascading failures resulting from increasing complexity and interdependent relations between critical infrastructure systems. Conducting the resilience analysis of interdependent critical infrastructure systems is to plan and implement practical and cost-efficient solutions to this urban community's challenge.

The purpose of this doctoral dissertation is to develop a framework that can evaluate the resilience of interdependent critical infrastructure systems in the face of potentially disruptive events by tracking post-disaster performance evolution. In addition to quantifying resilience, this framework can enhance the resilience of interdependent critical infrastructure systems by optimizing service distribution within infrastructure networks and resource allocation during the post-disaster recovery process. To this end, this doctoral dissertation includes the development of the ResQ-IOS framework for resilience analysis, its applications for community resilience enhancement, case studies for demonstration, and the ResQ-RDSS framework, a decision support system for implementing Community Resilience Enhancement Strategies (CRESs).

The ResQ-IOS is an Iterative Optimization-based Simulation (IOS) Framework comprising five modules: Risk Assessment, Simulation, Database, Optimization, and Controller. Transferring data and interaction between those five modules enable ResQ-IOS to model, optimize, quantify, and analyze the resilience of interdependent critical infrastructure systems to disruptive events. The capabilities of the ResQ-IOS framework are demonstrated by quantifying the seismic resilience of the case study interdependent critical infrastructure systems individually and jointly to evaluate the earthquake disaster resilience of the urban community in Shelby County (TN), USA.

The stakeholders can utilize the ResQ-IOS framework to plan, simulate, and appraise the impacts of implementing Community Resilience Enhancement Strategies (CRESs) on urban communities. Accordingly, the stakeholders will be able to identify the weak points of the urban community and choose the most effective CRES for improving the community's disaster resilience. The ResQ-IOS framework, with the ability to perform

parametric analysis, enables the stakeholders to explore the parameters influencing the resilience of urban communities. Depending on the task requested from the framework, ResQ-IOS can provide seven optimized quantities, namely, minimum joint accumulated loss of resilience for the urban community (SoCIS-ALR metric), optimal daily dispatching of services within infrastructure networks, optimal recovery strategy with the minimum total recovery cost, optimal portfolio for repair packages, and three optimized quantities related to deploying backup systems (optimal number, location, and schedule). The ResQ-IOS framework, as a robust and versatile computational tool, can be incorporated into urban planning procedures to design resilience-oriented plans for future developments of urban regions.

The ResQ-RDSS, the extension of ResQ-IOS with an application for rural areas, is a Resilience Quantification-based Regional Decision Support System. The objective of developing the ResQ-RDSS framework is to incorporate the resilience concept and resilience enhancement strategies in the long-term planning of rural electrification. The ResQ-RDSS framework consists of four modules: Spatial Techno-Economic Assessment (STEA), Earthquake-induced Risk Assessment (ERA), Flood-induced Risk Assessment (FRA), and Decision Maker (DM). These four modules work together to devise resilient electrification strategies (off-grid or on-grid) to mitigate the lack of electricity access problem globally. In other words, ResQ-RDSS, as a decision support system, helps stakeholders select the best CRES for rural communities. In addition to identifying the resilient electrification strategy for each village in the considered region, the ResQ-RDSS can be applied to rural areas in developed countries to identify more vulnerable rural settlements to diverse natural hazards and to plan various resilience enhancement strategies and implement them in a timely and cost-effective manner.

The ResQ-IOS and ResQ-RDSS frameworks are widely applicable to other case studies worldwide because of their generalized methodologies. However, particular applications require data on local hazard scenarios, exposure (vulnerability) models, and recovery models specific to the community whose resilience is modeled, quantified, and investigated for improvements.

Zusammenfassung

Kritische Infrastruktursysteme spielen eine entscheidende Rolle im reibungslosen Funktionieren städtischer Gemeinschaften. Wenn diese Systeme jedoch extremen Ereignissen ausgesetzt sind, besteht die Gefahr eines längeren Ausfalls von Infrastrukturdiensten in der Stadt. Dies kann auf verschiedene Faktoren zurückzuführen sein, darunter die unzureichende Resilienz einzelner Infrastruktursysteme sowie kaskadenartige Ausfälle, die sich aus der zunehmenden Komplexität und den Abhängigkeiten zwischen kritischen Infrastruktursystemen ergeben. Die Durchführung einer Resilienzanalyse dieser voneinander abhängigen Systeme ermöglicht es, praktische und kosteneffiziente Lösungen für Herausforderung in städtischen Gemeinschaften zu planen und umzusetzen.

Das Hauptziel dieser Dissertation ist es, ein Framework zu entwickeln, das es ermöglicht, die Resilienz voneinander abhängiger kritischer Infrastruktursysteme gegenüber potenziell störenden Ereignissen zu bewerten, indem die Leistungsentwicklung nach einer Katastrophe verfolgt wird. Dieses Framework, genannt ResQ-IOS, zielt darauf ab, nicht nur Resilienz zu quantifizieren, sondern auch durch die Optimierung der Verteilung von Diensten innerhalb der Infrastrukturnetze und der Ressourcenzuweisung während des Wiederherstellungsprozesses nach einer Katastrophe die Resilienz dieser Systeme zu verbessern. Die Dissertation beinhaltet auch die Anwendung des ResQ-IOS-Frameworks zur Verbesserung der Resilienz von Gemeinschaften, Fallstudien zur Demonstration sowie das ResQ-RDSS-Framework, ein Entscheidungshilfesystem für die Umsetzung von Resilienzstrategien für die Gemeinschaft (Community Resilience Enhancement Strategies, CRES).

Der ResQ-IOS ist ein Simulationsframework basierend auf iterativer Optimierung (Iterative Optimization-based Simulation, IOS), das fünf Module umfasst: Risikobewertung, Simulation, Datenbank, Optimierung und Controller. Durch den Austausch von Daten und die Interaktion zwischen diesen Modulen ermöglicht das ResQ-IOS die Modellierung, Optimierung, Quantifizierung und Analyse der Resilienz voneinander abhängiger kritischer Infrastruktursysteme gegenüber Störereignissen. Die Leistungsfähigkeit des ResQ-IOS wird durch die Quantifizierung der seismischen Resilienz einzelner und abhängiger kritischen Infrastruktursysteme in einer Fallstudie

demonstriert, in der die Resilienz der Gemeinschaft im Shelby County (TN), USA, gegenüber Erdbebenkatastrophen zu bewerten.

Die Stakeholder können das ResQ-IOS-Framework nutzen, um die Auswirkungen der Umsetzung von Strategien zur Verbesserung der Resilienz der Gemeinschaft (Community Resilience Enhancement Strategies, CRES) auf städtische Gemeinschaften zu planen, zu simulieren und zu bewerten. Dadurch sind sie in der Lage, Schwachstellen der städtischen Gemeinschaft zu identifizieren und die effektivsten CRES auszuwählen, um die Katastrophenresilienz der Gemeinschaft zu verbessern. Das ResQ-IOS-Framework ermöglicht parametrische Analysen, wodurch die Stakeholder die Parameter untersuchen können, die die Resilienz städtischer Gemeinschaften beeinflussen. Je nach den Anforderungen können im ResQ-IOS sieben optimierte Größen bereitgestellt werden: die minimale kumulierte Verlustgröße für die Resilienz der städtischen Gemeinschaft (SoCIS-ALR-Metrik), die optimale tägliche Verteilung von Diensten innerhalb von Infrastrukturnetzen, die optimale Wiederherstellungsstrategie mit den geringsten Gesamtkosten, das optimale Portfolio für Instandsetzungspakete und drei optimierte Größen im Zusammenhang mit dem Einsatz von Sicherungssystemen (optimale Anzahl, Standort und Zeitplan). Der ResQ-IOS-Rahmen kann als robustes und vielseitiges Berechnungsinstrument in städtische Planungsverfahren integriert werden, um resilienzorientierte Pläne für die zukünftige Entwicklung von Stadtregionen zu entwickeln.

Das ResQ-RDSS, eine Erweiterung des ResQ-IOS mit einer speziellen Anwendung für ländliche Gebiete, ist ein regionales Entscheidungsunterstützungssystem, das auf der Quantifizierung von Resilienz basiert. Ziel der Entwicklung des ResQ-RDSS-Frameworks ist es, das Konzept der Resilienz sowie Strategien zur Verbesserung der Resilienz in die langfristige Planung der ländlichen Elektrifizierung zu integrieren. Das ResQ-RDSS-Framework besteht aus vier Modulen: Räumliche Techno-Ökonomische Bewertung (Spatial Techno-Economic Assessment, STEA), Bewertung von Erdbebenrisiken (Earthquake-induced Risk Assessment, ERA), Bewertung von Hochwasserrisiken (Flood-induced Risk Assessment, FRA) und Entscheidungsträger (Decision Maker, DM). Diese Module arbeiten zusammen, um widerstandsfähige Elektrifizierungsstrategien zu entwickeln, sei es netzunabhängig oder netzgebunden, um das weltweite Problem des fehlenden Stromzugangs zu abzumildern. Mit anderen Worten: Das ResQ-RDSS dient als Entscheidungshilfesystem für Stakeholder, um die

besten CRES für ländliche Gemeinden auszuwählen. Es ermöglicht nicht nur die Bestimmung der geeigneten Elektrifizierungsstrategie für jedes Dorf in der betrachteten Region, sondern kann auch auf ländliche Gebiete in Industrieländern angewendet werden, um die Anfälligkeit ländlicher Gemeinschaften für diverse Naturgefahren zu ermitteln, verschiedene Strategien zur Verbesserung der Resilienz zu planen und sie zeitnah und kostengünstig umzusetzen.

Die Frameworks ResQ-IOS und ResQ-RDSS sind aufgrund ihrer generalisierten Methodik weitgehend für weitere Fallstudien weltweit anwendbar. Allerdings erfordern bestimmte Anwendungen Daten zu lokalen Gefahrenszenarien, Expositions- (Vulnerabilitäts-) und Wiederherstellungsmodellen, die spezifisch für die jeweilige Gemeinschaft sind. Diese Daten werden benötigt, um die Resilienz der Gemeinschaft zu modellieren, zu quantifizieren und Verbesserungen zu untersuchen.

Acknowledgments

I would like to express my sincere gratitude to my doctoral supervisor, Prof. Dr. Božidar Stojadinović, for offering me the opportunity to pursue my doctoral studies at ETH Zurich and allowing me to conduct research in my field of interest. I am deeply grateful for his invaluable mentorship and all the necessary support provided during the journey of this dissertation. I highly appreciate his kindness, unwavering support, and understanding during challenging moments.

I would also like to thank my second advisor, Prof. Dr. Bryan T. Adey, for his insightful feedback, helpful advice, and recommendations that improved this doctoral dissertation. I would like to thank all my doctoral committee members, Prof. Dr. Božidar Stojadinović, Prof. Dr. Bryan T. Adey, Prof. Dr. Edmond Lo Yat-Man, and Prof. Dr. Srijith Balakrishnan, for dedicating their time, energy, and efforts to review my doctoral dissertation and provide constructive feedback.

I would like to express my deepest gratitude to my parents for their endless love, patience, sacrifices, unwavering support, and continuous encouragement throughout my whole life. I am profoundly grateful to my brothers and my family for their love, kindness, understanding, continuous support, and constant encouragement during this demanding journey.

I would like to acknowledge that the present doctoral research was conducted at the Chair of Structural Dynamics and Earthquake Engineering at ETH Zurich and the Future Resilient Systems at the Singapore-ETH Centre. The Singapore-ETH Centre was established collaboratively between ETH Zurich and the National Research Foundation of Singapore. This research was supported by the National Research Foundation of Singapore (NRF) under its Campus for Research Excellence and Technological Enterprise (CREATE) program.

I am thankful to Dr. Jonas Joerin, Ms. Jean Tang at the Singapore-ETH Centre, and Ms. Nicole Benz at ETH Zurich for managing the administrative aspects of my doctoral studies. Lastly, I would like to thank my good friends and colleagues in Zurich and Singapore for their support, particularly Mr. Ting-Hsiang (Lawrence) Tseng, Dr. Nikola Blagojević, Dr. Johanna Woerle, and Dr. Mateusz Iwo Dubaniowski.

This dissertation is dedicated to my beloved parents.

Contents

List of Figures

List of Tables

Nomenclature

Abbreviations	
ResQ-IOS	Resilience Quantification Iterative Optimization-based Simulation Framework
ResQ-RDSS	Resilience Quantification-based Regional Decision Support System
IOS	Iterative Optimization-based Simulation
CISs	Critical Infrastructure Systems
EISs	Energy Infrastructure Systems
OS	Optimization-Simulation
MILP	Mixed-Integer Linear Programming
PGD	Peak Ground Displacement
PGV	Peak Ground Velocity
PGA	Peak Ground Acceleration
LR	Loss of Resilience
ALR	Accumulated Loss of Resilience
SoCIS-ALR	Joint Accumulated Loss of Resilience (for a system of CISs)
R&M	Repair and Maintenance
GTPP	Gas Turbine Power Plant
CCPP	Combined-Cycle Power Plant
PGS	Power Gate Station
LNGT	Liquefied Natural Gas Terminal
NGPP	Natural Gas Processing Plant
NGGS	Natural Gas Gate Station
ESS	Electric Substation
BSU	Building Stock Unit
NGCS	Natural Gas Compressor Station
WSF	Water Supply Facility

WPS	Water Pump Station
WST	Water Storage Tank
CRES	Community Resilience Enhancement Strategy
RRE	Resilient Rural Electrification
RE	Renewable Energy
RESs	Renewable Energy Sources
GHG	Greenhouse Gas
GIS	Geographic Information System
MCDM	Multi-Criteria Decision Making
SE	Solar Energy
MHRA	Multi-Hazard Risk Assessment
STEA	Spatial Techno-Economic Assessment
ERA	Earthquake-induced Risk Assessment
FRA	Flood-induced Risk Assessment
DM	Decision Maker
PV	Photovoltaic
GHI	Global Horizontal Irradiance
HPTN	Hypothetical Power Transmission Network
LHS	Latin Hypercube Sampling
FGO	Fuzzy Gamma Operator
AAT	Average Annual Temperature
SI	Solar Irradiance
ARN	Accessibility to the Road Network
DUA	Distance to Urban Areas
SIS	Slope of Installation Site
PPTL	Proximity to Power Transmission Lines
CFG	Combined Fuzzy Grade

Indices and sets	
i	Index of critical infrastructure systems
CIS	Set of critical infrastructure systems
s	Index of nodes in the critical infrastructure system
SN^i	Set of nodes in the critical infrastructure system i
f	Index of facilities in the critical infrastructure system
SF^i	Set of facilities in the critical infrastructure system i
m	Index of nodes in the power network
n	Index of nodes in the natural gas network
j	Index of nodes in the water network
p	Index of powerlines in the power network
q	Index of pipelines in the natural gas network
l	Index of pipelines in the water network
NE	Set of nodes in the power network
NG	Set of nodes in the natural gas network
NW	Set of nodes in the water network
LE	Set of power lines in the power network
LG	Set of pipelines in the natural gas network
LW	Set of pipelines in the water network
t	Index of time steps
T	Set of total time steps between t_E and t_R
f_e	Index of facilities in the power network
FE	Set of facilities in the power network
f_g	Index of facilities in the natural gas network
FG	Set of facilities in the natural gas network
f_w	Index of facilities in the water network

FW	Set of facilities in the water network
$IGtE$	Set of interdependent nodes coupled between the natural gas and power networks (Gas to Power)
$IWtE$	Set of interdependent nodes coupled between the water and power networks (Water to Power)
$IEtG$	Set of interdependent nodes coupled between the power and natural gas networks (Power to Gas)
$IEtW$	Set of interdependent nodes coupled between the power and water networks (Power to Water)

Variables	
R^i	Accumulated loss of resilience for an individual infrastructure system over the disruption period
R^{SoCIS}	Joint accumulated loss of resilience for interdependent infrastructure systems over the disruption period
R_t^{SoCIS}	Joint accumulated loss of resilience for interdependent infrastructure systems at time t
P_{pre}^i	Pre-disruption performance of an individual infrastructure system
P_{post}^i	Post-disruption performance of an individual infrastructure system
$C_{sys}^{pre,i}$	Total consumption of the service in the infrastructure network i before disruption
$D_{sys}^{pre,i}$	Total demand for the service in the infrastructure network i before disruption
$C_{sys}^{post,i}$	Total consumption of the service in the infrastructure network i after disruption
$D_{sys}^{post,i}$	Total demand for the service in the infrastructure network i after disruption
$E_{G,t}^m$	Total electric power generation at electric node m at time t
$E_{C,t}^m$	Total electric power consumption at electric node m at time t
e_t^p	Electric power flow through the powerline p at time t
$E_{G,t}^{GTPP,m}$	Electric power generation of GTPP at electric node m at time t
$E_{G,t}^{CCPP,m}$	Electric power generation of CCPP at electric node m at time t
$E_{G,t}^{PGS,m}$	Electric power imported by PGS at electric node m at time t
$E_{C,t}^{GTPP,m}$	Electric power consumption for GTPP at electric node m at time t
$E_{C,t}^{CCPP,m}$	Electric power consumption for CCPP at electric node m at time t
$E_{C,t}^{ESS.m}$	Electric power consumption for ESS at electric node m at time t
$E_{C,t}^{NGPP,m}$	Electric power consumption for NGPP at electric node m at time t
$E_{C,t}^{LNGT,m}$	Electric power consumption for LNGT at electric node m at time t
$E_{C,t}^{NGCS,m}$	Electric power consumption for NGCS at electric node m at time t

$E_{C,t}^{WSF,m}$	Electric power consumption for WSF at electric node m at time t
$E_{C,t}^{WPS,m}$	Electric power consumption for WPS at electric node m at time t
$E_{C,t}^{H}$	Electric power consumption for BSU H located in the service area of electric node m at time t
$z_{E,t}^{p}$	Binary variable indicating the operating state of powerline p at time t
$x_{E,t}^{m}$	Binary variable indicating the operating state of electric node m at time t
g_{t}^{q}	Natural gas flow through the pipeline q at time t
$G_{G,t}^{n}$	Total natural gas production at gas node n at time t
$G_{C,t}^{n}$	Total natural gas consumption at gas node n at time t
$G_{G,t}^{LNGT,n}$	Natural gas production of LNGT at gas node n at time t
$G_{G,t}^{NGPP,n}$	Natural gas production of NGPP at gas node n at time t
$G_{G,t}^{NGGS,n}$	Natural gas imported by NGGS at gas node n at time t
$G_{C,t}^{GTPP,n}$	Natural gas consumption for GTPP at gas node n at time t
$G_{C,t}^{CCPP,n}$	Natural gas consumption for CCPP at gas node n at time t
$G_{C,t}^{NGPP,n}$	Natural gas consumption for NGPP at gas node n at time t
$G_{C,t}^{LNGT,n}$	Natural gas consumption for LNGT at gas node n at time t
$G_{C,t}^{NGCS,n}$	Natural gas consumption for NGCS at gas node n at time t
$G_{C,t}^{H}$	Natural gas consumption for BSU H located in the service area of gas node n at time t
$z_{G,t}^{q}$	Binary variable indicating the operating state of gas pipeline q at time t
$x_{G,t}^{n}$	Binary variable indicating the operating state of gas node n at time t
w_{t}^{l}	Water flow through the pipeline l at time t
$W_{G,t}^{j}$	Total water supply at water node j at time t
$W_{C,t}^{j}$	Total water consumption at water node j at time t

$W_{G,t}^{WSF,j}$	Water supply by WSF at water node j at time t
$W_{G,t}^{WST,j}$	Water supply by WST at water node j at time t
$W_{C,t}^{CCPP,j}$	Water consumption for CCPP at water node j at time t
$W_{C,t}^{H}$	Water consumption for BSU H located in the service area of water node j at time t
$z_{W,t}^{l}$	Binary variable indicating the operating state of water pipeline l at time t
$x_{W,t}^{j}$	Binary variable indicating the operating state of water node j at time t
$\varphi_{E,t}^{GTPP,m}$	Binary variable indicating the operating state of GTPP at electric node m at time t
$\theta_{t}^{GTPP,n}$	Binary variable indicating the operating state of the interdependency link from gas node n to GTPP at electric node m at time t
$\delta_{t}^{GTPP,n}$	Binary variable indicating the operating state of gas supply system for GTPP at gas node n at time t
$\varphi_{E,t}^{CCPP,m}$	Binary variable indicating the operating state of CCPP at electric node m at time t
$\theta_{t}^{CCPP,n}$	Binary variable indicating the operating state of the interdependency link from gas node n to CCPP at electric node m at time t
$\delta_{t}^{CCPP,n}$	Binary variable indicating the operating state of gas supply system for CCPP at gas node n at time t
$\sigma_{t}^{CCPP,j}$	Binary variable indicating the operating state of the interdependency link from water node j to CCPP at electric node m at time t
$\gamma_{t}^{CCPP,j}$	Binary variable indicating the operating state of water supply system for CCPP at water node j at time t
$\varphi_{E,t}^{PGS,m}$	Binary variable indicating the operating state of PGS at electric node m at time t
$\varphi_{E,t}^{ESS,m}$	Binary variable indicating the operating state of ESS at electric node m at time t
$\varphi_{G,t}^{LNGT,n}$	Binary variable indicating the operating state of LNGT at gas node n at time t
$\alpha_{t}^{LNGT,m}$	Binary variable indicating the operating state of the interdependency link from electric node m to LNGT at gas node n at time t

$\pi_t^{LNGT,m}$	Binary variable indicating the operating state of power supply system for LNGT at electric node m at time t
$\varphi_{G,t}^{NGPP,n}$	Binary variable indicating the operating state of NGPP at gas node n at time t
$\alpha_t^{NGPP,m}$	Binary variable indicating the operating state of the interdependency link from electric node m to NGPP at gas node n at time t
$\pi_t^{NGPP,m}$	Binary variable indicating the operating state of power supply system for NGPP at electric node m at time t
$\varphi_{G,t}^{NGGS,n}$	Binary variable indicating the operating state of NGGS at gas node n at time t
$\varphi_{G,t}^{NGCS,n}$	Binary variable indicating the operating state of NGCS at gas node n at time t
$\alpha_t^{NGCS,m}$	Binary variable indicating the operating state of the interdependency link from electric node m to NGCS at gas node n at time t
$\pi_t^{NGCS,m}$	Binary variable indicating the operating state of power supply system for NGCS at electric node m at time t
$\varphi_{W,t}^{WSF,j}$	Binary variable indicating the operating state of WSF at water node j at time t
$\beta_t^{WSF,m}$	Binary variable indicating the operating state of the interdependency link from electric node m to WSF at water node j at time t
$\pi_t^{WSF,m}$	Binary variable indicating the operating state of power supply system for WSF at electric node m at time t
$\varphi_{W,t}^{WPS,j}$	Binary variable indicating the operating state of WPS at water node j at time t
$\beta_t^{WPS,m}$	Binary variable indicating the operating state of the interdependency link from electric node m to WPS at water node j at time t
$\pi_t^{WPS,m}$	Binary variable indicating the operating state of power supply system for WPS at electric node m at time t
$\varphi_{W,t}^{WST,j}$	Binary variable indicating the operating state of WST at water node j at time t
$MG_{W,t}^{E,j}$	Binary variable indicating whether a truck-mounted mobile generator is deployed at water node j at time t

Parameters	
t_E	Beginning time of system disruption
t_R	Ending time of the recovery process
ω_i	Pre-determined weights related to the relative importance of infrastructure systems
$S(link)$	Start node of the link
$T(link)$	Terminal node of the link
e_{cap}^{p}	Flow capacity of the powerline p
g_{cap}^{q}	Flow capacity of the gas pipeline q
w_{cap}^{l}	Flow capacity of the water pipeline l
$\tau_{E,t}^{m}$	Binary parameter indicating whether the recovery process started at electric node m at time t
$\tau_{G,t}^{n}$	Binary parameter indicating whether the recovery process started at gas node n at time t
$\tau_{W,t}^{j}$	Binary parameter indicating whether the recovery process started at water node j at time t
$S_{E,t}^{GTPP,m}$	Electric power generation capacity of GTPP at electric node m at time t
$D_{E,t}^{GTPP,m}$	Electric power demand of GTPP at electric node m at time t
$D_{G,t}^{GTPP,n}$	Natural gas demand of GTPP at gas node n at time t
$S_{E,t}^{CCPP,m}$	Electric power generation capacity of CCPP at electric node m at time t
$D_{E,t}^{CCPP,m}$	Electric power demand of CCPP at electric node m at time t
$D_{G,t}^{CCPP,n}$	Natural gas demand of CCPP at gas node n at time t
$D_{W,t}^{CCPP,j}$	Water demand of CCPP at water node j at time t
$S_{E,t}^{PGS,m}$	Electric power import capacity of PGS at electric node m at time t
$D_{E,t}^{ESS,m}$	Electric power demand of ESS at electric node m at time t
$D_{E,t}^{H}$	Electric power demand of BSU H located in the service area of electric node m at time t
$S_{G,t}^{LNGT,n}$	Natural gas production capacity of LNGT at gas node n at time t
$D_{G,t}^{LNGT,n}$	Natural gas demand of LNGT at gas node n at time t

$D_{E,t}^{LNGT,m}$	Electric power demand of LNGT at electric node m at time t
$S_{G,t}^{NGPP,n}$	Natural gas production capacity of NGPP at gas node n at time t
$D_{G,t}^{NGPP,n}$	Natural gas demand of NGPP at gas node n at time t
$D_{E,t}^{NGPP,m}$	Electric power demand of NGPP at electric node m at time t
$S_{G,t}^{NGGS,n}$	Natural gas import capacity of NGGS at gas node n at time t
$D_{G,t}^{NGCS,n}$	Natural gas demand of NGCS at gas node n at time t
$D_{E,t}^{NGCS,m}$	Electric power demand of NGCS at electric node m at time t
$D_{G,t}^{H}$	Natural gas demand of BSU H located in the service area of gas node n at time t
$S_{W,t}^{WSF,j}$	Water supply capacity of WSF at water node j at time t
$S_{W,t}^{WST,j}$	Water supply capacity of WST at water node j at time t
$D_{E,t}^{WSF,m}$	Electric power demand of WSF at electric node m at time t
$D_{E,t}^{WPS,m}$	Electric power demand of WPS at electric node m at time t
$D_{W,t}^{H}$	Water demand of BSU H located in the service area of water node j at time t
$\mu_{E,t}^{p}$	Binary parameter indicating whether the powerline p is restored at time t
$\mu_{G,t}^{q}$	Binary parameter indicating whether the gas pipeline q is restored at time t
$\mu_{W,t}^{l}$	Binary parameter indicating whether the water pipeline l is restored at time t
$N_{W,avail}^{E}$	Number of available truck-mounted mobile generators in the water network
UC_{SoCIS}	Unit cost of the SoCIS-ALR metric
UC_{RP}	Daily unit cost of the repair package
UC_{BS}	Daily unit cost of the backup system
L_i	Availability level of repair packages in the infrastructure network i
Nr_i^{BS}	Number of backup systems in the infrastructure network i

Chapter One

Introduction

The material of this chapter is directly or indirectly based on the following doctoral research plan and papers:

• Hamed Hafeznia. *Resilience Analysis of Interdependent Critical Infrastructure Systems*. Doctoral Research Plan, ETH Zurich, 2021.

• Hamed Hafeznia and Božidar Stojadinović. "ResQ-IOS: An iterative optimization-based simulation framework for quantifying the resilience of interdependent critical infrastructure systems to natural hazards," *Applied Energy*, vol. 349, p. 121558, Nov. 2023, doi: 10.1016/j.apenergy.2023.121558.

• Hamed Hafeznia and Božidar Stojadinović, "Resilience-based decision support system for installing standalone solar energy systems to improve disaster resilience of rural communities," submitted to Energy Strategy Reviews.

1.1. Problem statement and motivation

Countries' socio-economic development relies extensively on well-functioning Critical Infrastructure Systems (CISs) that provide essential resources and vital services, such as different types of energy, water, communication, and transportation [1], [2], [3]. In today's world, Critical Infrastructure Systems (CISs) such as power, natural gas, and water networks are becoming increasingly complex and, at the same time, highly interdependent, integrated, and interconnected with each other [4], [5], [6]. In light of the growing interdependencies between the CISs and other civil infrastructure networks, it is expected that a malfunction in a critical infrastructure system, such as the electrical power system, will lead to the inability to operate other interdependent civil infrastructure networks, like transportation and communication systems. Hence, the inoperability of critical infrastructure systems that serve as the backbone of a community may adversely affect the society's economic sectors [6], [7], [8], [9], [10], [11].

On the other hand, extreme events such as human-made threats and natural disasters, including earthquakes, floods, windstorms, etc., often disrupt the performance of CISs [8], [12], [13], [14]. Due to the many components in the structure of CISs, disruptions and shocks arising from the events mentioned earlier may cause temporary or permanent damage to technical equipment and, eventually, result in cascading failures. Considering that modern communities' functioning is dependent on the continuous services provided by interdependent infrastructure systems, policymakers, as well as community stakeholders, are concerned about the stability, reliability, and sustainability of supplying energy resources to support the economic and social growth in their communities [15], [16].

As part of their efforts to reduce damage costs and economic losses after disruptions in the performance of interdependent CISs, government agencies, policymakers, stakeholders, and infrastructure managers have adopted resilience enhancement strategies for critical infrastructure systems against extreme events [3], [6], [17], [18], [19], [20], [21], [22], [23], [24]. Community Resilience Enhancement Strategies (CRESs) aim to reduce vulnerability and damage costs, boost infrastructure networks' flexibility and tolerance to disruptive events, improve adaptability to the

changing environment, and expedite post-disruption recovery [3], [6], [17], [18], [19], [20], [22], [23], [24].

1.2. Research Questions

Considering the importance of maintaining and improving the resilience of urban and rural communities to natural hazards, the following research questions guided this doctoral dissertation:

1- How can we build the resilience assessment framework using a system-of-systems approach to track the post-disruption performance evolution of critical infrastructure systems while considering the interdependency relations between them?
2- How to mathematically model infrastructure systems' components to represent their real-world conditions during the recovery process?
3- How can we develop the framework to simultaneously quantify and enhance resilience over the recovery period?
4- How to conceptualize, model, and simulate the implementation of Community Resilience Enhancement Strategies (CRESs)?
5- How can the multi-hazard resilience assessment framework be applied to regional development planning?

1.3. Research Objectives

The purpose of this doctoral dissertation is to develop a framework that can evaluate the resilience of interdependent critical infrastructure systems in the face of potentially disruptive events by tracking post-disaster performance evolution. In addition to the ability of resilience quantification, this framework can enhance the resilience of interdependent critical infrastructure systems by optimizing service distribution within infrastructure networks and resource allocation during the post-disaster recovery process. To answer the research questions, the following research objectives are defined for this doctoral dissertation:

1- Create a framework to quantify the resilience of interdependent critical infrastructure systems against natural hazards using a system-of-systems approach.
2- Develop a detailed modeling approach to better represent the status of infrastructure systems' components during recovery.
3- Integrate optimization into the simulation-based methodology of the resilience assessment framework to benefit from simultaneous resilience quantification and improvement.
4- Model and conduct the feasibility study of implementing Community Resilience Enhancement Strategies (CRESs).
5- Incorporate a multi-hazard resilience assessment framework into the regional development planning.

1.4. State-of-the-art review

To better understand the literature review on the resilience assessment of interdependent infrastructure systems conducted for the doctoral dissertation, this section represents the state-of-the-art review of the resilience analysis of the CISs in four subsections, namely, Definition of Resilience, Modeling Approach, Performance Modeling, and Assessment Methods, as shown in Figure 1.1.

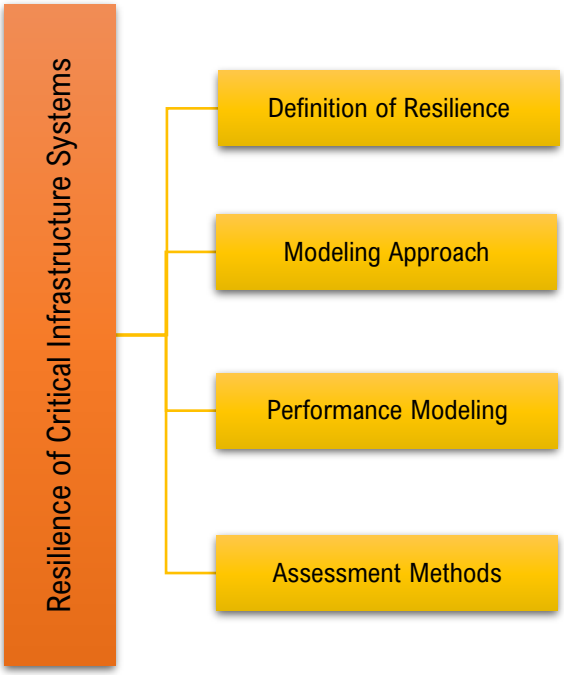

Fig. 1.1. Structure and four subsections of the state-of-the-art review section.

1.4.1. Definition of Resilience

Although understanding the definition of resilience is essential, conducting the literature review demonstrates flexibility in defining the concept of resilience, especially when research objectives, methodology, and case studies vary widely, from purely technical systems to purely societal aspects of a community exposed to disruption. In other words, there is no general agreement on the resilience definition, indicators, and quantitative metrics for critical infrastructure systems, including energy systems [3]. In this doctoral dissertation, an infrastructure system's resilience is defined as the ability of that system to minimize the consequences of the disturbance by anticipating, absorbing, adapting to, and recovering from the disruption.

1.4.2. Modeling Approach

One of the key steps in infrastructure resilience assessment is selecting a modeling approach. Various approaches can be applied to model the post-disaster performance and components' status of infrastructure systems. Ahmadi et al. [3] have conducted a literature review on approaches to modeling the resilience of energy systems. Based on their findings, the resilience modeling approaches can be categorized into three main groups: optimization, stochastic, and agent-based modeling. Other modeling approaches, including purely simulation-based, system dynamic, and indicator-based modeling, are less frequent. The classification of modeling approaches for resilience evaluation of infrastructure systems is shown in Figure 1.2.

In optimization-based models, the process of resilience quantification for infrastructure systems is modeled as an optimization problem whose objective function(s) may address the various aspects of system performance after disruption, such as recovery duration, potential costs and losses, and restoration sequence. In general, the optimization problem aims to improve the system's post-disaster performance by shortening the recovery process and reducing potential economic losses and system component damage.

Kong et al. [6] developed an optimization framework to improve the resilience of interdependent infrastructure systems to natural disasters. The objective of this framework was to find the optimal set of strategies to maximize the disaster resilience of infrastructure systems. Sang et al. [25] proposed an optimization model comprising a mixed-integer linear programming problem to find the optimal restoration sequence

of damaged components in interdependent gas and electricity infrastructure systems. Zhou et al. [26] provided a resilience enhancement framework to mitigate the impact of cascading failures by minimizing the costs of restoring failed components, hardening the system, and damages imposed by cascading failures. To solve the optimization model, they proposed mixed-integer genetic algorithms.

Liu et al. [27] provided a multi-objective optimization problem in a hierarchical framework to specify the optimal strategies for the resilience enhancement of interdependent power and natural gas infrastructure systems. Their optimization model aims to maximize infrastructure resilience while minimizing the cost of resilience improvement strategies. A multi-objective optimization model was developed by Almoghathawi et al. [28] to maximize the resilience of interdependent power and water networks while minimizing recovery costs. This model consists of a mixed-integer programming problem to determine the restoration priority of damaged components. In another research study, Almoghathawi et al. [29] presented an optimization model to boost the resilience of physically interdependent infrastructure systems by specifying the priority order of restoration tasks. They implemented the optimization model, which is a mixed-integer programming problem, for interdependent infrastructure systems located in Shelby County (TN), USA.

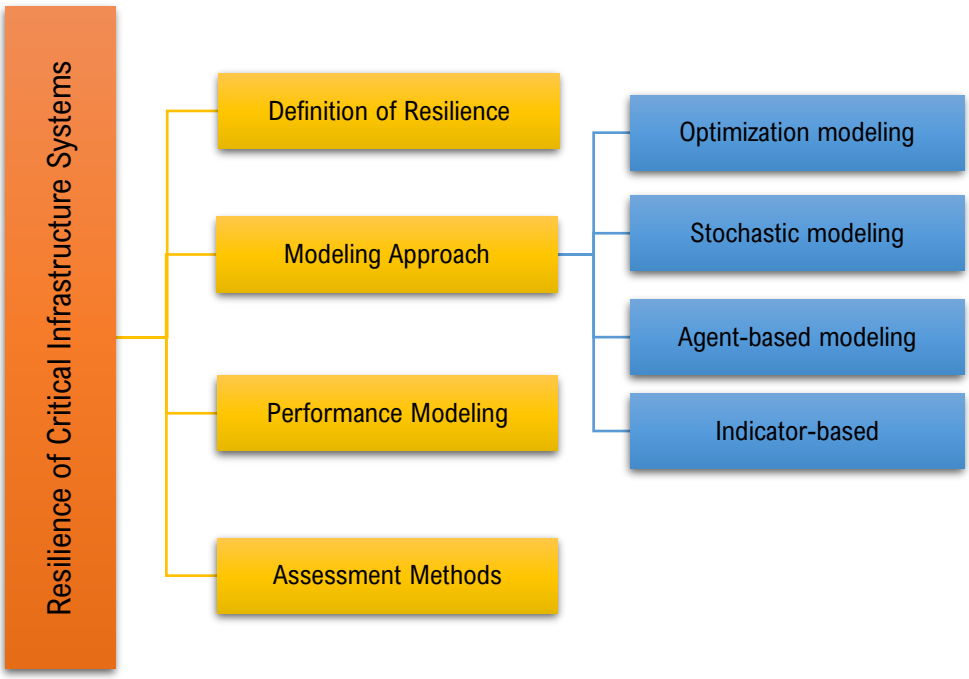

Fig. 1.2. Modeling approaches for infrastructure resilience assessment.

As part of stochastic modeling, Monte Carlo simulation methods are widely utilized to quantify the uncertainties in assessing the resilience of infrastructure systems. Research studies [30], [31], [32] proposed applying simulation-based methods to analyze the resilience of electricity networks against extreme weather events like hurricanes. Panteli and Mancarella [30] presented a time-series simulation model that was combined with the Monte Carlo method to evaluate the resilience of power infrastructure systems under intense climatic conditions. Balakrishnan and Cassottana [33] developed an open-source simulation package called InfraRisk for evaluating the resilience of interconnected infrastructure systems, focusing on power, water, and transportation networks.

Younesi et al. [13] proposed a quantitative framework for the resilience assessment of power networks against wide-area natural hazards. Applying Monte Carlo simulations, this framework accounts for the uncertainties involved in some characteristics of natural hazards, such as location, type, and severity level. Blagojevic et al. [34] developed a probability-based resilience assessment model for a virtual community. To carry out the stochastic modeling, many scenarios were simulated to quantify the virtual community's resilience against earthquakes. In a different study, Blagojevic et al. [35] presented a Monte Carlo-based simulation method to measure the importance of interdependent infrastructure systems' components for community resilience. The components of infrastructure systems were ranked based on the results of Sobol' indices.

As examples of agent-based modeling, the research studies [36] and [37] applied this type of modeling approach to the resilience analysis of infrastructure networks. For modeling the interdependencies between the infrastructure networks and the community, including the households and businesses, Dubaniowski and Heinimann [38] developed an agent-based Input-Output (IO) framework. They implemented the developed IO framework for assessing the resilience of an urban community in Singapore [39]. Sun et al. [40] proposed an agent-based recovery model for appraising the seismic resilience of communities. Furthermore, they presented a framework for quantifying the resilience of integrated civil infrastructure systems [41].

The application of indicator-based modeling for the resilience analysis of technical systems has lower frequency in resilience-related literature. For instance, Yazdi et al.

[42] provided a qualitative resilience evaluation framework for hydrogen-based energy infrastructure systems by jointly considering resilience and sustainability indicators. Gasser et al. [43] assessed the resilience of electricity supply in 140 countries using Multi-Criteria Decision Analysis (MCDA). They developed a metric for quantifying electricity supply resilience at the national level with an indicator-based approach. Arvin et al. [44] developed an infrastructure resilience assessment framework integrating the Geographic Information System (GIS) data and Multi-Criteria Decision Making (MCDM) techniques. The MCDM techniques consider 25 indicators to rank the case study counties based on resilience to three types of hazards: earthquake, flood, and landslide.

1.4.3. Performance Modeling

In modeling critical energy systems for resilience assessment, the system's performance is often considered a continuous variable. However, some research studies have applied discrete multistate models to evaluate the resilience of critical systems (Fig. 1.3). As an example of the application of multistate models, Zeng et al. [8] proposed a Markov reward process-based framework to quantify the resilience of nuclear power plants. They applied a multistate performance model for the nuclear power plant and analyzed the recovery process of the power plant by using a continuous time discrete state Markov chain. The capability of controlling the complexity of the modeling process is the advantage of using discrete multistate models. However, multistate models may not be applicable to interdependent critical infrastructure systems with numerous components. After disruption, components can be fully functional, partially functional, or completely failed. Contrary to this, some studies [6], [28], [45] relying on optimization models for resilience quantification assume a post-disruption binary state for components (failed or functional). That is to say, those research studies did not consider continuous functionality recovery for components.

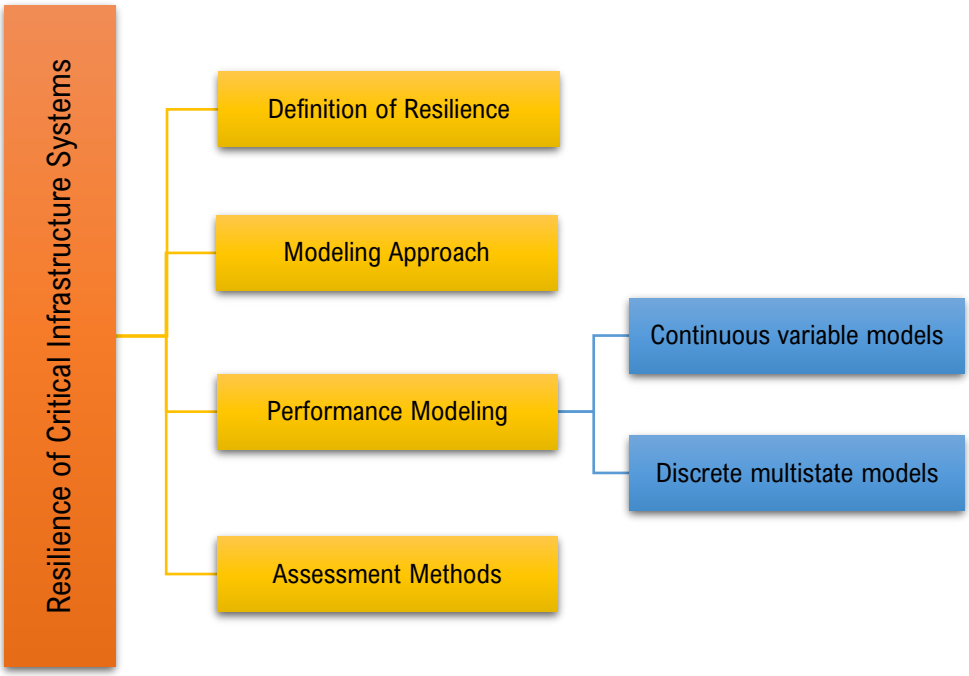

Fig. 1.3. Performance models for infrastructure resilience assessment.

1.4.4. Assessment Methods

Hosseini et al. [46] classified the system resilience assessment methods into two groups, namely, general measure-based and structure-based methods (Fig. 1.4). The general measure-based methods are developed based on empirically observable quantities [8], [46]. In other words, these methods quantify resilience regardless of the system-specific characteristics, such as system structure and the type of relationship between the components of the system [8], [46]. The resilience triangle model developed by Bruneau et al. [47] is a general measure-based method that quantifies resilience.

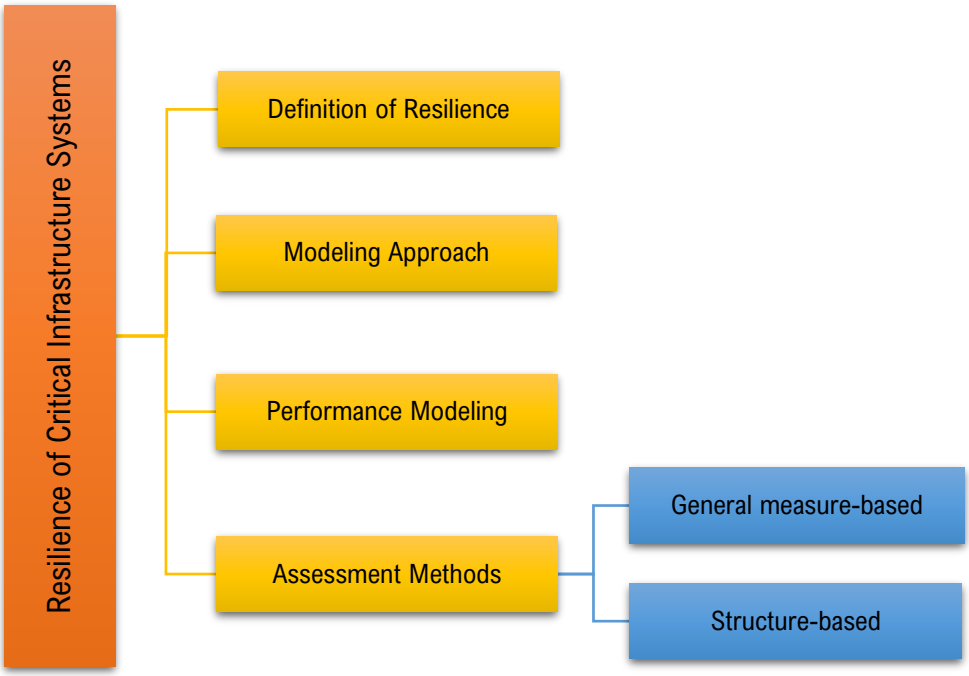

Fig. 1.4. Assessment methods for infrastructure resilience.

Structure-based methods consider system-specific characteristics, like structural topology. In topology-based methods, as a subset of structure-based methods, the resilience is quantified by applying network models that follow the topological structure of the concerned system [46], [48]. Chen et al. [49] studied the vulnerability of power transmission systems by integrating topological models with some characteristics of power grids. Liu et al. [50] assessed the resilience of interconnected power and gas networks by combining the topological model with a dynamic one. Wang et al. [51] proposed a three-stage framework for the modeling and resilience analysis of power grids using network theory.

1.4.5. Resilience Metrics

There are a few candidates for a metric to quantify the joint disruption resilience of interdependent CISs. In some research studies [3], [6], [52], [53], [54], [55], the resilience of an individual infrastructure system is calculated by the ratio of the area under the curve representing the time evolution of the actual performance of the infrastructure system with respect to the target performance of the system over the period starting from the occurrence of a disruptive event and ending when the recovery process is completed.

Some researchers [47], [56] quantified the resilience of an infrastructure system as the instantaneous difference between the actual and target system performance at certain time points during the recovery process. Another example of an instantaneous measure is the resilience metric proposed in the NIST SP-1190 report [57]. However, both groups of researchers use different indicators for infrastructure system performance.

1.4.6. Community Resilience Enhancement Strategy (CRES)

This section aims to illustrate how implementing Community Resilience Enhancement Strategies (CRESs) can improve community resilience against extreme events. The resilience of interdependent infrastructure systems of an urban community to disruptive events such as earthquakes, floods, windstorms, etc., can be evaluated by four indicators, namely, redundancy, robustness, resourcefulness, and rapidity [6]. They are illustrated in Fig. 1.5, displaying an infrastructure system's typical performance evolution curve after an extreme event. As shown in Fig. 1.5, the redundancy indicator measures the descending rate of the post-disruption performance of the infrastructure system. The robustness indicator is the minimum level of infrastructure performance after an extreme event occurrence. The resourcefulness indicator measures the ascending rate of the infrastructure system's performance after the recovery process starts. The rapidity indicator considers the time required for full functional recovery of the infrastructure system [6].

The objective of implementing CRESs is to improve the resilience indicators for infrastructure systems after a disaster [58], [59], [60], [61]. To investigate the impacts of CRESs on improving the disaster resilience of a community, these four indicators are employed to conceptualize CRESs and model their implementations. Such strategies are followed before the extreme events, representing a class of *pre-disruption* CRESs, or during the long-term recovery after the extreme event, representing a class of *post-disruption* CRESs. In addition, *peri-disruption* CRESs aimed at resolving the interdependencies among the CISs are followed during the short-term emergency interventions after the extreme event.

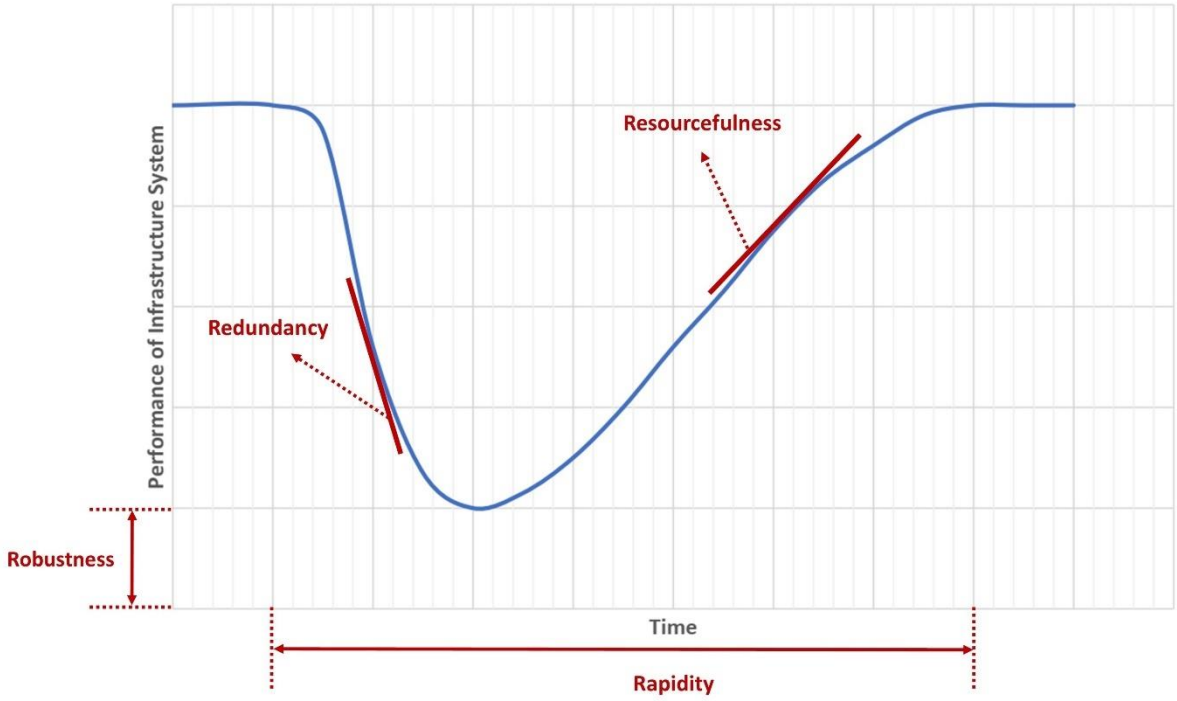

Fig. 1.5. The performance evolution of an infrastructure system after an extreme event and four respective resilience evaluation indices.

1.5. Research gaps in the resilience analysis of interdependent infrastructure systems

This section addresses existing research gaps identified through the critical literature review on the resilience analysis of interdependent infrastructure systems. The ResQ-IOS framework takes advantage of both simulation-based and optimization-based approaches to address existing research gaps. The research gaps in quantifying infrastructure resilience and the contributions of the ResQ-IOS framework to fill the gaps are as follows:

1- The simulation-based and agent-based methods employed for resilience quantification do not necessarily guarantee the optimal distribution of resources and services throughout infrastructure networks. The ResQ-IOS resilience quantification framework can determine the optimal flow of resources and services from and to each node in the network to maximize the resilience of

interdependent infrastructure systems at each time step of the simulation and thus deliver a realistic resilience assessment.

2- To reduce the computational burden, some papers consider a specific group of infrastructure systems' components for the resilience assessment, even though all components are subject to damage by natural hazards. The proposed ResQ-IOS framework assumes that all components of the considered systems may be damaged during the disaster.

3- Some research studies applying optimization models for resilience quantification consider a binary state for the operating condition of components after the disruption (failed or fully functional). In the ResQ-IOS framework, the initial operating state of components after disruption can be completely failed, partially functional, or fully functional.

4- Some reviewed research assumes that the demands posed by the components are constant and equal to their pre-disruption demands during the entire resilience assessment process, whereas it is an unrealistic assumption. For example, demands for electric power, natural gas, and potable water in the network may decrease after a disaster that damages residential buildings since the residents of damaged buildings have to move to safe locations outside the network. In the proposed ResQ-IOS framework, the demand for resources and services evolves in time after a disruptive event occurs. Thus, the demand for resources and services is a time-dependent function during the resilience assessment period. The ResQ-IOS framework makes it possible to consider the temporary loads that may be imposed on infrastructure networks during the recovery process.

5- To the best of our knowledge, it is necessary to develop a regional decision-making support system that simultaneously considers multi-hazard risk and resilience evaluation and techno-economic assessment to improve electricity access in rural areas. The ResQ-RDSS framework was designed to fill this gap.

1.6. Main contributions

This doctoral dissertation aims to develop a powerful and versatile computational tool called ResQ-IOS for modeling, quantifying, optimizing, and analyzing the resilience of interdependent critical infrastructure systems against potentially disruptive events. This framework applies a bottom-up approach to assessing an urban community's resilience, from estimating the damage level of infrastructure components to evaluating the infrastructure systems' performance and quantifying the urban community's disaster resilience. Considering the state-of-the-art in resilience analysis of interdependent infrastructure systems, the ResQ-IOS framework aims to minimize post-disaster disruption in an urban community by determining the optimal dispatching of infrastructure services during the recovery process. In this doctoral dissertation, the following items are the main contributions:

1- The ResQ-IOS framework can provide the stakeholders with seven optimal quantities related to the post-disaster recovery of urban communities:
   - Optimal daily dispatching of infrastructure services
   - Minimum loss of resilience (i.e., SoCIS-ALR metric)
   - Minimum total recovery cost
   - Optimal number of backup systems
   - Optimal portfolio for repair packages
   - Optimal locations of backup systems
   - Optimal schedule for deploying backup systems.

2- The ResQ-IOS framework enables the stakeholders to conduct feasibility studies on implementing Community Resilience Enhancement Strategies (CRESs). This ability enables the stakeholders to plan, simulate, and assess the impact of pre-disruption, peri-disruption, and post-disruption CRESs on improving community resilience.

3- The ResQ-IOS framework enables stakeholders to perform parametric analyses of community resilience against disasters to gain insight into the parameters influencing the recovery of urban and rural communities.

4- ResQ-RDSS, as a regional decision support system for analyzing various CRESs, is among only a few research studies that quantify the resilience of rural communities, moving from qualitative and conceptual studies toward implementation.

5- The ResQ-RDSS framework integrates multi-hazard risk assessment, optimization, and resilience quantification into Multi-Criteria Decision Making (MCDM).

1.7. Structure of the Dissertation

This dissertation is divided into five chapters. Chapter 1 discusses the problem statement and motivation, introduces the research questions and objectives of this doctoral dissertation, and surveys the current state-of-the-art concerning infrastructure resilience assessment. This chapter identifies the research gaps and describes the dissertation's main contributions to the state-of-the-art related to the resilience analysis of interdependent infrastructure systems.

Chapter 2 introduces the Iterative Optimization-based Simulation (IOS) methodology and explains the importance of developing such a computational framework to achieve the dissertation's research objectives. Then, this chapter outlines the structure of the ResQ-IOS, the Resilience Quantification Iterative Optimization-based Simulation framework developed in this doctoral research for evaluating the resilience of interdependent Critical Infrastructure Systems (CISs). Finally, Chapter 2 presents the mathematical model of interdependent CISs' performance and formulates a Mixed-Integer Linear Programming (MILP) problem for optimizing the resilience of interdependent CISs.

Chapter 3 aims to demonstrate the capabilities of the ResQ-IOS in evaluating the resilience of interdependent CISs. To this end, a realistic example of Shelby County (TN), USA, as a relatively dense urban community is introduced, followed by assessing the seismic resilience of Shelby County. This chapter also investigates the impacts of implementing three CRESs on the disaster resilience of Shelby County and carries out the parametric analysis of urban disaster resilience by taking Shelby County as an example. Finally, Chapter 3 identifies the optimal recovery strategies for minimizing the total recovery cost.

Chapter 4 explains the problem statement and motivation for developing the ResQ-RDSS, the extension of the ResQ-IOS, a resilience-based regional decision support system for installing off-grid solar power systems to improve disaster resilience of rural communities. This chapter describes the structure of the ResQ-RDSS. In order to

demonstrate the capabilities of the ResQ-RDSS, the rural settlements of Birjand County, Iran, are introduced as a low-density region case study. At the end of this chapter, the result of implementing the ResQ-RDSS for the resilient rural electrification of the case study is analyzed.

Chapter 5 comprises a summary of conclusions and suggestions for the potential extension of the research conducted in this doctoral dissertation.

Chapter Two

ResQ-IOS: An Iterative Optimization-based Simulation Framework for the Resilience Quantification of Interdependent Critical Infrastructure Systems

This chapter introduces the Iterative Optimization-based Simulation (IOS) framework of the ResQ-IOS and its structure, which comprises five modules for the resilience analysis of interdependent infrastructure systems. This chapter also provides the mathematical model of interdependent critical infrastructure systems for optimizing the disaster resilience of urban communities. The material of this chapter is published in the following paper:

• Hamed Hafeznia and Božidar Stojadinović. "ResQ-IOS: An iterative optimization-based simulation framework for quantifying the resilience of interdependent critical infrastructure systems to natural hazards," *Applied Energy*, vol. 349, p. 121558, Nov. 2023, doi: 10.1016/j.apenergy.2023.121558.

2.1. Introduction to Iterative Optimization-based Simulation

The capabilities of modern simulation tools to analyze complex systems' behavior by assessing their performance through creating 'what-if' scenarios make simulation a robust methodology for solving real-world problems [62], [63], [64]. The simulation process computes system's performance measures for different model alternatives to evaluate the effects of model parameters on systems' behavior. However, an optimization process is needed to find the best configuration of the systems by exploring the systems' performance measures space generated by simulation. Integration of simulation and optimization is, therefore, a promising methodology for solving large and complex problems in the real-world environment [65].

Optimization approaches utilizing traditional mathematical optimization are readily applicable to small, deterministic, and less complex systems. As the system's size, uncertainty, and complexity increase, mathematical modeling may fail to find an optimal solution [66], [67], [68], [69], [70]. In contrast, hybrid Optimization-Simulation (OS) approaches can deal with the uncertainty and complexity of large-scale systems. Accordingly, OS models are more suitable for real-world stochastic and complex systems with sizable details and intricate relationships between their components [67], [71], [72]. Models using OS approaches can also consider the system's non-linear relationships, dynamic features, and qualitative aspects [70]. Significant progress in computational capacities has led to meaningful growth in applying OS models to various research fields, such as risk management, healthcare, and industrial engineering [65], [73], [74], [75], [76]. In the field of disaster resilience modeling, assessment, and quantification of interacting civil infrastructures system, Optimization-Simulation (OS) is particularly useful. This is particularly important when the involved systems have different disruption reaction times. For example, depending on the source of electric power (nuclear, natural gas, oil, coal, wind, water, solar), the time to stabilize the system after a disruption and restore its function may be very different.

Considering the advantages of the hybrid Optimization-Simulation (OS) approach discussed above, it is essential to develop an Iterative Optimization-based Simulation (IOS) computational framework for modeling, quantifying, optimizing, and analyzing the resilience of interdependent CISs to achieve this doctoral dissertation's objectives.

The dissertation's objectives, addressed in this Chapter and stated earlier in Chapter 1 (Objectives No. 1, 2, and 3), are as follows:

- Create a framework to quantify the resilience of interdependent critical infrastructure systems against natural hazards using a system-of-systems approach.
- Develop a detailed modeling approach to better represent the status of infrastructure systems' components during recovery.
- Integrate optimization into the simulation-based methodology of the resilience assessment framework to benefit from simultaneous resilience quantification and improvement.

The general structure of an Iterative Optimization-based Simulation (IOS) framework is illustrated in Figure 2.1. According to this figure, an optimization solver is embedded into a simulation model in the structure of the proposed Iterative Optimization-based Simulation (IOS) framework. As shown in Fig. 2.1, the optimization solver is called repeatedly at each operational step of the IOS framework to optimize the simulated systems' state variables. Specifically, the simulation run is temporarily paused, and the state variables of the simulated system are transferred to the optimization solver as input to the analytical modeling of the system that is formulated as an optimization problem according to the current state of the simulated system. After the optimizer solves the mathematical model of the system and finds the solution, the framework updates the system's configuration according to the optimal solution and resumes the simulation run. This process is iterated between the optimization and simulation frequently until a pre-set stopping criterion is satisfied.

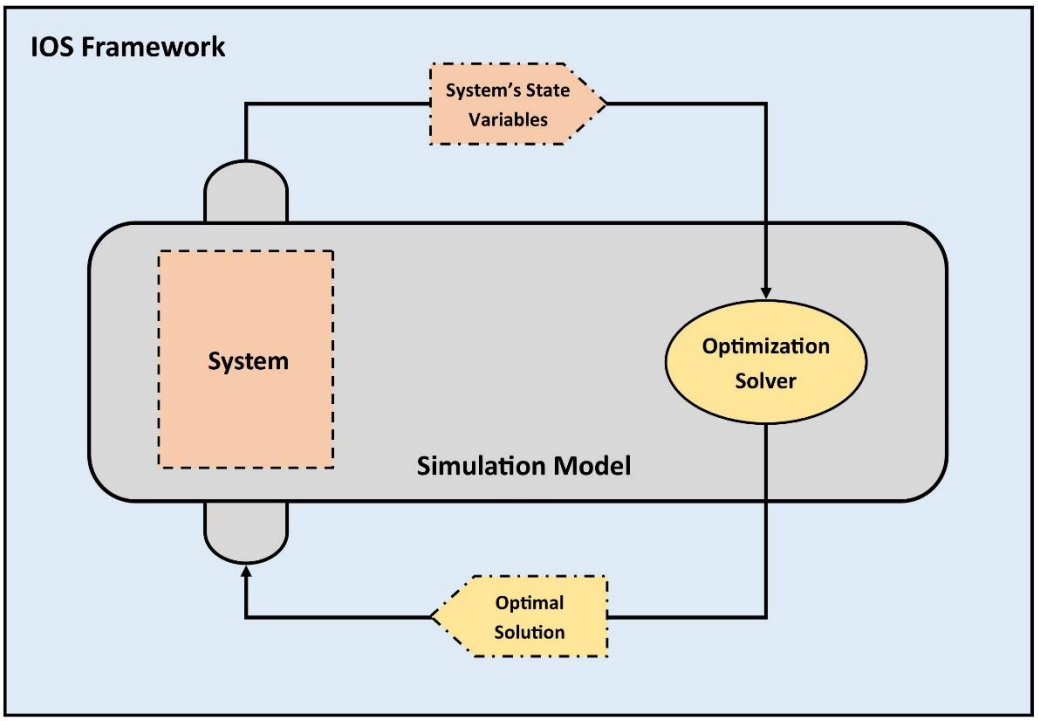

Fig. 2.1. An illustrative structure of the Iterative Optimization-based Simulation (IOS) framework.

2.2. Structure of the ResQ-IOS

This section introduces resilience quantification into an IOS framework by combining simulation and optimization. As shown in Fig. 2.2, the proposed Resilience Quantification Iterative Optimization-based Simulation (ResQ-IOS) framework for quantifying the resilience of interdependent CISs benefits from a modular workflow to establish logical relationships between the different sections of the framework. This IOS framework consists of five modules: risk assessment, simulation, optimization, database, and controller. They are described subsequently.

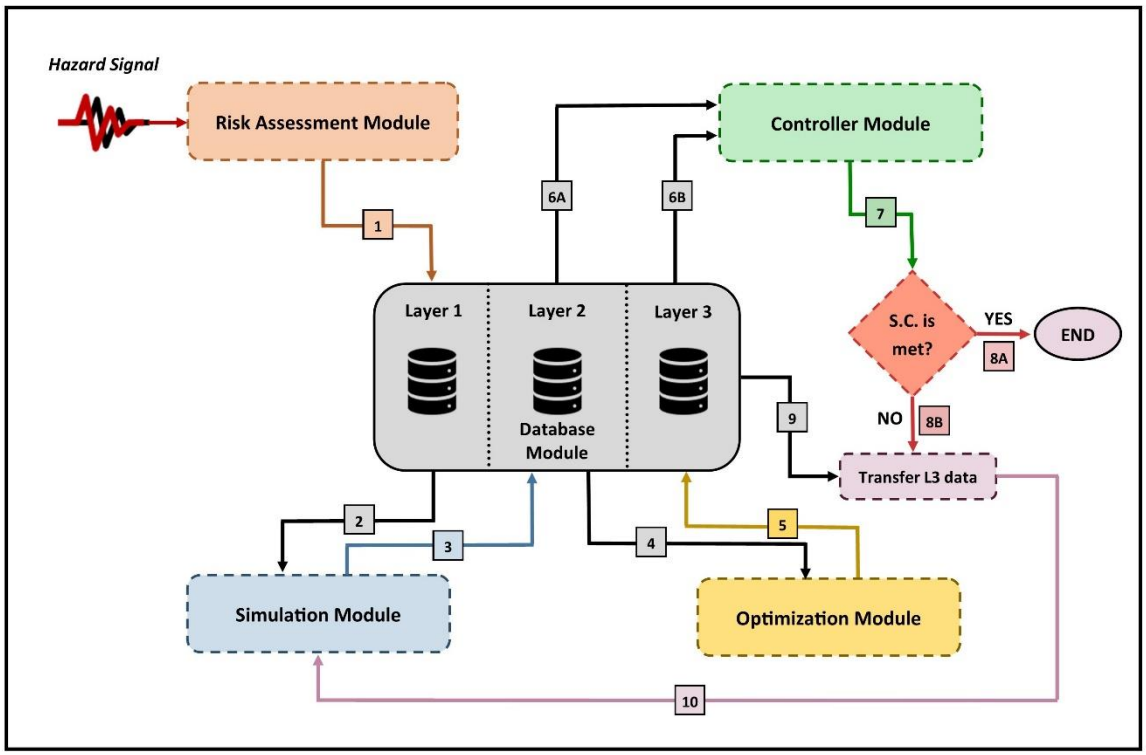

Fig. 2.2. The proposed ResQ-IOS framework for quantifying and optimizing the resilience of interdependent CISs.

The block diagram of the process by which the ResQ-IOS models and quantifies the resilience of interdependent CISs is given in Fig. 2.3. The diagram comprises five major modules: Risk Assessment, Simulation, Optimization, Database and Controller. These five modules work together to evaluate the resilience of interdependent infrastructure systems. As depicted in Fig. 2.3, the first module that triggers the ResQ-IOS framework to operate is the risk assessment module. This module simulates the hazard and, accordingly, evaluates the vulnerability of the components of the infrastructure networks. Then, data related to the post-disaster status of the infrastructure networks as the output of the risk assessment module is conveyed to the database module. In the next step, the simulation module uses this data to simulate the functional recovery evolution of infrastructure networks' performance by tracing the functionality of components on both supply and demand sides according to their damage level and repair progress. This simulated data is populated to the database module and is utilized by the optimization module to maximize the post-disruption performance of the considered interdependent CISs. The optimization module solves a Mixed-Integer Linear Programming (MILP) problem to determine the optimal

distribution of services and resources in the infrastructure networks with the objective of minimizing unmet demands. Then, the optimal configuration for supply and demand is transferred to the database module. Concerning the infrastructure systems' optimal performance configuration stored in the database, the simulation module reconfigures the supply and demand patterns in infrastructure networks. It then simulates the performance evolution of infrastructure networks for the next time step in the recovery process. This time-stepping Optimization-Simulation (OS) procedure is iterated between the simulation, database, and optimization modules. The controller module computes the loss of resilience for the infrastructure networks at each time step using the data of the supply and demand whose distribution is optimized. The controller module ends the OS process when a set of pre-defined simulation stopping criteria is met.

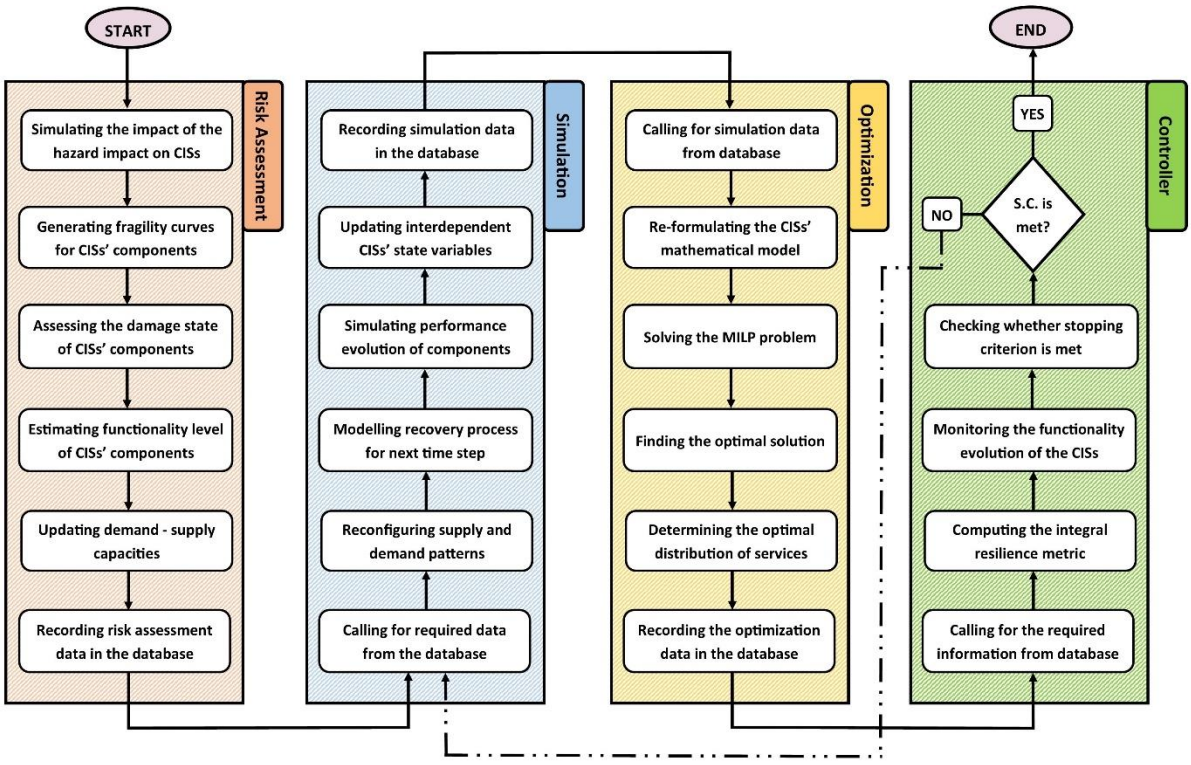

Fig. 2.3. The block diagram of the process used in the ResQ-IOS for modeling and quantifying the resilience of interdependent CISs.

2.2.1. Risk Assessment Module

The ResQ-IOS framework incorporates the risk assessment module to model how a hazard-induced disruption affects the functioning of a community and its interdependent infrastructure systems. The role of this module is to estimate the impact of the hazard on the performance of infrastructure systems' components. This module is the starter of workflow in the ResQ-IOS framework for the resilience assessment of interdependent CISs.

After the hazard-related disruption information is received, the risk assessment module begins to simulate the regional-scale impacts of the hazard on the infrastructure networks, considering the type and magnitude of the hazard. In this doctoral dissertation, the interdependent CISs' loss of functionality due to natural hazards is classified into two groups: direct and indirect functionality loss. Direct functionality loss is referred to the physical damage to the components of infrastructure networks. The physical damage includes structural and non-structural damage. For instance, the structural damage of a water pump station can be a partial collapse of the pump station building, and non-structural damage can be referred to as the equipment failure of the electrical power supply system in the pump station. Indirect functionality loss is referred to the inoperability of a component in the infrastructure system due to the malfunction in the performance of another infrastructure system that supplies the demand of that component in the dependent infrastructure system setting. For example, the water pump station, which remains intact after a natural hazard, may cease to operate if the electrical power network is damaged and not able to supply the pump station's demand. This type of functionality loss results from the interdependency between different infrastructure systems.

Taking an earthquake as an example of the hazard, the risk assessment module simulates the impact of the earthquake on the infrastructure network by estimating intensity measures at the geographical location of the infrastructure networks' components. The earthquake intensity measures such as PGD, PGV, and PGA are calculated from the ground motion characteristics. To estimate the intensity measures at the locations of the systems' components, attenuation models that are the function of the earthquake magnitude and epicenter location are used. Then, the risk assessment module utilizes the seismic fragility curves of the infrastructure networks' components provided within component specification data. Considering the fragility

curves and earthquake intensity measures at their location, the module assesses the components' vulnerability against the hazard and sets their initial post-disruption damage state. After producing the fragility curve for each component, based on the earthquake intensity measures like PGA at the location of the component, the damage state of the component is estimated. To this end, five damage states similar to the methodology of the FEMA-HAZUS Earthquake Model Technical Manual [77] are considered, namely, None, Slight, Moderate, Extensive, and Complete. The workflow of the risk assessment module is consistent with the Performance-Based Earthquake Engineering (PBEE) methodology developed by the Pacific Earthquake Engineering Research Center (PEER) [78]. Lastly, the risk assessment module sends information about the damage state of the components to the database module.

One of the strengths of the ResQ-IOS framework is that the resilience assessment process is formulated and implemented based on the time-dependent damage state of the components. Hence, this framework can evaluate the resilience of interdependent CISs under the impact of multiple natural hazards (e.g., floods or high winds) as well as triggered natural hazard cascades.

2.2.2. Simulation Module

The function of this module is to simulate the post-disruption performance of the interdependent CISs with a system-of-systems approach during the recovery process. This module models the interactions between different infrastructure networks during the post-disaster recovery process by tracking the CIS components' initial damage and function recovery to capture the interdependency between the infrastructure networks. Additionally, the simulation module of the ResQ-IOS framework employs a fuzzy logic model to continuously assess components' functionality.

According to the components' damage level data, which is stored in the first layer of the ResQ-IOS database, the simulation modules appraise the functionality level of the infrastructure networks. The operational state of the components is evaluated by fuzzy membership functions. Therefore, the operating state of a component after a disaster can be rated as fully functional, partially functional, or completely failed. The amount of time needed to restore a damaged component is a function of its immediate

post-disaster damage state and, thus, a function of the hazard's intensity at the location of the component and its vulnerability.

2.2.3. Optimization Module

An optimization solver is embedded into the ResQ-IOS framework to determine the optimal flow of resources and services from and to each node in the considered infrastructure networks to minimize the loss of resilience of interdependent CISs at each step of the recovery process. Section 2.3 introduces a resilience metric that computes the joint loss of resilience for interdependent infrastructure systems. Minimizing that resilience metric is the objective function of the optimization module. Thus, the optimization solver is called in each iteration of the ResQ-IOS framework. The optimization module calls for information about the current infrastructure network status stored in the second layer of the ResQ-IOS database. Then, the optimization module updates the mathematical model of the interdependent CISs according to the networks' status parameters. The main parts of the mathematical model, including the objective function and the constraints, stay unchanged; however, the model parameters and some decision variable coefficients may change in an optimization cycle.

2.2.4. Controller Module

The tasks of the controller module are to monitor the functionality evolution of critical infrastructure systems during the post-disruption recovery process, and to stop the time-stepping OS process once the stopping criteria are met. For these purposes, an integral resilience metric is defined in Section 2.3 to evaluate the joint recovery process of the interdependent CISs. The controller module computes this resilience metric in each of the ResQ-IOS framework cycle. The module stops the resilience quantification framework when the resilience metric exceeds the pre-set threshold.

2.2.5. Database Module

In the ResQ-IOS framework, the role of the database module is to store the output data from the risk assessment, simulation, and optimization modules and provide the

required data to those modules during iterative resilience quantification (Fig. 2.2). In other words, the database module fulfills the module interface and data exchange roles. The database module consists of three layers. The first layer is allocated to store the output data sent by the risk assessment module. This data includes the damage state of the infrastructure networks' components caused by the hazard. The simulation module uses the data in this layer to trace the performance evolution of the CISs after the occurrence of the hazard.

The second layer of the database is dedicated to the output data of the simulation module, comprising the current functionality level of the CIS components and the current demand recovery of the consumers. The data of the second layer is fed to the optimization module. This data, which are the state variables of the community, is utilized to re-formulate the MILP optimization problem that is representative of the community's mathematical model. As shown in Fig. 2.2, the optimal solution discovered by the optimization module is populated to the third layer of the database. The data stored in the third layer is then transferred to the simulation module to reconfigure the infrastructure networks and update the supply and demand patterns in the CISs and the community. The exchange of data between the ResQ-IOS framework's modules, as stated above, occurs until the controller module stops the time-stepping recovery OS process. The controller module takes the data from the second and third layers of the database to check whether the resilience quantification stopping criterion is satisfied. In other words, the controller module monitors changes in the value of the resilience metric defined for interdependent infrastructure systems.

2.3. Resilience metric for interdependent critical infrastructure systems

In this doctoral dissertation, a resilience metric was defined to measure the resilience of an individual infrastructure system with respect to its pre-and post-disruption performance. The resilience of the infrastructure system following a disruptive event is quantified by tracking the evolution path of system performance after the disruption through time. The resilience metric adopted in this dissertation is based on the Loss of Resilience metric proposed by Didier et. al [79]. An infrastructure

system encounters a loss of resilience when it is not able to supply the amount of demand for its service. The resilience metric R^i used in this doctoral dissertation is:

$$R^i = \int_{t_E}^{t_R} \left(P^i_{pre}(t) - P^i_{post}(t) \right) dt \qquad (E.1)$$

where P^i_{pre} and P^i_{post} denote the infrastructure system's i pre- and post-disruption performance, and t_E and t_R denote the times when the disruption occurs and the time when the recovery process ends, respectively. The instantaneous performance of the system $P^i(t)$ is the ratio of the instantaneous total consumption of its service (e.g., electrical power, water, etc.) $C^i_{sys}(t)$ and the instantaneous total demand for its service $D^i_{sys}(t)$ and measures its instantaneous Loss of Resilience (LR). By this definition, the performance of the system $P^i(t)$ is normalized and unitless, following [80], and takes values between 0 and 1. The resilience metric is then:

$$R^i = \int_{t_E}^{t_R} \left(\frac{C^{pre,i}_{sys}(t)}{D^{pre,i}_{sys}(t)} - \frac{C^{post,i}_{sys}(t)}{D^{post,i}_{sys}(t)} \right) dt \qquad (E.2)$$

In this dissertation, pre-disruption performance is assumed to have no Loss of Resilience, thus $P^i_{pre} = 1$, and the target post-disruption performance is assumed to be equal to the pre-disruption performance. Figure 2.4 graphically demonstrates that the resilience metric R^i is equal to the area between the target and the actual performance curves of the infrastructure system, computed by integrating the consumption/demand ratio difference in each time step. Thus, the resilience metric R^i for a CIS is called the Accumulated Loss of Resilience (ALR) in this doctoral dissertation.

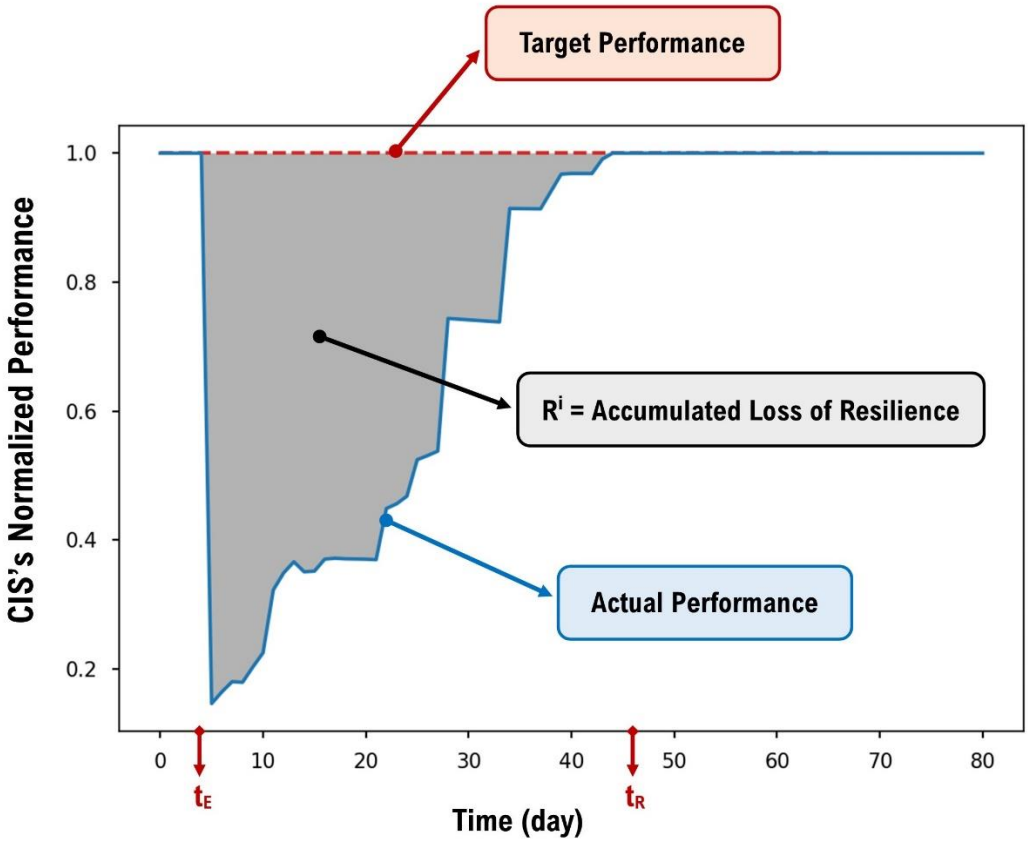

Fig. 2.4. Illustration of the Accumulated Loss of Resilience (ALR) for a CIS (R^i metric).

Due to connections, dependencies, and interactions between different infrastructure networks in a community, interdependent CISs are modeled as a "system-of-systems" [48]. As explained in the next section, a resilient behavior of interdependent system of CISs relies on the functioning of all individual infrastructure networks in the community. Conversely, the non-resilient behavior of the system of CISs may be induced by interdependencies and cascading failures, where non-performance of one CIS disables otherwise undamaged components of other CISs. To capture this system-of-CISs behavior in a single resilience metric, according to [80], a linear combination (i.e., weighted sum) of the performance of each infrastructure system, called the joint Accumulated Loss of Resilience (SoCIS-ALR) metric, is proposed as:

$$R^{SoCIS} = \sum_{i \in CIS} \omega_i R^i = \sum_{i \in CIS} \omega_i \cdot \int_{t_E}^{t_R} \left(\frac{C_{sys}^{pre,i}(t)}{D_{sys}^{pre,i}(t)} - \frac{C_{sys}^{post,i}(t)}{D_{sys}^{post,i}(t)} \right) dt \qquad (E.3)$$

$$s.t. \qquad \sum_{i \in CIS} \omega_i = 1 \tag{E.4}$$

where ω_i denotes the predetermined weights assigned to individual CISs, for example, according to the relative importance of each network in the community. In this doctoral dissertation, the relative importance of infrastructure networks in the community is considered equal for power, natural gas, and water networks. Since the SoCIS-ALR metric (R^{SoCIS}) is normalized and unitless, it can evaluate the performance of interdependent CISs jointly regardless of the type of service provided by the infrastructure system. Moreover, using R^{SoCIS} metric facilitates computing the community resilience performance goals proposed in NIST SP-1190 [57].

2.4. Modeling of Interdependent Critical Infrastructure Systems

Different types of interdependencies exist between the infrastructure systems, such as physical, cyber, geographical, and logical [4]. According to the relevant studies on resilience quantification, a multi-layer network model can be used to represent interdependent CISs [6], [80], [81]. In this model, different CISs can operate and interact through the interdependency links connecting nodes from different CISs. An illustrative example of a multi-layer network with interdependency links is provided in Fig. 2.5. As depicted in this figure, the service inputs necessary for continuing the functionality of an infrastructure network are transferred from other infrastructure networks through such interdependency links. These interdependency links represent the physical interdependencies between various infrastructure networks. The principal interdependencies between power, natural gas, and water networks are physical [28], [80]. In addition to physical, the simulation module in the Res-IOS framework considers the geographical interdependencies between the infrastructure networks. Geographical interdependencies between CISs occur when their components are in proximity to one another so that those components may be simultaneously affected by the same natural hazard [6]. Cyber and logical interdependencies are not modeled in this research.

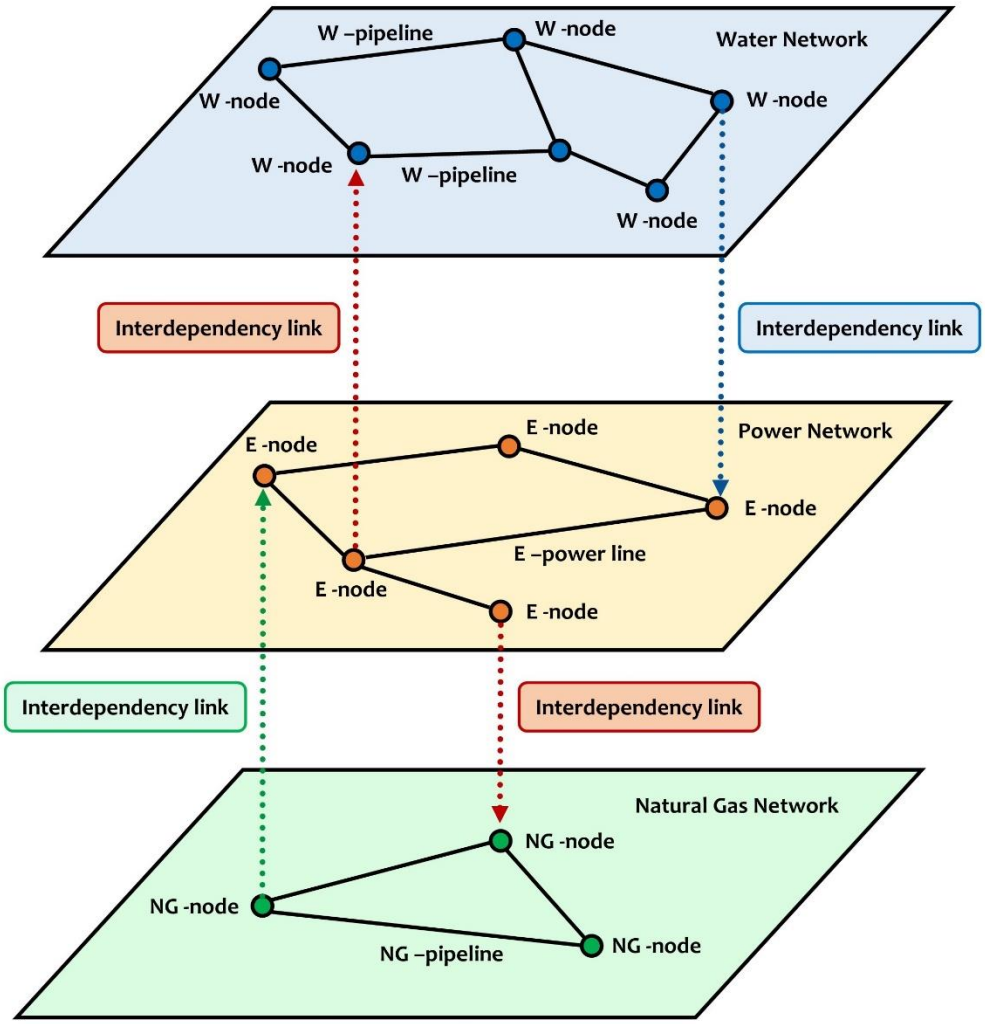

Fig. 2.5. An illustrative example of a multilayer network with interdependency links.

2.5. Network flow-based model of an infrastructure system

There are different CIS operation models for analyzing the performance of infrastructure systems and its evaluation through the post-disaster recovery process [82], [83], [84], [85]. Considering the characteristics of the CISs addressed in this doctoral dissertation, power, natural gas, and water, a network flow-based operation model is selected to capture the evolution of infrastructure systems' performance according to [6], [25], [86], [87], [88]. In this operation model, the function of each infrastructure system is to generate and convey a specific type of service throughout its network.

To represent an infrastructure system as a network, it is crucial to map the physical facilities in the infrastructure system to the set of nodes and links describing the actual functional role of those facilities. The network flow-based model has three types of nodes to differentiate the physical facilities in the infrastructure system by their function type: supply, demand, and transmission. The supply nodes are the facilities in the infrastructure network that generate a service. The demand nodes are the locations in the infrastructure network where the services are delivered to the end users. The transmission nodes are the facilities in the infrastructure network that facilitate service transfer between supply and demand nodes. Another flow-based network component is the links, which connect two nodes to transfer services.

2.6. Modeling the recovery process

The recovery process in the simulation module is modeled for three types of interdependent infrastructure systems: electrical power, water, and natural gas. Since the risk assessment module estimates the impact of the disaster on the components of both the demand and supply sides, not only the restoration of infrastructure networks' components but also the demand evolution of consumers is considered in the modeling of the recovery process. In addition to considering time-dependent demands for resources and services during the recovery process, the recovery model of the ResQ-IOS framework can deal with temporary fluctuations of the demands for services in the course of the restoration of the damaged components.

According to the components' damage level data, which is stored in the first layer of the ResQ-IOS database, the simulation modules appraise the functionality level of the infrastructure networks. The operational state of the components is evaluated by fuzzy membership functions. Therefore, the operating state of a component after a disaster can be rated as fully functional, partially functional, or completely failed. The amount of time needed to restore a damaged component is a function of its immediate post-disaster damage state and, thus, a function of the hazard's intensity at the location of the component and its vulnerability.

The recovery model developed for the ResQ-IOS framework can apply different restoration functions to the damaged CIS components. Besides binary and linear restoration functions, the recovery model implements nonlinear restoration functions.

A nonlinear restoration model considers different repair rates throughout the recovery process, made possible by the Iterative Optimization-based Simulation framework of the ResQ-IOS.

2.7. Mathematical formulation of the optimization model

In the optimization module, the performance of interdependent infrastructure systems is formulated as a Mixed-Integer Linear Programming (MILP) problem. The resilience of these interdependent infrastructure systems is then quantified by solving the optimization problem. In this doctoral dissertation, the resilience of an infrastructure system is quantified using the resilience metric defined by Equation (E.3). Measuring the best performance of considered interdependent CISs in each recovery process step is essential. An infrastructure system with optimal service distribution throughout its network may cope with the aftermaths of a natural disaster better than an infrastructure system with random service dispatching. The optimal service dispatch within a network usually reduces the unmet demand and results in a higher resilience value for that network. The objective of the optimization module is to minimize the SoCIS-ALR metric, which measures the loss of resilience for a system of interdependent CISs after a disruption, and it is expressible as follows:

$$\min_{DV} R_t^{SoCIS} = \min_{DV} \sum_{i \in CIS} \omega_i R_t^i = \min_{DV} \sum_{i \in CIS} \omega_i \cdot \left(\frac{C_{sys}^{pre,i}(t)}{D_{sys}^{pre,i}(t)} - \frac{C_{sys}^{post,i}(t)}{D_{sys}^{post,i}(t)} \right) \qquad (E.5)$$

where R_t^{SoCIS} is the joint accumulated loss of resilience for the system of interdependent infrastructure systems at time t and ω_i and R_t^i denote the predetermined weights assigned to individual CISs and the accumulated loss of resilience for an individual CIS at time t, respectively. In the objective function (Equation E.5), R_t^i , the accumulated loss of resilience for an individual CIS, is the difference between the instantaneous target (i.e., pre-disruption) and the instantaneous actual (i.e., post-disruption) performance of the concerned CIS. The performance of the concerned CIS at time t is the ratio of the instantaneous total consumption of its service $C_{sys}^i(t)$ and the instantaneous total demand for its service $D_{sys}^i(t)$. The pre-disruption and post-disruption performances of the concerned CIS i at time step t are the following ratios:

$\left(\frac{C_{sys}^{pre,i}(t)}{D_{sys}^{pre,i}(t)}\right)$: pre-disruption performance

$\left(\frac{C_{sys}^{post,i}(t)}{D_{sys}^{post,i}(t)}\right)$: post-disruption performance

Then, to minimize the loss of resilience at each time step of the resilience assessment period, the optimal post-disruption performance of the interdependent infrastructure systems is calculated by considering the constraints related to the network topology, the operating state of facilities and components, and interdependencies between the infrastructure systems. The objective function of the optimization model considering the SoCIS-ALR metric for the three interdependent CISs (power, natural gas, and water) is formulated as follows:

$$\begin{aligned}
\min_{DV} R_t^{SoCIS} &= \min_{DV} \sum_{i \in CIS} \omega_i \cdot \left(\frac{C_{sys}^{pre,i}(t)}{D_{sys}^{pre,i}(t)} - \frac{C_{sys}^{post,i}(t)}{D_{sys}^{post,i}(t)} \right) \\
&= \min_{DV} \sum_{i \in CIS} \omega_i \cdot \left(\frac{\sum_{s \in SN^i} \sum_{f \in SF^i} C_{f,s,t}^{pre,i}}{\sum_{s \in SN^i} \sum_{f \in SF^i} D_{f,s,t}^{pre,i}} - \frac{\sum_{s \in SN^i} \sum_{f \in SF^i} C_{f,s,t}^{post,i}}{\sum_{s \in SN^i} \sum_{f \in SF^i} D_{f,s,t}^{post,i}} \right) \\
&= \min_{DV} \Bigg[\omega_E \cdot \left(\frac{\sum_{m \in NE} \sum_{f_e \in FE} E_{C,t}^{f_e,m,pre}}{\sum_{m \in NE} \sum_{f_e \in FE} D_{E,t}^{f_e,m,pre}} - \frac{\sum_{m \in NE} \sum_{f_e \in FE} E_{C,t}^{f_e,m,post}}{\sum_{m \in NE} \sum_{f_e \in FE} D_{E,t}^{f_e,m,post}} \right) \\
&+ \omega_G \cdot \left(\frac{\sum_{n \in NG} \sum_{f_g \in FG} G_{C,t}^{f_g,n,pre}}{\sum_{n \in NG} \sum_{f_g \in FG} D_{G,t}^{f_g,n,pre}} - \frac{\sum_{n \in NG} \sum_{f_g \in FG} G_{C,t}^{f_g,n,post}}{\sum_{n \in NG} \sum_{f_g \in FG} D_{G,t}^{f_g,n,post}} \right) \\
&+ \omega_W \cdot \left(\frac{\sum_{j \in NW} \sum_{f_w \in FW} W_{C,t}^{f_w,j,pre}}{\sum_{j \in NW} \sum_{f_w \in FW} D_{W,t}^{f_w,j,pre}} - \frac{\sum_{j \in NW} \sum_{f_w \in FW} W_{C,t}^{f_w,j,post}}{\sum_{j \in NW} \sum_{f_w \in FW} D_{W,t}^{f_w,j,post}} \right) \Bigg] \quad (E.6)
\end{aligned}$$

$$s.t. \quad sets\ of\ constraints\ [Eqs.(E.7) - (E.92)]$$

where R_t^{SoCIS} denotes the instantaneous joint accumulated loss of resilience for interdependent CISs. ω_i is assigned weights to each infrastructure system. ω_E, ω_G, and ω_W represent the predetermined weights of the power, natural gas, and water networks. As explained earlier for Eq. (E.5), $C_{sys}^{i}(t)$ and $D_{sys}^{i}(t)$ are the total consumption and demand for the service provided by the concerned CIS i at time t. The variable $C_{f,s,t}^{post,i}$ denotes that the total consumption of the service in CIS i at time t after the disruption equals the total service consumption by facilities f belonging to the

CIS i (SF^i) and located at the node s in the network of the CIS i (SN^i). The variable $D_{f,s,t}^{post,i}$ denotes that the total demand for the service provided by the CIS i at time t equals the total post-disruption demands for the service requested by facilities f belonging to the CIS i (SF^i) and located at the node s in the network of the CIS i (SN^i). The same definitions apply to pre-disruption situations. Symbols $E_{C,t}$, $G_{C,t}$, and $W_{C,t}$ denote the instantaneous consumption of electric power, natural gas, and water, respectively. $D_{E,t}$, $D_{G,t}$, and $D_{W,t}$ are the instantaneous demand for electric power, natural gas, and water, respectively. The information about other indices and variables in Eq. (E.6) is given in the nomenclature table of this doctoral dissertation.

To construct the optimization model for resilience assessment, it is necessary to develop the constraints according to the network flow-based model of infrastructure systems. The constraints of the MILP problem for the power, natural gas, and water CISs used for the optimization model of this doctoral dissertation are presented in the following sub-sections.

2.7.1. Power network operating constraints

In the network flow-based model of the power system, the supply nodes are the electrical power generation sites and the gate stations for electricity import. This doctoral dissertation considers two types of power plants: Gas Turbine Power Plants (GTPPs) and Combined-Cycle Power Plants (CCPPs). A Power Gate Station (PGS) used for electricity import is considered a supply node in this doctoral dissertation. The transmission nodes are the electric substations. The demand nodes are the locations where the power is delivered to the end users, such as building stock units, water pump stations, etc. The links represent power transmission lines installed between various parts of the power network.

The constraints of the power network are represented by Equations (E.7)-(E.12). Equation (E.7) guarantees the flow conservation at each power network node. Equation (E.8) states that the power flow injected to each node at each time step comprises the electricity imported by the PGSs and the electrical power output of GTPP and CCPP units. Equation (E.9) describes that the power flow out of each node at each time step is equal to the accumulated electrical power consumed by the GTPP,

CCPP, and ESS units in the power network, NGPP, LNG terminals, and NGCS units from the natural gas network, WSF, and WPS units in the water network and building stock units including different types of buildings. Equation (E.10) ensures that the power flow through each power transmission line at each time step cannot exceed the power line's capacity if the power line is operational. The logical relationships between the operating state of the power line and the operating state of its start and terminal nodes are represented by Equations (E.11)-(E.12).

$$\sum_{(p \in LE \mid T(p)=m)} e_t^p - \sum_{(p \in LE \mid S(p)=m)} e_t^p + E_{G,t}^m - E_{C,t}^m = 0 \qquad \forall m \in NE, \forall t \in T \qquad (E.7)$$

$$E_{G,t}^m = E_{G,t}^{GTPP,m} + E_{G,t}^{CCPP,m} + E_{G,t}^{PGS,m} \qquad \forall m \in NE, \forall t \in T \qquad (E.8)$$

$$E_{C,t}^m = E_{C,t}^{GTPP,m} + E_{C,t}^{CCPP,m} + E_{C,t}^{ESS,m} + E_{C,t}^{NGPP,m} + E_{C,t}^{LNGT,m} + E_{C,t}^{NGCS,m} + E_{C,t}^{WSF,m} + E_{C,t}^{WPS,m} + \sum_{(H \in BSU \mid loc(H)=m)} E_{C,t}^H \qquad \forall m \in NE, \forall t \in T \qquad (E.9)$$

$$0 \leq e_t^p \leq z_{E,t}^p \cdot e_{cap}^p \qquad \forall p \in LE, \forall t \in T \qquad (E.10)$$

$$z_{E,t}^p \leq x_{E,t}^{S(p)} \qquad \forall p \in LE, \forall t \in T \qquad (E.11)$$

$$z_{E,t}^p \leq x_{E,t}^{T(p)} \qquad \forall p \in LE, \forall t \in T \qquad (E.12)$$

2.7.2. Natural gas network operating constraints

Regarding the natural gas system's network flow-based model, the supply nodes represent the facilities where natural gas is prepared for sending out into the transmission grid, such as LNG terminals, Natural Gas Processing Plants (NGPP), and Natural Gas Gate Stations (NGGS) employed for natural gas imports. Transmission nodes are representative of the natural gas compressor stations. The demand nodes provide natural gas to consumers, such as power plants, building stock units, etc. The links are the natural gas pipelines connecting the gas network nodes.

Equations (E.13)-(E.18) represent the constraints of the natural gas network. The conservation of flow at each node of the natural gas network is represented by Equation (E.13). Equation (E.14) states that the inflow of natural gas at each node at each time step includes the natural gas imported by NGGS and the natural gas processed by the NGPP unit and LNG terminal. Equation (E.15) describes that the natural gas outflow at each node at each time step is the accumulated natural gas consumed by the GTPP and CCPP units in the power network, NGPP unit, LNG terminal, and NGCS units in the natural gas network, and building stock units. Equation (E.16) ensures that the natural gas flow through each pipeline at each time step does not exceed the pipeline's capacity, provided that the pipeline is operational. Equations (E.17)-(E.18) describe the logical relationships between the operating state of the pipeline and the nodes connected to the pipeline.

$$\sum_{(q\in LG\,|\,T(q)=n)} g_t^q \;-\; \sum_{(q\in LG\,|S(q)=n)} g_t^q + G_{G,t}^n \;-\; G_{C,t}^n = 0 \qquad \forall n \in NG, \forall t \in T \qquad (E.13)$$

$$G_{G,t}^n = \; G_{G,t}^{LNGT,n} + \; G_{G,t}^{NGPP,n} + \; G_{G,t}^{NGGS,n} \qquad \forall n \in NG, \forall t \in T \qquad (E.14)$$

$$G_{C,t}^n = G_{C,t}^{GTPP,n} + G_{C,t}^{CCPP,n} + G_{C,t}^{NGPP,n} + G_{C,t}^{LNGT,n} + G_{C,t}^{NGCS,n} + \sum_{(H\in BSU|loc(H)=n)} G_{C,t}^H \qquad \forall n \in NG, \forall t \in T \qquad (E.15)$$

$$0 \;\le g_t^q \le \; z_{G,t}^q \cdot g_{cap}^q \qquad \forall q \in LG, \forall t \in T \qquad (E.16)$$

$$z_{G,t}^q \le \; x_{G,t}^{S(q)} \qquad \forall q \in LG, \forall t \in T \qquad (E.17)$$

$$z_{G,t}^q \le \; x_{G,t}^{T(q)} \qquad \forall q \in LG, \forall t \in T \qquad (E.18)$$

2.7.3. Water network operating constraints

The supply and transmission nodes represent the water supply facilities, water storage tanks, and pump stations in the water system's network flow-based model.

Demand nodes are where water is provided to the consumers, like building stock units. Links are representative of the water pipelines located between different parts of the water network.

Equations (E.19)-(E.24) constitute the constraints of the water network. Equation (E.19) displays the water flow balance equation at each water network node at each time step. Equation (E.20) declares that the inflow of water at each node at each time step equals the amount of water supplied by the WSF and WST units. Equation (E.21) states that the water flow out of each node at each time step consists of the water consumed by the CCPP and building stock units. Equation (E.22) demonstrates that if the pipeline is operational, the water flow at each time step does not exceed the pipeline's capacity. A water pipeline's operating state relies on the nodes' operating state at the end of that pipeline, as shown in Equations (E.23)-(E.24).

$$\sum_{(l \in LW \mid T(l)=j)} w_t^l - \sum_{(l \in LW \mid S(l)=j)} w_t^l + W_{G,t}^j - W_{C,t}^j = 0 \qquad \forall j \in NW, \forall t \in T \qquad (E.19)$$

$$W_{G,t}^j = W_{G,t}^{WSF,j} + W_{G,t}^{WST,j} \qquad \forall j \in NW, \forall t \in T \qquad (E.20)$$

$$W_{C,t}^j = W_{C,t}^{CCPP,j} + \sum_{(H \in BSU \mid loc(H)=j)} W_{C,t}^H \qquad \forall j \in NW, \forall t \in T \qquad (E.21)$$

$$0 \leq w_t^l \leq z_{W,t}^l \cdot w_{cap}^l \qquad \forall l \in LW, \forall t \in T \qquad (E.22)$$

$$z_{W,t}^l \leq x_{W,t}^{S(l)} \qquad \forall l \in LW, \forall t \in T \qquad (E.23)$$

$$z_{W,t}^l \leq x_{W,t}^{T(l)} \qquad \forall l \in LW, \forall t \in T \qquad (E.24)$$

2.7.4. Modeling the interdependencies between the infrastructure systems

In this doctoral research, interdependency between two infrastructure systems refers to two aspects of the relationship between the infrastructure systems. The first aspect is the reliance of an infrastructure system's performance on the service delivery

of another infrastructure system. Taking a water pump station as an example, the functionality of the pump station is dependent on the electric power supplied by the power network. This aspect is modeled by interdependency links coupling two nodes from two infrastructure networks interacting with one another. This interdependency link transfers the service from a node in the supplier infrastructure network to another node in the consumer infrastructure network. In the case of a pump station, the electric power needed for the pump station's functionality is transferred by the interdependency link from the supplier node in the power network to the consumer node in the water network. The supplier node, which delivers service to consumer nodes in other infrastructure networks, often acts as a demand node in its network [80], [86]. The operating state of the interdependency link is considered a binary (0-1) variable [87], [89]. If the supplier node meets the required demand of the consumer node in another network, then the interdependency link will be operational. Otherwise, the service transfer between supplier and consumer nodes through the interdependency link will cease. The inoperability of the interdependency link may lead to the loss of operation in the consumer node’s network.

The second aspect of interdependency considered in this doctoral research is that the recovery process of an infrastructure system may adversely affect the restoration of the facilities in another infrastructure network. For instance, the structural damage to the pump station may be fully restored after an earthquake, but the station is still not functional due to the lack of power supply. Hence, the power network's recovery process can delay the restoration of the pump station in the water network. The constraints described in the following section represent both aspects of the considered interdependency.

2.7.5. Interdependency constraints

This section presents the interdependency constraints of facilities belonging to three types of infrastructure networks: power, natural gas, and water. As for the power network, the interdependency constraints of GTPP, CCPP, PGS, ESS, and BSU are provided. Interdependency constraints are developed for LNGT, NGPP, NGGS, NGCS, and BSU in the natural gas network. Regarding the water network, WSF, WPS, WST, and BSU are considered for interdependency constraints. Equations (E.25)-

(E.27) represent the time delay in starting the recovery process at each node, including the response time needed for the decision-making on the recovery of damaged nodes. For instance, if a node in the power network faces a 5-day delay in providing the prerequisites of the recovery process because of the road closure, this delay may postpone the beginning of the restoration of facilities located at the respective node.

Equations (E.28)-(E.34) state that the performance of a GTPP depends on the availability of the coupled gas node with the electric node where the facility is located, as well as the operation state of the interdependency link between those nodes. Equations (E.35)-(E.45) declare that the operation of a CCPP is dependent on the availability of the coupled gas and water nodes with the electric node where the CCPP is located and the functionality of two interdependency links originating from the connected gas and water nodes. Equations (E.46) and (E.47) represent the constraints concerning the restoration of a PGS. Equations (E.48)-(E.50) represent the interdependency constraints regarding the restoration of an ESS. Equation (E.51) describes that electric power consumed by BSUs located in the service area of an electric node will not exceed their time-dependent demand if the respective electric node is operational.

$$x_{E,t}^{m} \leq \tau_{E,t}^{m} \qquad \forall m \in NE, \forall t \in T \qquad (E.25)$$

$$x_{G,t}^{n} \leq \tau_{G,t}^{n} \qquad \forall n \in NG, \forall t \in T \qquad (E.26)$$

$$x_{W,t}^{j} \leq \tau_{W,t}^{j} \qquad \forall j \in NW, \forall t \in T \qquad (E.27)$$

$$0 \leq E_{G,t}^{GTPP,m} \leq \varphi_{E,t}^{GTPP,m} . S_{E,t}^{GTPP,m} \qquad \forall m \in NE, \forall t \in T \qquad (E.28)$$

$$0 \leq E_{C,t}^{GTPP,m} \leq \varphi_{E,t}^{GTPP,m} . D_{E,t}^{GTPP,m} \qquad \forall m \in NE, \forall t \in T \qquad (E.29)$$

$$0 \leq G_{C,t}^{GTPP,n} \leq \delta_{t}^{GTPP,n} . D_{G,t}^{GTPP,n} \qquad \forall n \in NG, \forall t \in T \qquad (E.30)$$

$$\varphi_{E,t}^{GTPP,m} \leq x_{E,t}^{m} \qquad \forall m \in NE, \forall t \in T \qquad (E.31)$$

$$\delta_{t}^{GTPP,n} \leq x_{G,t}^{n} \qquad \forall n \in NG, \forall t \in T \qquad (E.32)$$

$$G_{C,t}^{GTPP,n} - \theta_{t}^{GTPP,n} . D_{G,t}^{GTPP,n} \geq 0 \qquad \forall n \in NG, \forall t \in T \qquad (E.33)$$

$$\varphi_{E,t}^{GTPP,m} \leq \theta_{t}^{GTPP,n} \qquad \forall (n,m) \in IGtE, \forall t \in T \qquad (E.34)$$

$$0 \le E_{G,t}^{CCPP,m} \le \varphi_{E,t}^{CCPP,m} . S_{E,t}^{CCPP,m} \qquad \forall m \in NE, \forall t \in T \qquad (E.35)$$

$$0 \le E_{C,t}^{CCPP,m} \le \varphi_{E,t}^{CCPP,m} . D_{E,t}^{CCPP,m} \qquad \forall m \in NE, \forall t \in T \qquad (E.36)$$

$$0 \le G_{C,t}^{CCPP,n} \le \delta_t^{CCPP,n} . D_{G,t}^{CCPP,n} \qquad \forall n \in NG, \forall t \in T \qquad (E.37)$$

$$\varphi_{E,t}^{CCPP,m} \le x_{E,t}^{m} \qquad \forall m \in NE, \forall t \in T \qquad (E.38)$$

$$\delta_t^{CCPP,n} \le x_{G,t}^{n} \qquad \forall n \in NG, \forall t \in T \qquad (E.39)$$

$$G_{C,t}^{CCPP,n} - \theta_t^{CCPP,n} . D_{G,t}^{CCPP,n} \ge 0 \qquad \forall n \in NG, \forall t \in T \qquad (E.40)$$

$$\varphi_{E,t}^{CCPP,m} \le \theta_t^{CCPP,n} \qquad \forall (n,m) \in IGtE, \forall t \in T \qquad (E.41)$$

$$0 \le W_{C,t}^{CCPP,j} \le \gamma_t^{CCPP,j} . D_{W,t}^{CCPP,j} \qquad \forall j \in NW, \forall t \in T \qquad (E.42)$$

$$\gamma_t^{CCPP,j} \le x_{W,t}^{j} \qquad \forall j \in NW, \forall t \in T \qquad (E.43)$$

$$W_{C,t}^{CCPP,j} - \sigma_t^{CCPP,j} . D_{W,t}^{CCPP,j} \ge 0 \qquad \forall j \in NW, \forall t \in T \qquad (E.44)$$

$$\varphi_{E,t}^{CCPP,m} \le \sigma_t^{CCPP,j} \qquad \forall (j,m) \in IWtE, \forall t \in T \qquad (E.45)$$

$$0 \le E_{G,t}^{PGS,m} \le \varphi_{E,t}^{PGS,m} . S_{E,t}^{PGS,m} \qquad \forall m \in NE, \forall t \in T \qquad (E.46)$$

$$\varphi_{E,t}^{PGS,m} \le x_{E,t}^{m} \qquad \forall m \in NE, \forall t \in T \qquad (E.47)$$

$$0 \le E_{C,t}^{ESS,m} \le \varphi_{E,t}^{ESS,m} . D_{E,t}^{ESS,m} \qquad \forall m \in NE, \forall t \in T \qquad (E.48)$$

$$\varphi_{E,t}^{ESS,m} \le x_{E,t}^{m} \qquad \forall m \in NE, \forall t \in T \qquad (E.49)$$

$$E_{C,t}^{ESS,m} - x_{E,t}^{m} . D_{E,t}^{ESS,m} \ge 0 \qquad \forall m \in NE, \forall t \in T \qquad (E.50)$$

$$0 \le \sum_{(H \in BSU | loc(H) = m)} E_{C,t}^{H} \le x_{E,t}^{m} . \sum_{(H \in BSU | loc(H) = m)} D_{E,t}^{H} \qquad \forall m \in NE, \forall t \in T \qquad (E.51)$$

Equations (E.52)-(E.58) describe that the operating state of a LNGT relies on the availability of the coupled electric node with the gas node where the LNGT is located and the functionality of the interdependency link between those gas and electric

nodes. Equations (E.59)-(E.65) mean that a NGPP's performance is dependent on the availability of the coupled electric node with the gas node where the NGPP is located and the operation state of the interdependency link between those nodes. Equations (E.66) and (E.67) represent the constraints regarding the restoration of a NGGS. The interdependency constraints related to the NGCS are constituted by Equations (E.68)-(E.74). Equation (E.75) ensures that the amount of natural gas consumed by BSUs located in the service area of a gas node cannot exceed their demand if the respective gas node is operational.

$$0 \leq G_{G,t}^{LNGT,n} \leq \varphi_{G,t}^{LNGT,n} . S_{G,t}^{LNGT,n} \qquad \forall n \in NG, \forall t \in T \qquad (E.52)$$

$$0 \leq G_{C,t}^{LNGT,n} \leq \varphi_{G,t}^{LNGT,n} . D_{G,t}^{LNGT,n} \qquad \forall n \in NG, \forall t \in T \qquad (E.53)$$

$$0 \leq E_{C,t}^{LNGT,m} \leq \pi_{t}^{LNGT,m} . D_{E,t}^{LNGT,m} \qquad \forall m \in NE, \forall t \in T \qquad (E.54)$$

$$\varphi_{G,t}^{LNGT,n} \leq x_{G,t}^{n} \qquad \forall n \in NG, \forall t \in T \qquad (E.55)$$

$$\pi_{t}^{LNGT,m} \leq x_{E,t}^{m} \qquad \forall m \in NE, \forall t \in T \qquad (E.56)$$

$$E_{C,t}^{LNGT,m} - \alpha_{t}^{LNGT,m} . D_{E,t}^{LNGT,m} \geq 0 \qquad \forall m \in NE, \forall t \in T \qquad (E.57)$$

$$\varphi_{G,t}^{LNGT,n} \leq \alpha_{t}^{LNGT,m} \qquad \forall (m,n) \in IEtG, \forall t \in T \qquad (E.58)$$

$$0 \leq G_{G,t}^{NGPP,n} \leq \varphi_{G,t}^{NGPP,n} . S_{G,t}^{NGPP,n} \qquad \forall n \in NG, \forall t \in T \qquad (E.59)$$

$$0 \leq G_{C,t}^{NGPP,n} \leq \varphi_{G,t}^{NGPP,n} . D_{G,t}^{NGPP,n} \qquad \forall n \in NG, \forall t \in T \qquad (E.60)$$

$$0 \leq E_{C,t}^{NGPP,m} \leq \pi_{t}^{NGPP,m} . D_{E,t}^{NGPP,m} \qquad \forall m \in NE, \forall t \in T \qquad (E.61)$$

$$\varphi_{G,t}^{NGPP,n} \leq x_{G,t}^{n} \qquad \forall n \in NG, \forall t \in T \qquad (E.62)$$

$$\pi_{t}^{NGPP,m} \leq x_{E,t}^{m} \qquad \forall m \in NE, \forall t \in T \qquad (E.63)$$

$$E_{C,t}^{NGPP,m} - \alpha_{t}^{NGPP,m} . D_{E,t}^{NGPP,m} \geq 0 \qquad \forall m \in NE, \forall t \in T \qquad (E.64)$$

$$\varphi_{G,t}^{NGPP,n} \leq \alpha_{t}^{NGPP,m} \qquad \forall (m,n) \in IEtG, \forall t \in T \qquad (E.65)$$

$$0 \leq G_{G,t}^{NGGS,n} \leq \varphi_{G,t}^{NGGS,n} . S_{G,t}^{NGGS,n} \qquad \forall n \in NG, \forall t \in T \qquad (E.66)$$

$$\varphi_{G,t}^{NGGS,n} \leq x_{G,t}^{n} \qquad \forall n \in NG, \forall t \in T \qquad (E.67)$$

$$0 \le G_{C,t}^{NGCS,n} \le \varphi_{G,t}^{NGCS,n} . D_{G,t}^{NGCS,n} \qquad \forall n \in NG, \forall t \in T \qquad (E.68)$$

$$\varphi_{G,t}^{NGCS,n} \le x_{G,t}^{n} \qquad \forall n \in NG, \forall t \in T \qquad (E.69)$$

$$G_{C,t}^{NGCS,n} - x_{G,t}^{n} . D_{G,t}^{NGCS,n} \ge 0 \qquad \forall n \in NG, \forall t \in T \qquad (E.70)$$

$$0 \le E_{C,t}^{NGCS,m} \le \pi_{t}^{NGCS,m} . D_{E,t}^{NGCS,m} \qquad \forall m \in NE, \forall t \in T \qquad (E.71)$$

$$\pi_{t}^{NGCS,m} \le x_{E,t}^{m} \qquad \forall m \in NE, \forall t \in T \qquad (E.72)$$

$$E_{C,t}^{NGCS,m} - \alpha_{t}^{NGCS,m} . D_{E,t}^{NGCS,m} \ge 0 \qquad \forall m \in NE, \forall t \in T \qquad (E.73)$$

$$\varphi_{G,t}^{NGCS,n} \le \alpha_{t}^{NGCS,m} \qquad \forall (m,n) \in IEtG, \forall t \in T \qquad (E.74)$$

$$0 \le \sum_{(H \in BSU | loc(H) = n)} G_{C,t}^{H} \le x_{G,t}^{n} . \sum_{(H \in BSU | loc(H) = n)} D_{G,t}^{H} \qquad \forall n \in NG, \forall t \in T \qquad (E.75)$$

Equations (E.76)-(E.81) represent that the restoration of a WSF depends on the availability of the coupled electric node with the water node where the facility is located and the operating state of the interdependency link between those water and electric nodes. Equations (E.82)-(E.86) display that the recovery of a WPS relies on the availability of the coupled electric node with the water node where the WPS is located and the operation state of the interdependency link between those nodes. Equations (E.87) and (E.88) represent the constraints concerning the restoration of a WST. Equation (E.89) reveals that if a water node is operational, the amount of water consumed by BSUs in that water node's service area cannot exceed their demand.

$$0 \le W_{G,t}^{WSF,j} \le \varphi_{W,t}^{WSF,j} . S_{W,t}^{WSF,j} \qquad \forall j \in NW, \forall t \in T \qquad (E.76)$$

$$0 \le E_{C,t}^{WSF,m} \le \pi_{t}^{WSF,m} . D_{E,t}^{WSF,m} \qquad \forall m \in NE, \forall t \in T \qquad (E.77)$$

$$\varphi_{W,t}^{WSF,j} \le x_{W,t}^{j} \qquad \forall j \in NW, \forall t \in T \qquad (E.78)$$

$$\pi_{t}^{WSF,m} \le x_{E,t}^{m} \qquad \forall m \in NE, \forall t \in T \qquad (E.79)$$

$$E_{C,t}^{WSF,m} - \beta_{t}^{WSF,m} . D_{E,t}^{WSF,m} \ge 0 \qquad \forall m \in NE, \forall t \in T \qquad (E.80)$$

$$\varphi_{W,t}^{WSF,j} \leq \beta_t^{WSF,m} \qquad \forall (m,j) \in IEtW, \forall t \in T \qquad (E.81)$$

$$\varphi_{W,t}^{WPS,j} \leq x_{W,t}^{j} \qquad \forall j \in NW, \forall t \in T \qquad (E.82)$$

$$0 \leq E_{C,t}^{WPS,m} \leq \pi_t^{WPS,m} . D_{E,t}^{WPS,m} \qquad \forall m \in NE, \forall t \in T \qquad (E.83)$$

$$\pi_t^{WPS,m} \leq x_{E,t}^{m} \qquad \forall m \in NE, \forall t \in T \qquad (E.84)$$

$$E_{C,t}^{WPS,m} - \beta_t^{WPS,m} . D_{E,t}^{WPS,m} \geq 0 \qquad \forall m \in NE, \forall t \in T \qquad (E.85)$$

$$\varphi_{W,t}^{WPS,j} \leq \beta_t^{WPS,m} \qquad \forall (m,j) \in IEtW, \forall t \in T \qquad (E.86)$$

$$0 \leq W_{G,t}^{WST,j} \leq \varphi_{W,t}^{WST,j} . S_{W,t}^{WST,j} \qquad \forall j \in NW, \forall t \in T \qquad (E.87)$$

$$\varphi_{W,t}^{WST,j} \leq x_{W,t}^{j} \qquad \forall j \in NW, \forall t \in T \qquad (E.88)$$

$$0 \leq \sum_{(H \in BSU | loc(H) = j)} W_{C,t}^{H} \leq x_{W,t}^{j} . \sum_{(H \in BSU | loc(H) = j)} D_{W,t}^{H} \qquad \forall j \in NW, \forall t \in T \qquad (E.89)$$

Equations (E.90)-(E.92) state that the links in different infrastructure networks (i.e., power lines, pipelines) can convey flow if they are not damaged. In other words, full recovery is a necessary condition for links to be operational in the network.

$$z_{E,t}^{p} \leq \mu_{E,t}^{p} \qquad \forall p \in LE, \forall t \in T \qquad (E.90)$$

$$z_{G,t}^{q} \leq \mu_{G,t}^{q} \qquad \forall q \in LG, \forall t \in T \qquad (E.91)$$

$$z_{W,t}^{l} \leq \mu_{W,t}^{l} \qquad \forall l \in LW, \forall t \in T \qquad (E.92)$$

2.8. Implementation of the ResQ-IOS framework

This section aims to explain how the ResQ-IOS framework implements the resilience assessment of interdependent infrastructure systems. Since many parameters and factors influence an urban community's recovery after the occurrence of extreme events, the resilience analysis of interdependent infrastructure systems is a complex issue. For this reason, considering assumptions and simplifications in

resilience quantification is inevitable to reduce the complexity of the problem. The existence of uncertainties in evaluating the disaster resilience of an urban community is the main challenge. The uncertainties in the process of resilience assessment can be grouped into the following categories:

- uncertainties in the characteristics of the extreme event
- uncertainties in the damage functions
- uncertainties in the restoration functions
- uncertainties in the available budget and recovery resources

The flowchart, shown in Fig. 2.6, describes the process by which the ResQ-IOS framework evaluates the resilience of an urban community after a disaster. To capture the uncertainties in the characteristics of the natural hazard, ResQ-IOS allows the user to implement the resilience assessment process for either one scenario or many natural hazard scenarios. For instance, to take into account the uncertainties in the occurrence of the earthquake hazard, the resilience assessment can be performed for several seismic hazard scenarios with varying return periods and epicenters in the case study. According to Fig. 2.6, to carry out a probabilistic resilience analysis for an urban community with many disruption scenarios, ResQ-IOS follows the route from A to B in the flowchart. Fig. 2.7 displays the flowchart of the route from A to B. In this part, the user can specify the characteristics of the natural hazard, such as type, severity, damage, and proximity. Based on these characteristics of the natural hazard, a disruption scenario is generated. This procedure can be repeated for the desired number of disruption scenarios.

The ResQ-IOS framework assumes that all components of the considered infrastructure systems may be damaged during the disaster. This framework can apply both deterministic and probabilistic approaches to estimating the damage state of the infrastructure systems' components and produce different damage states for the same disruption scenario. This ability allows ResQ-IOS to capture the uncertainties in the damage functions of components. In the ResQ-IOS framework, the required time for restoring the failed components depends on the failed component's damage state, which is a function of the characteristics of the hazard. Therefore, restoring damaged components may take several time steps in the resilience assessment period.

To consider the uncertainties in restoring failed components, ResQ-IOS follows the route from C to D in the flowchart (Fig. 2.8). The recovery model developed for the ResQ-IOS framework can apply different restoration functions to the damaged infrastructure components. Besides binary and linear restoration functions, the recovery model can implement nonlinear restoration functions. A nonlinear restoration model considers different repair rates throughout the recovery process, which is made possible by the Iterative Optimization-based Simulation framework of the ResQ-IOS. Therefore, the user can select the proper recovery model for each type of infrastructure component in the resilience assessment process. Also, the ResQ-IOS framework can rate the functionality level of the components continuously by using a fuzzy logic-based model.

Both deterministic and probabilistic approaches can be applied to the repair rates for restoring the damaged components to capture the uncertainties in the restoration of infrastructure components. The last category of uncertainties in the resilience assessment is related to the available budget and recovery resources like repair teams. To quantify this type of uncertainty, the ResQ-IOS framework can be implemented at different levels of recovery resource availability. It is noteworthy that considering many hazard scenarios and availability levels of recovery resources simultaneously for the resilience analysis of an urban community leads to a substantial computational burden.

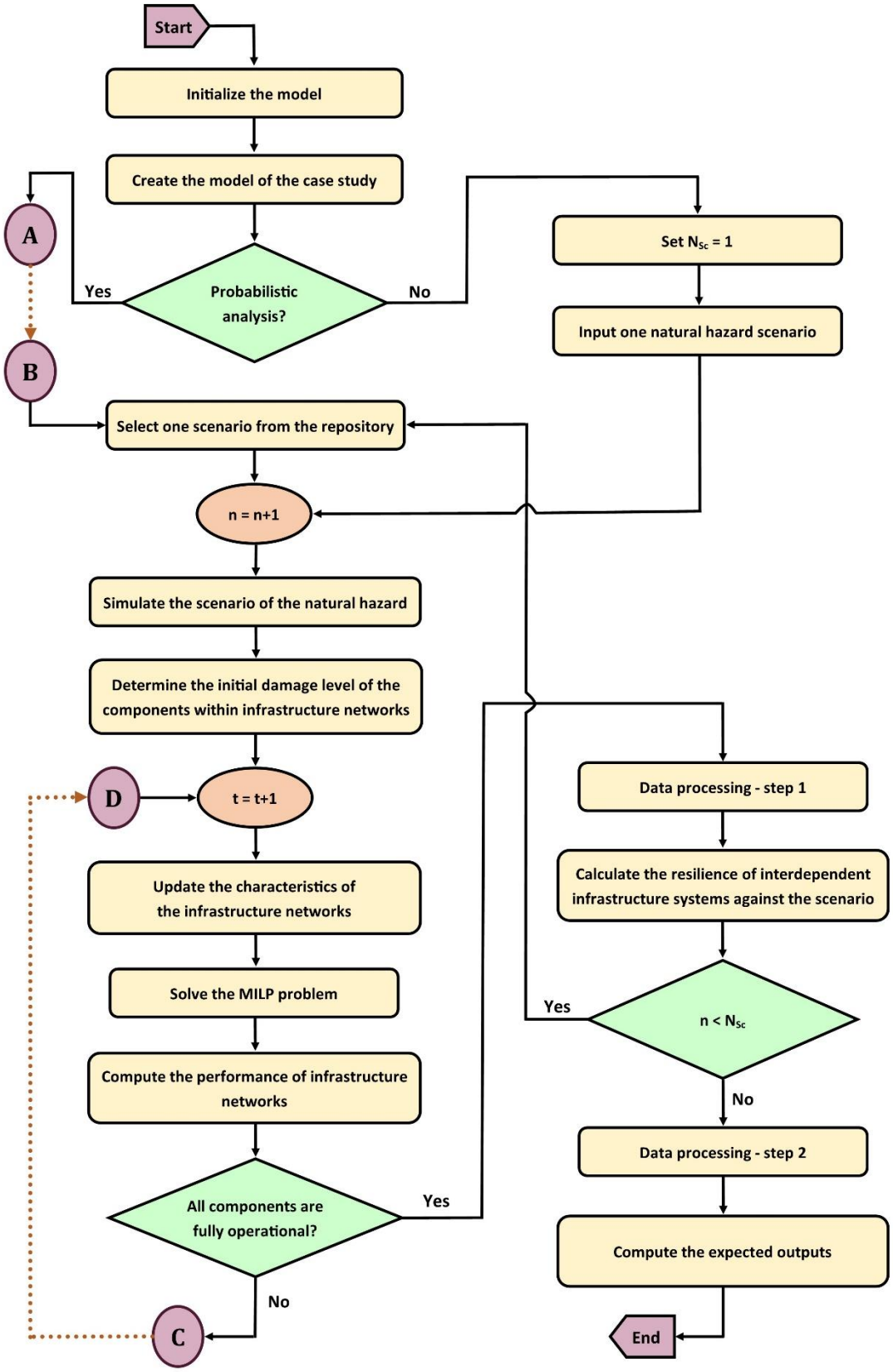

Fig. 2.6. The implementation flowchart of the ResQ-IOS framework.

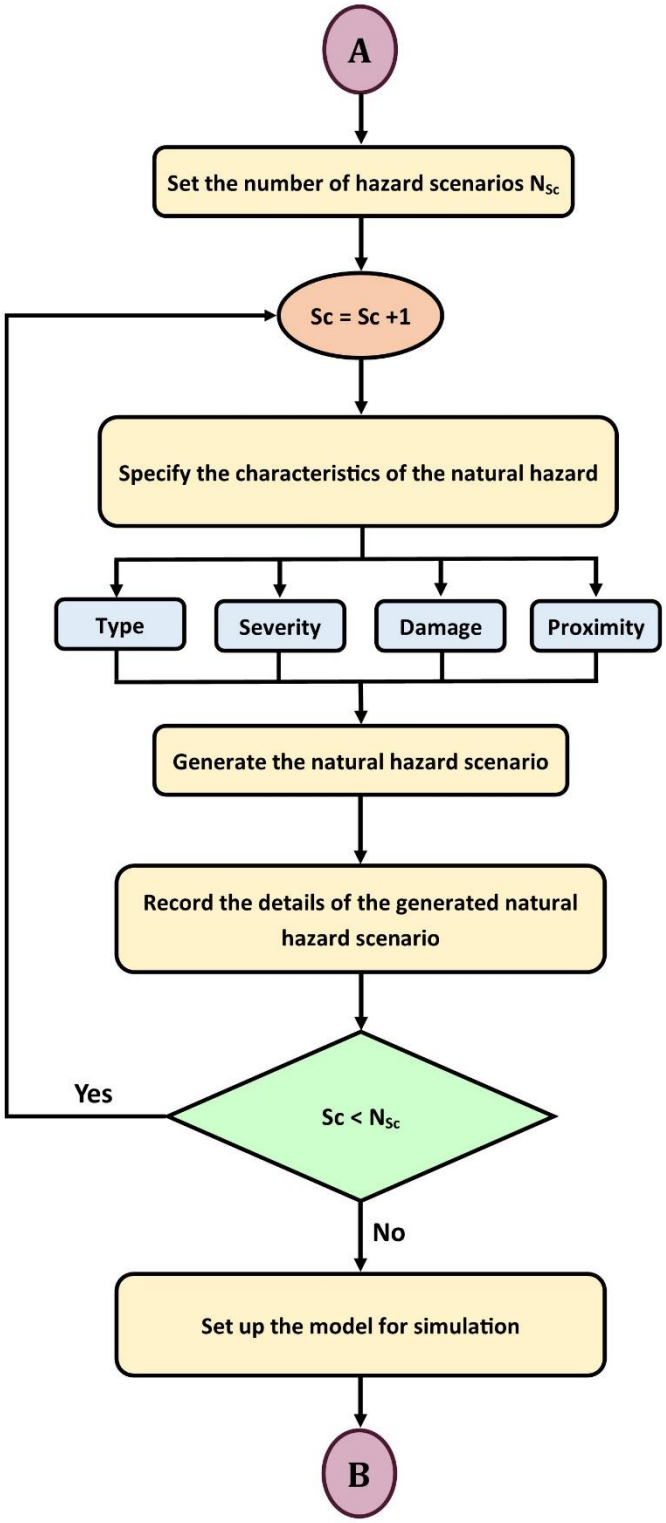

Fig. 2.7. The flowchart of hazard scenario generation in the ResQ-IOS framework.

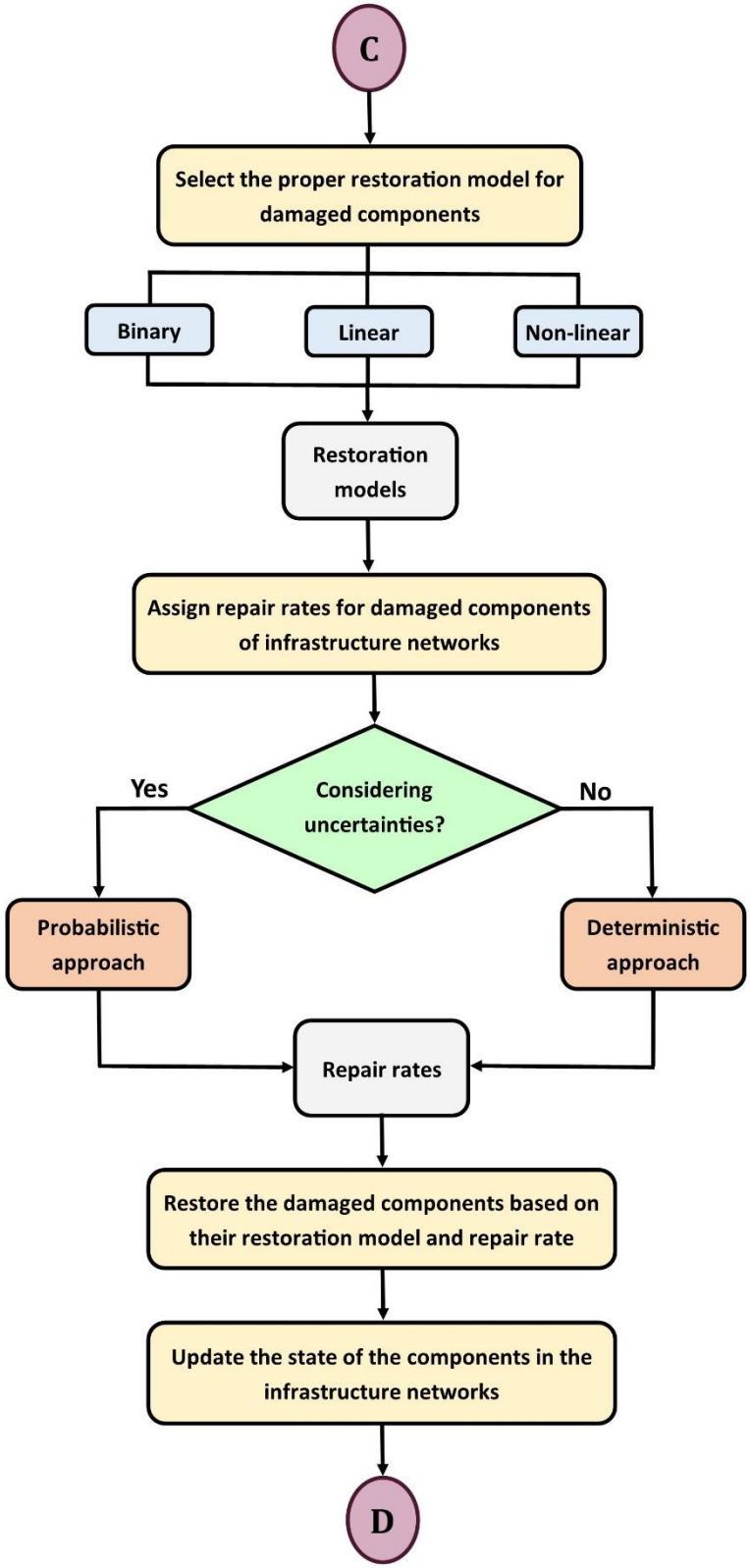

Fig. 2.8. The flowchart of restoration process in the ResQ-IOS framework.

2.9. Conclusion

In this chapter, the advantages of using the hybrid Optimization-Simulation (OS) approach for modeling complex and stochastic large-scale systems such as interdependent infrastructure networks were discussed. Due to the benefits of the OS approach, ResQ-IOS, an Iterative Optimization-based Simulation framework, was developed for quantifying and optimizing the disaster resilience of interdependent CISs. After outlining the ResQ-IOS's structure, a resilience metric was formulated to measure the joint accumulated loss of resilience for a system of interdependent critical infrastructure systems. This chapter provided the mathematical model of interdependent CISs' performance and formulated the Mixed-Integer Linear Programming (MILP) problem of the optimization model. Also, the constraints of the MILP problem for the power, natural gas, and water networks, including interdependencies between those networks, were presented in detail. To demonstrate the capabilities of the developed ResQ-IOS framework, the disaster resilience of an urban community in the USA will be quantified and analyzed in the next chapter.

Chapter Three

Application of the ResQ-IOS: Urban Community Resilience Assessment

This chapter evaluates the seismic resilience of a realistic example of Shelby County (TN), USA, to demonstrate the capabilities of the ResQ-IOS, the Resilience Quantification Iterative Optimization-based Simulation Framework developed in Chapter 2. In addition to performing the parametric analysis of urban disaster resilience in this chapter, implementing different Community Resilience Enhancement Strategies (CRESs) is investigated, and accordingly, the optimal recovery strategies for minimizing total recovery cost are identified. Some material from this chapter is published in the following paper:

- Hamed Hafeznia and Božidar Stojadinović. "ResQ-IOS: An iterative optimization-based simulation framework for quantifying the resilience of interdependent critical infrastructure systems to natural hazards," *Applied Energy*, vol. 349, p. 121558, Nov. 2023, doi: 10.1016/j.apenergy.2023.121558.

3.1. Case Study: A realistic example of Shelby County, USA

To conduct the resilience analysis of urban communities against natural hazards, ResQ-IOS was coded in the MATLAB [90] software environment using the YALMIP toolbox [91]. The IBM CPLEX solver [92] is utilized to solve the MILP problem of the optimization model. The dissertation's objectives, addressed in this Chapter and stated earlier in Chapter 1 (Objectives No. 3 and 4), are as follows:

- Integrate optimization into the simulation-based methodology of the resilience assessment framework to benefit from simultaneous resilience quantification and improvement.
- Model and conduct the feasibility study of implementing Community Resilience Enhancement Strategies (CRESs).

As discussed in Section 2.8, the ResQ-IOS can conduct the resilience assessment process for either one natural hazard scenario or multiple hazard scenarios to capture the uncertainties in quantifying the resilience of an urban community. For example, the resilience of an urban community to earthquakes can be evaluated by considering multiple seismic events with varying return periods and epicenters. This ability of the ResQ-IOS enables the stakeholders to consider the uncertainties of the seismic hazards in the decision-making process to enhance the resilience of their urban community. The initial sections of this chapter appraise the seismic resilience of a case study against one seismic hazard scenario. Then, in the parametric analyses section of this chapter, multiple earthquake intensities are considered to highlight the uncertainties in the resilience assessment process for decision-making to improve urban disaster resilience. In this research, the probabilistic implications of seismic hazard scenarios on decision-making were not considered.

Shelby County, located in Tennessee (TN), USA, is selected to demonstrate the ResQ-IOS framework proposed in this doctoral dissertation. The power, natural gas, and water networks of Shelby County can be considered realistic examples for the resilience assessment of interdependent infrastructure networks. The data on Shelby County's power, natural gas, and water networks, including the topology, demand, supply capacity, and interdependencies between the infrastructure networks, is obtained from [93], [94]. However, some missing data, particularly for the natural gas network, was reasonably assumed. For better understanding, the nodal demands are

normalized to the total demand of the respective infrastructure network. This normalization applies to the nodal supply capacities as well.

In this doctoral dissertation, a slightly modified version of Shelby County's infrastructure networks is employed to demonstrate the capabilities of the ResQ-IOS framework for quantifying the resilience of interdependent CISs. For instance, there is no power plant in Shelby County. To resolve such a problem, a node in the power network containing a Power Gate Station (PGS) is replaced with a Combined-Cycle Power Plant (CCPP) such that the power generation capacity of the CCPP is equal to the amount of electrical power imported into Shelby County by the PGS. This assumption is made to avoid changing the actual flow pattern in the network. Subsequently, this modification creates more interdependencies between the gas, power, and water networks.

The interdependency relations between infrastructure networks in Shelby County are illustrated in Fig. 3.1. This figure demonstrates how different sectors of the power, gas, and water networks are interconnected. Two bi-directional interdependency relations exist: one between the power generation and natural gas production sectors and another between the power generation and water supply sectors. Also, this figure shows that the operability of the water and natural gas transmission sectors relies on the proper functioning of the power transmission grid. For instance, the production capacity of the natural gas network can be affected adversely by natural hazards like an earthquake. This reduction in natural gas supply capacity can curtail the electricity generation capacity and, subsequently, influence the power supply to the transmission and supply components of the water network. Thus, a disruption in the natural gas network can reduce water service delivery to consumers, whereas there is no direct interdependency relation between the natural gas and water networks, according to Fig. 3.1.

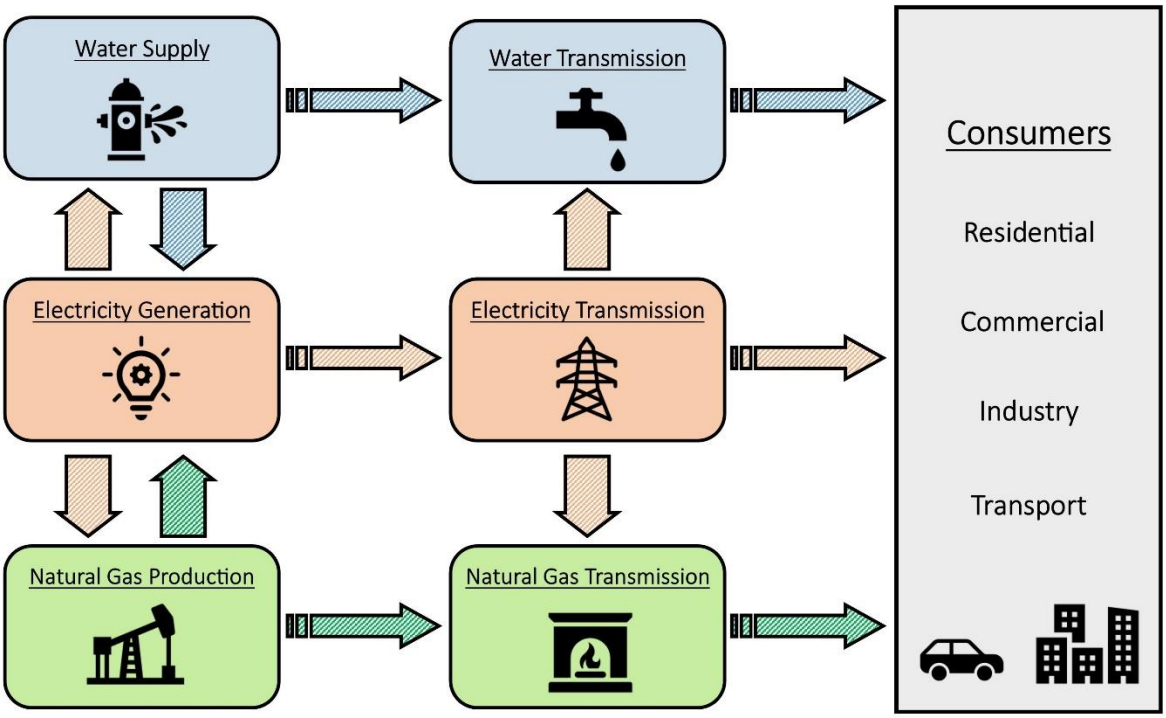

Fig. 3.1. The interdependency relations between infrastructure networks in the case study.

Figure 3.2 displays the topologies of Shelby County's infrastructure networks at the transmission level. The power, natural gas, and water networks are depicted in red, green, and blue colors, respectively. The modified power network comprises 73 powerlines and 59 electric nodes: one Combined-Cycle Power Plant (CCPP), two Gas Turbine Power Plants (GTPPs), 5 Power Gate Stations (PGSs), seventeen 23-kV Electric Substations (ESSs), twenty 12-kV ESSs, and 14 power intersections. The modified natural gas network contains 17 pipelines and 16 gas nodes: one Liquefied Natural Gas Terminal (LNGT), one Natural Gas Processing Plant (NGPP), two Natural Gas Compressor Stations (NGCSs), one Natural Gas Gate Station (NGGS), and 11 regular distribution stations. The modified water infrastructure network consists of 49 water nodes and 71 pipelines. There are 6 Water Storage Tanks (WSTs), 4 Water Pump Stations (WPSs), and 5 Water Supply Facilities (WSFs). The remaining nodes are water intersections that deliver water to the end users. In this dissertation, it is assumed that all nodes and links within Shelby County's infrastructure networks are subject to the destructive impacts of the considered natural hazard.

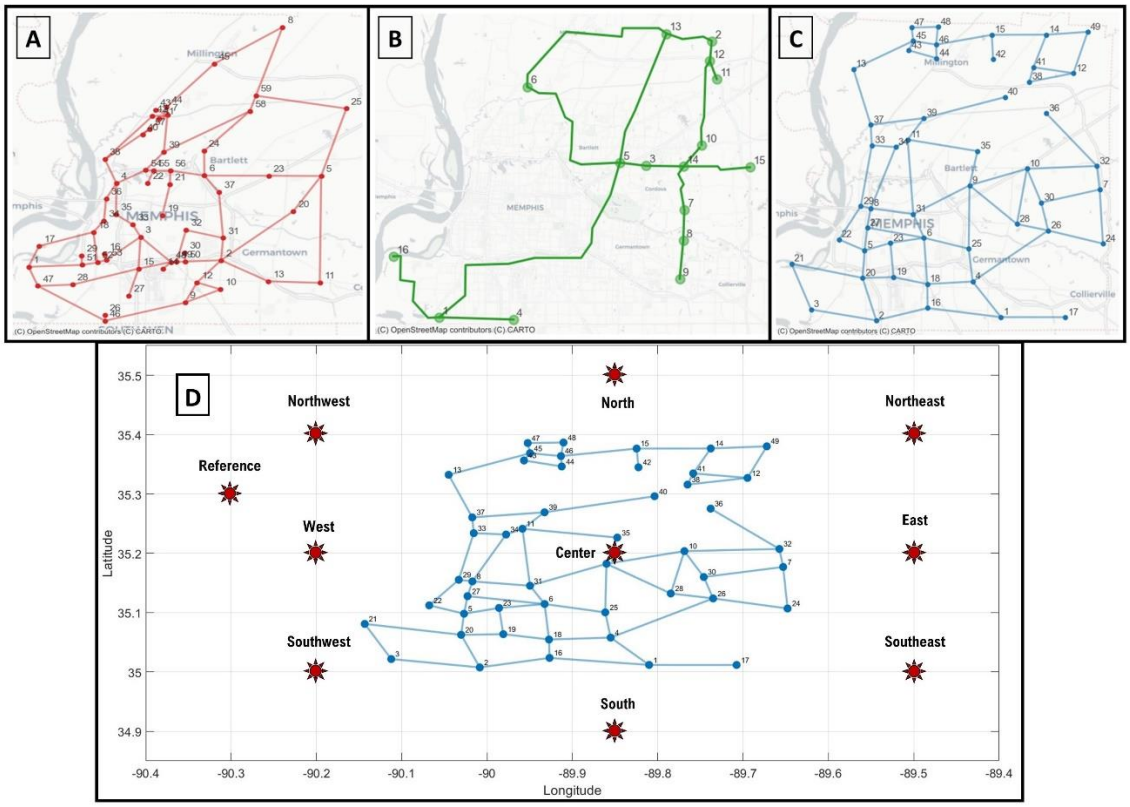

Fig. 3.2. Topologies of the (A) power, (B) natural gas, (C) water infrastructure networks in Shelby County (TN), USA (Map tiles by CARTO, under CC-BY 4.0), and (D) epicenter locations of earthquake scenarios defined in this dissertation (background: water network).

3.2. Urban Community Resilience Analysis of Shelby County

To demonstrate the capabilities of the ResQ-IOS framework to model the interdependency between the infrastructure systems and evaluate the resilience of those interdependent systems against disasters, the seismic resilience of the interdependent CISs located in Shelby County (TN), USA is quantified. The data relating to damage functions, functionality levels, and the details of the recovery process for the CISs' components (e.g., the required time for restoring a component) is obtained from Section 8.1 for potable water systems, Section 8.4 for natural gas systems, and Section 8.5 for electric power systems of the HAZUS Earthquake Model Technical Manual (HAZUS 5.1) published by the Federal Emergency Management Agency (FEMA) in July 2022 [77].

To show the performance evolution of infrastructure networks (power, natural gas, and water) after a disaster, a hazard scenario is defined similarly to the realistic earthquake scenario in Shelby County provided by [95]. The hazard scenario simulates an earthquake with a magnitude of Mw = 7.7 and an epicenter located at 35.3 N and 90.3 W (situated in the northwest of Shelby County – the epicenter location labeled as *Reference,* shown in Fig. 3.2). Ground motion intensity measures at the infrastructure components' location are estimated using attenuation models that are the function of the earthquake magnitude and the epicenter location. The performance evolution of the Shelby County infrastructure networks after this earthquake scenario is shown in Fig. 3.3. This figure displays the changes in the actual performance of power, natural gas, and water networks considering the hazard occurs on day 0, and the recovery process starts on day 1.

To calculate the resilience metric defined by Equation (E.2) (i.e., accumulated loss of resilience), the area between the target and the actual performance of each network is computed according to Fig. 2.4. The Accumulated Loss of Resilience (ALR) metrics for the power, natural gas, and water CISs are 9.47, 12.32, and 15.37 days, respectively. For a better understanding of ALR, we can interpret the ALR of an infrastructure network as the equivalent number of days that the infrastructure network of interest is completely shut down (i.e., the met demand is zero). For instance, the ALR of the power network is 9.47 days, meaning total unmet demand during the recovery process that takes 54 days to complete equals 9.47 days with zero power supply. The minimum instantaneous performance of the power system $P^i(t)$ (the ratio of consumption to demand) was 17.3 percent of the daily demand in this earthquake scenario.

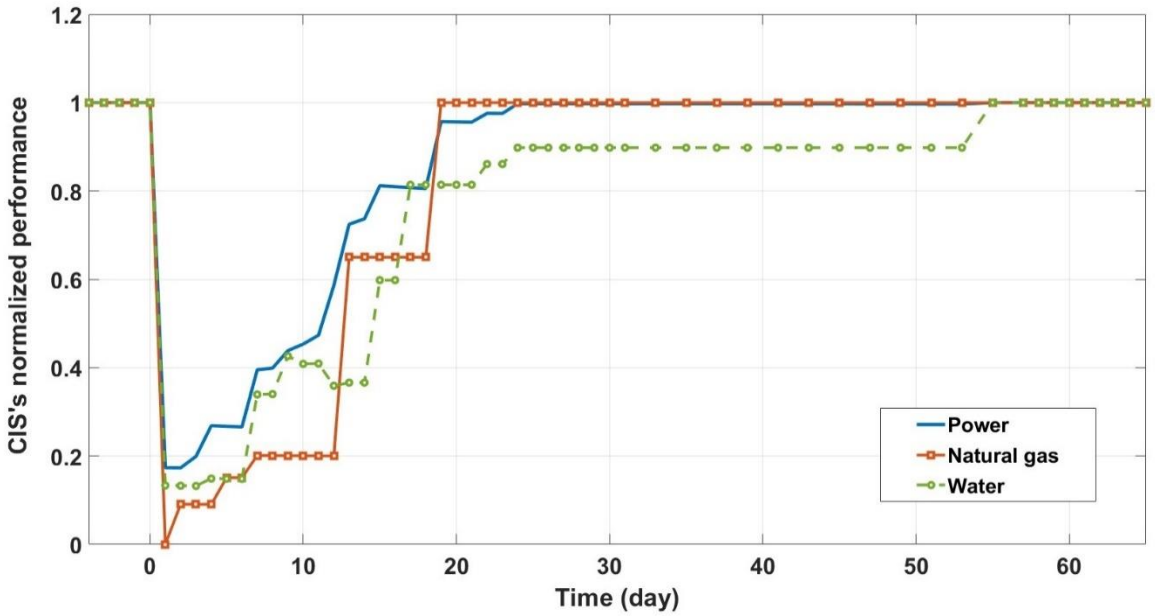

Fig. 3.3. The normalized performance evolution of the Shelby County CISs in the investigated earthquake scenario (M_w=7.7).

It is noteworthy that the ALR determines the amount of unmet demand during the recovery process of an infrastructure network after the disaster. Still, this ALR resilience metric does not specify the speed of the recovery process. In other words, an infrastructure network with a lower ALR value may have a more extended recovery period; for example, the case study (Fig. 3.3) reveals that the ALR for the natural gas network (12.32) is higher than power network (9.47), while the function recovery of the natural gas network is completed in 18 days, 36 days sooner than the power network's recovery period (54 days). Although the natural gas network holds the fastest rate in the recovery process, this network is the only infrastructure network in the case study that totally failed for a short period (one day), as shown in Fig. 3.3.

According to the results of resilience quantification, the water network has the highest ALR among the three Shelby County CISs; however, the water network is not the last infrastructure system recovered from earthquake-induced failures. Figure 3.4 indicates the daily percentage of partially and fully damaged nodes in the CISs' networks in Shelby County during the recovery process after the earthquake. According to Fig. 3.4, the restoration of the water network's components has been completed in 12 days, almost 4.5 times faster than that of the power network. Despite the relatively fast restoration of the damaged components in the water network, the

resilience indicator for the water network cannot approach value of one earlier than the 54th day of the recovery process. The main reason for such post-disaster recovery of the water network is the interdependency between the power and water networks.

Due to the slower recovery rate of the power network, the operability of some components in the water network, such as water pump stations, is conditioned on the functionality level of the power network's elements, like substations and power lines. Namely, the constant part of the water network's resilience curve between the 23rd day and 52nd day of the recovery process in Fig. 3.3 (the recovery process starts on day 1) is due to the water pump station located at node 11 being out of service during the period mentioned above even though its earthquake-induced damage is fully restored and the water pipelines connected to the pump station are ready to operate. The reason for the inoperability of this water pump station is the lack of power supply delivered by the connected 12-kV electric substation due to ongoing components' restoration in the power network.

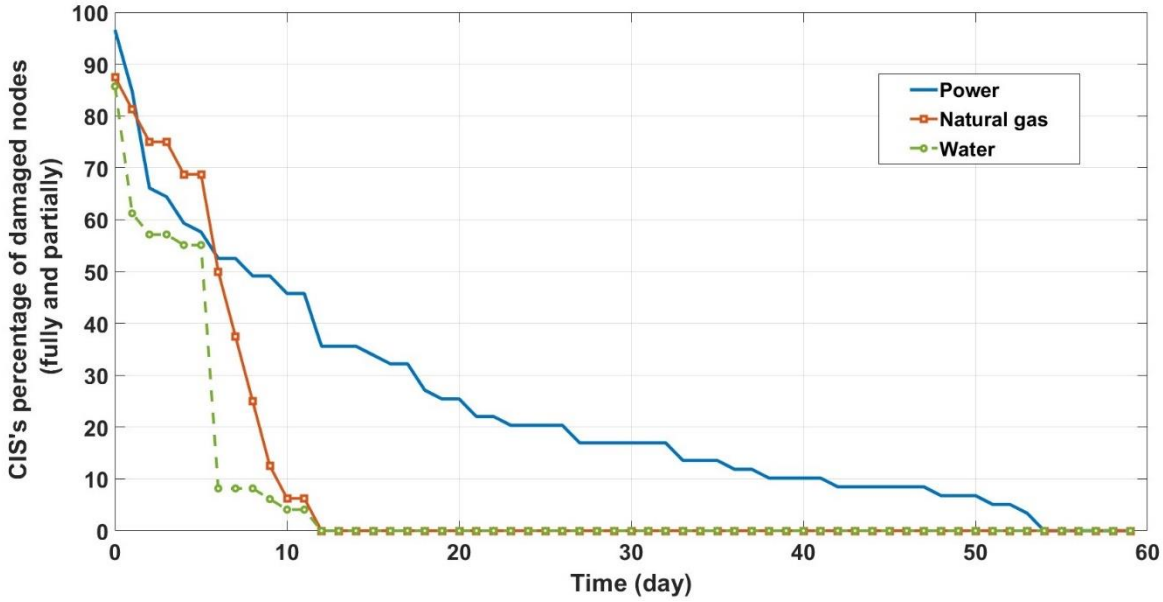

Fig. 3.4. The daily percentage of partially and fully damaged nodes in the Shelby County CISs during the recovery process after the investigated earthquake scenario (M_w=7.7).

It is important to note that the damage recovery of the natural gas network (i.e., the restoration of direct earthquake-induced damage to the natural gas network) is completed in 12 days, according to Fig. 3.4, whereas the function recovery of the natural gas network is completed in 18 days according to Fig. 3.3. The main reason

for this 6-day delay in the function recovery of the gas network is the interdependency between the power and natural gas networks. In other words, the natural gas network cannot reach full production capacity after the 12th day because of insufficient power supply by the electricity grid.

Figure 3.4 also provides some information concerning the robustness of the individual CISs in the case study. According to this figure, the power network has the lowest robustness to the earthquake scenario since 96.6 percent of its nodes are partially or fully damaged on the first day after the occurrence of the earthquake. In contrast, the water network is the most robust infrastructure network in Shelby County after the earthquake. In Fig. 3.4, the slope of the curve indicates the instantaneous (daily) rate of damage recovery (i.e., the restoration of direct earthquake-induced damage) for the concerned infrastructure network in Shelby County. It is noteworthy that changes in some parameters, such as the characteristics of the earthquake scenario, the restoration sequence of failed components, and the availability of repair teams, can affect the results of the resilience analysis presented above. If the restoration functions other than those in Sections 8.1, 8.4, and 8.5 of the HAZUS Earthquake Model Technical Manual (HAZUS 5.1) [77] are considered, the outcome may change. For instance, a reduction in the number of repair teams in the water network may cause a delay in the restoration of water pipelines, or a change in the magnitude and epicenter of the earthquake may increase the number of damaged water pipelines. Therefore, the faster recovery of the water network compared to the power network in this example should not be concluded as a general feature of the water network in Shelby County.

The ResQ-IOS framework enables the evaluation of the functional recovery metrics proposed in the NIST SP-1190 report [57] to quantify the function restoration time aspect of the recovery process. Table 3.1 shows the required time to restore the different percentages of interdependent CISs' services in the case study.

Table 3.1. The required time to restore the different percentages of the Shelby County interdependent CISs' services.

Required time (days)		Percentage of service recovery			
		30%	60%	90%	100%
Network	Power	7	13	19	54
	Natural gas	13	13	18	18
	Water	7	16	54	54

To evaluate the resilience of an urban community against natural hazards, it is essential to jointly quantify the resilience of the community's interdependent CISs. The SoCIS-ALR metric for the system-of-CISs in this Shelby Count case study is calculated using Equation (E.3). Figure 3.5 depicts the evolution of the SoCIS resilience metric for three earthquake scenarios with magnitudes 6.8, 7.7, and 8.2 and the same epicenter. The computed SoCIS-ALR values for the three earthquakes are 4.40, 12.36, and 18.53, while the recovery period for the community, starting from day 1, lasts 20, 54, and 62 days, respectively, as shown in Fig. 3.5.

This figure demonstrates the capability of the ResQ-IOS to consider all components of interdependent CISs for community resilience assessment. The capability to carry out individual resilience assessments for each infrastructure system and joint assessments for the urban community using instantaneous and cumulative resilience metrics reflects other contributions of this doctoral dissertation.

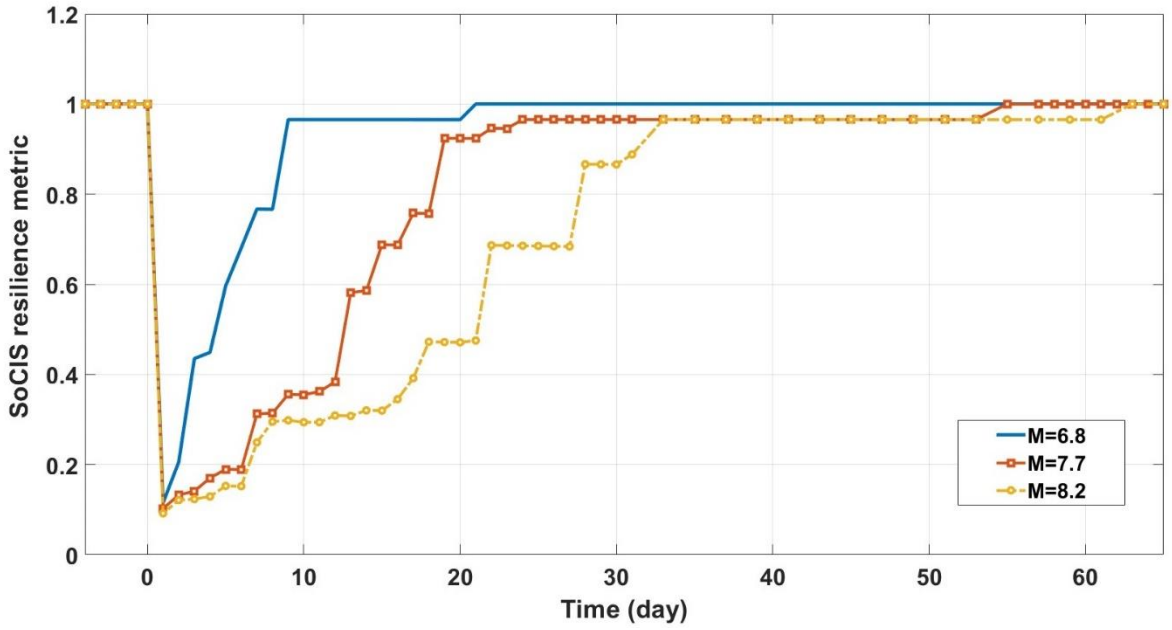

Fig. 3.5. The evolution of the SoCIS resilience metric of the Shelby County CISs for three earthquake scenarios.

3.3. Improving Urban Disaster Resilience of Shelby County

This section examines three Community Resilience Enhancement Strategies (CRESs). The aim of each CRES is to improve one resilience evaluation indicator or two for the urban community of Shelby County as the case study of this dissertation. The first, pre-disaster, CRES aims to address robustness and redundancy indicators through actions taken before an extreme event. The second, post-disaster, CRE strategy addresses the recovery process after the extreme event to increase its resourcefulness and rapidity and provide better allocation of constrained resources. The third, peri-disaster, CRE strategy indirectly addresses the rapidity indicator by aiming to mitigate the interdependencies among the CISs through emergency interventions during the recovery.

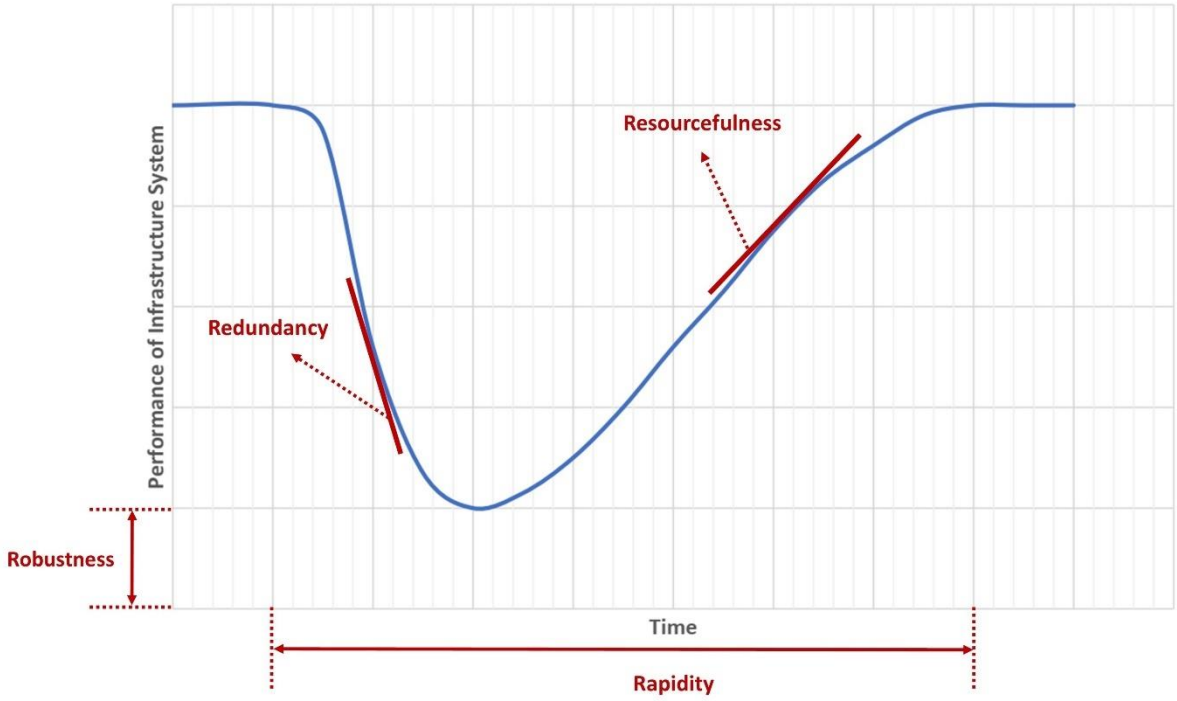

Fig. 3.6. The performance evolution of an infrastructure system after an extreme event and four respective resilience evaluation indices.

3.3.1. Enhancing Robustness and Redundancy

The first, pre-disaster, CRES aims to improve the redundancy and robustness indicators of the individual CIS. In the Shelby County case study, this CRES provides extra supply capacity margins for the interdependent CISs. The effect of this CRES is two-fold: primarily, it increases the robustness of each CIS, while secondarily, it increases the redundancy of the linkages among the interdependent CISs. Three scenarios are devised to determine whether adding extra supply capacity to the infrastructure networks significantly impacts the seismic resilience of the Shelby County system-of-CISs. Those three scenarios consider a 10% increment in the supply capacity of each of the power, natural gas, and water networks, respectively, while keeping the supply capacity of the other two networks unchanged. The results of the resilience analyses for these scenarios are given in Table 3.2.

Table 3.2. The fully functional recovery duration and SoCIS-ALR metric values for the Shelby County interdependent CISs after the earthquake with M_w= 7.7 with varying supply margins.

Scenario	SoCIS-ALR	% Changes wrt. the initial case	Recovery duration (days)	% Changes wrt. the initial case
Initial case	12.36	---	54	---
+10% in the supply capacity of the power network	12.22	1.133 %	54	0 %
+10% in the supply capacity of the natural gas network	12.20	1.295 %	54	0 %
+10% in the supply capacity of the water network	10.92	11.65 %	24	55.5 %

While the 10% increase in the supply capacity of the power grid and natural gas network improves the Shelby County SoCIS-ALR metric slightly, a 10% percent increment in the water network's supply capacity significantly shortens the time to fully recover the function of all three Shelby County CISs. It is important to note that after the community returns to normal conditions on the 24th day of the recovery process, restoring the failed components in the power network will continue until the 54th day. Also, the water pump station at node 11 is still out of service after the 24th day due to the lack of power supply. Nevertheless, the water network provides water to meet the nodal demands previously supplied by the water pump station located at node 11 because of the increased capacity of other water supply facilities that can compensate for the inoperability of the pump station at node 11. The network distributes the water flow by optimally mapping new routes from the supply nodes to the demand nodes, dependent on the pump station at node 11.

Concerning the performance of the power network, since the power supply of the pump station at node 11 is no longer a top priority demand, the ResQ-IOS optimization module re-dispatches the power supply to other nodes with higher priority. On the 24th day, the power network can supply the total demand, except for the pump station at node 11. This reflects that the ResQ-IOS can rebalance the components' time-dependent demands and temporary loads that may be imposed on infrastructure

networks during the recovery process and adjust the operation of the CISs to maximize the resilience of the combined system-of-systems. Hence, all infrastructure networks in the case study can meet the daily demands after the day 24th, which means the function of the Shelby County CISs is fully restored after the case study earthquake scenario. On the 54th day, the power network's recovery is completed, and the aforementioned water pump station can start supplying water to the connected nodes. Notably, after the 54th day, the water network utilizes about 91% of its supply capacity.

3.3.2. Enhancing Resourcefulness and Rapidity

For improved infrastructure resilience to natural hazards, modifying the Repair and Maintenance (R&M) teams' allocation may be an effective and practical Community Resilience Enhancement Strategy (CRES) owing to post-disaster recovery budget constraints. The second, post-disaster, CRES aims to strengthen the resourcefulness indicator of the Shelby County urban community. To illustrate the usefulness of altering the allocation of R&M teams in the recovery process, the seismic resilience of the interdependent CISs for two cases of R&M teams' allocation after an earthquake with a magnitude of 7.7 is quantified. In addition to the case with the initial number of R&M teams, a modified case evaluates the resilience of Shelby County CISs, considering a 50% increase in the number of the power network's R&M teams and a simultaneous 50% decrease in the number of the water network's R&M teams.

Figure 3.7 displays the evolution of the SoCIS resilience metric to compare the initial and rebalanced R&M team assignment. The results of this figure point out that rebalancing the assignment of R&M teams (i.e., new allocation) improves the SoCIS-ALR measure by 30.8 percent. Also, the rebalancing of R&M team assignments leads to the recovery of the Shelby County CISs in 36 days, 18 days sooner than with the initial R&M team assignment. As discussed earlier, the reason for this resilience improvement is that the power network is the controlling infrastructure in the recovery of the Shelby County CISs after the case study earthquake. It means the power-dependent infrastructure systems like the water network and, accordingly, the community cannot return to their normal conditions before the power network's recovery process is completed.

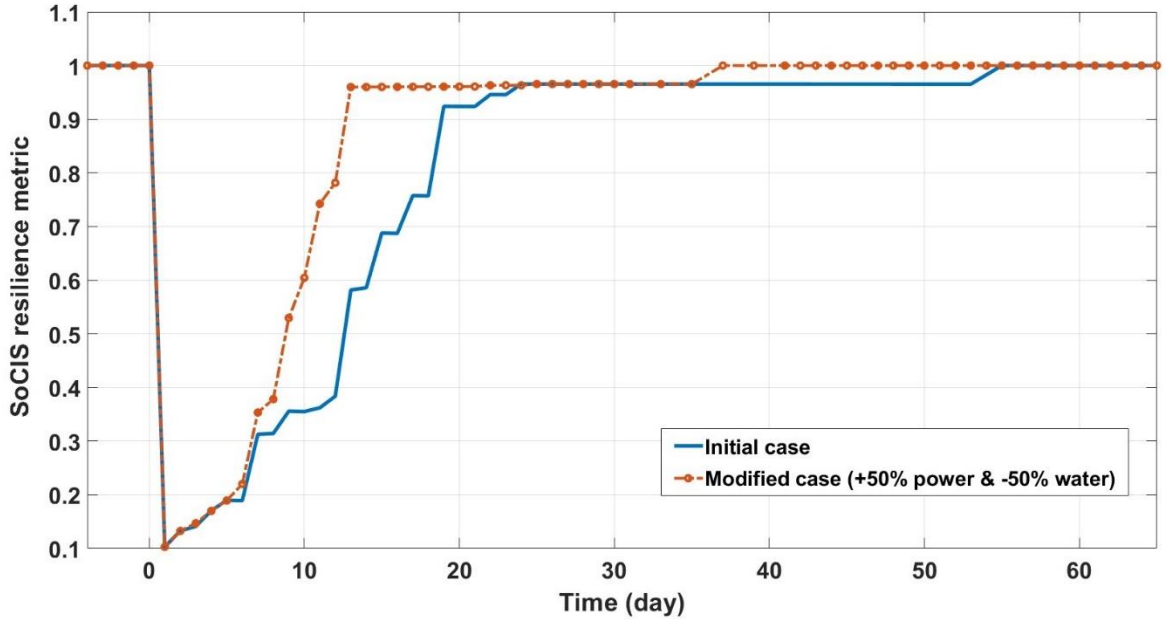

Fig. 3.7. The evolution of the SoCIS resilience metric of the Shelby County interdependent CISs comparing the initial and the re-balanced R&M team assignments in the magnitude 7.7 earthquake scenario.

3.3.3. Mitigating Interdependencies

The third, peri-disaster, CRES aims to improve the rapidity indicator of Shelby County urban resilience by deploying truck-mounted mobile power generators during the recovery process of the water network. As discussed earlier in section 3.2, the main reason for the prolonged function recovery of the water network despite the relatively fast restoration of damaged components is the interdependency relations between the water and power networks in Shelby County. The purpose of implementing the third CRES is to mitigate the adverse effect of interdependencies between the components of these two networks (power and water). In other words, the electric power demand of water facilities and pump stations can be supplied by truck-mounted mobile generators. The advantage of following this resilience enhancement strategy is that truck-mounted mobile generators act as portable power backup systems for the facilities in the water network. Since the objective of the ResQ-IOS is to maximize the resilience of urban communities after the occurrence of the disruption, the main question raised here is how to optimize the schedule and site selection for deploying the available truck-mounted mobile generators in the water

network. To this end, Equations (E.81) and (E.86) are modified and the new version of those Equations, (E.93) and (E.94), are added to the main body of the optimization model embedded in the structure of the ResQ-IOS:

$$\varphi_{W,t}^{WSF,j} \leq \beta_t^{WSF,m} + MG_{W,t}^{E,j} \qquad \forall (m,j) \in IEtW, \forall t \in T \qquad (E.93)$$

$$\varphi_{W,t}^{WPS,j} \leq \beta_t^{WPS,m} + MG_{W,t}^{E,j} \qquad \forall (m,j) \in IEtW, \forall t \in T \qquad (E.94)$$

Since the number of truck-mounted mobile generators that are available for deploying in the water network is limited, the following constraint is added to the optimization model as Equation (E.95):

$$\sum_j MG_{W,t}^{E,j} \leq N_{W,avail}^{E} \qquad \forall (m,j) \in IEtW, \forall t \in T \qquad (E.95)$$

A numerical experiment is designed to investigate the impact of deploying mobile generators on the resilience enhancement of the Shelby County urban community. Since nine water facilities and pump stations exist in Shelby County's water network, the experiment comprises ten cases for the seismic resilience assessment of Shelby County after an earthquake with a magnitude of 7.7. In the first case, it is assumed that there is no truck-mounted mobile power generator for deploying in the water network during the recovery process. From the second case onwards, the available number of mobile generators increases one by one. In the last case (the 10th case), all water facilities and pump stations are equipped with a truck-mounted mobile generator.

The results of this numerical experiment, considering the low availability of R&M teams, indicate that the CRES mentioned above can improve the rapidity indicator significantly. According to Fig. 3.8, deploying only one mobile generator can reduce the recovery duration of the urban community from 111 days to 46 days (about a 58.6% improvement in the value of the rapidity indicator). As shown in Fig. 3.8, it is important to note that deploying more than three mobile generators simultaneously no longer shortens the duration of the community recovery. In other words, 38 days is the minimum recovery duration that can be reached by implementing this resilience enhancement strategy for the case study of this numerical experiment. Hence, it can be concluded that three truck-mounted mobile generators are the optimal number of

this type of portable backup system to reach the minimum duration for the post-earthquake recovery process.

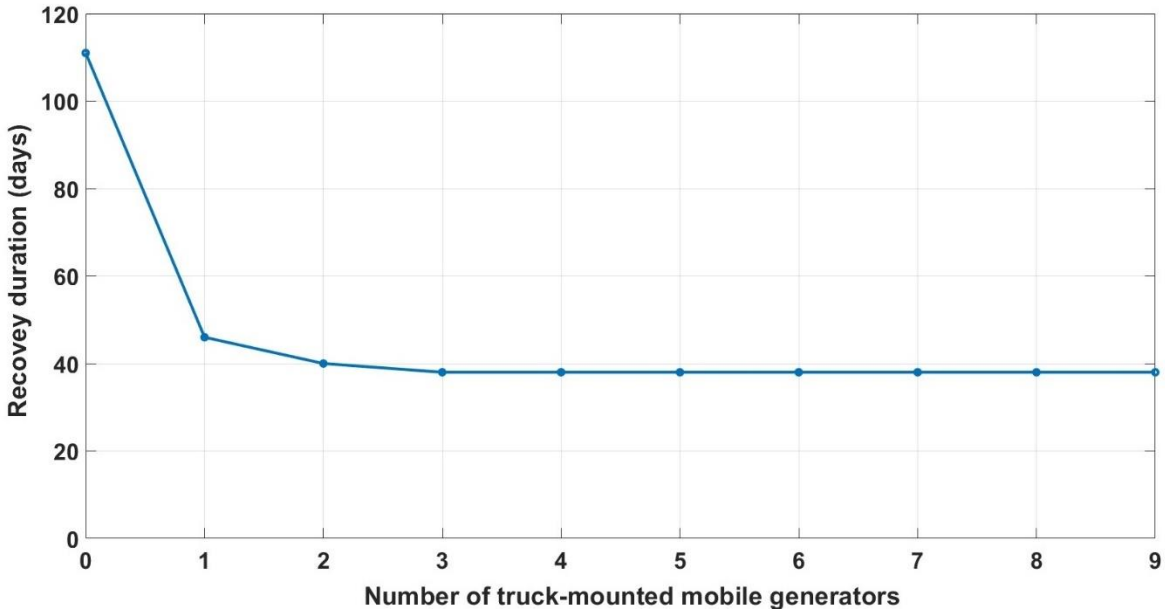

Fig. 3.8. The community recovery duration for different numbers of truck-mounted mobile generators deployed in the water network in the magnitude 7.7 earthquake scenario.

In terms of the SoCIS-ALR resilience metric, the strategy of deploying mobile generators results in lower values of loss of resilience. Fig. 3.9 displays the evolution of the SoCIS-ALR resilience metric for the case study of this numerical experiment. However, the SoCIS-ALR metric curve still decreases when more than three mobile generators are deployed during the recovery process. The reason for such behavior can be that water facilities and pump stations utilize mobile generators for power supply instead of consuming electricity from the power grid. This action lets the power grid manage its capacity for supplying less important nodal demands like residential buildings, which leads to reduced loss of resilience and a lower SoCIS-ALR resilience metric value as well.

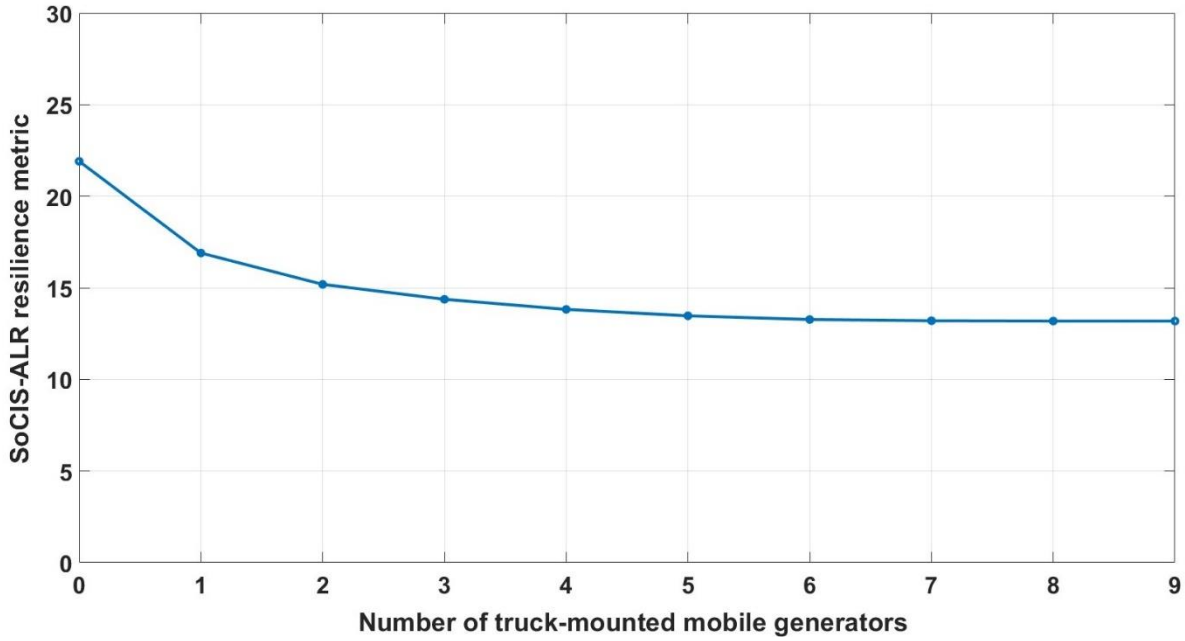

Fig. 3.9. The evolution of the SoCIS-ALR resilience metric for different numbers of truck-mounted mobile generators deployed in the water network in the magnitude 7.7 earthquake scenario.

Although deploying truck-mounted mobile generators improves the urban community's resilience against disruptive events, the objective of ResQ-IOS is to maximize this resilience improvement. For this purpose, the ResQ-IOS framework aims to optimize the implementation of this resilience enhancement strategy by determining the optimal schedule and locations for truck-mounted mobile generators during the recovery of the water network. As an example, the optimization results of the ResQ-IOS, including the optimal schedule and optimal locations for deploying three mobile generators in Shelby County's water network, are given in Table 3.3. For better illustration, the optimal locations for three truck-mounted mobile generators in the case study water network on the 6th and 33rd days are displayed in Figs. 3.10 and 3.11.

Table 3.3. Optimal schedule and locations for deploying three truck-mounted mobile generators in Shelby County's water network under the low availability of R&M teams after an earthquake with M_w=7.7 (MG: Mobile Generator, N: Node).

Optimal Location											
Optimal Schedule	Day	1	2	3	4	5	6	7	8	9	10
	MG1	N 4	N 4	N 4	N 4	N 4	N 4	N 4	N 4	N 4	N 4
	MG2	N 5	N 5	N 5	N 5	N 5	N 5	N 5	N 5	N 5	N 5
	MG3	N 6	N 6	N 6	N 6	N 6	N 6	N 6	N 6	N 2	N 6
	Day	11	12	13	14	15	16	17	18	19	20
	MG1	N 2	N 11	N 11	N 11	N 11	N 11	N 11	N 11	N 11	N 11
	MG2	N 5	N 5	N 5	N 5	N 5	N 5	N 5	N 5	N 5	N 5
	MG3	N 6	N 6	N 6	N 6	N 6	N 6	N 6	N 6	N 3	N 3
	Day	21	22	23	24	25	26	27	28	29	30
	MG1	N 11	N 11	N 11	N 11	N 11	N 11	N 11	N 11	N 11	N 11
	MG2	N 5	N 5	N 5	N 5	N 5	N 5	N 5	N 5	N 5	N 5
	MG3	N 3	N 3	N 3	N 3	N 3	N 3	N 3	N 3	N 3	N 3
	Day	31	32	33	34	35	36	37	38	39	40
	MG1	N 11	N 11	N 11	N 11	N 11	N 11	N 11	N 11	-	-
	MG2	N 5	N 8	N 8	N 8	Dismissed	Dismissed	Dismissed	Dismissed	-	-
	MG3	N 3	N 3	N 3	N 3	N 3	Dismissed	Dismissed	Dismissed	-	-

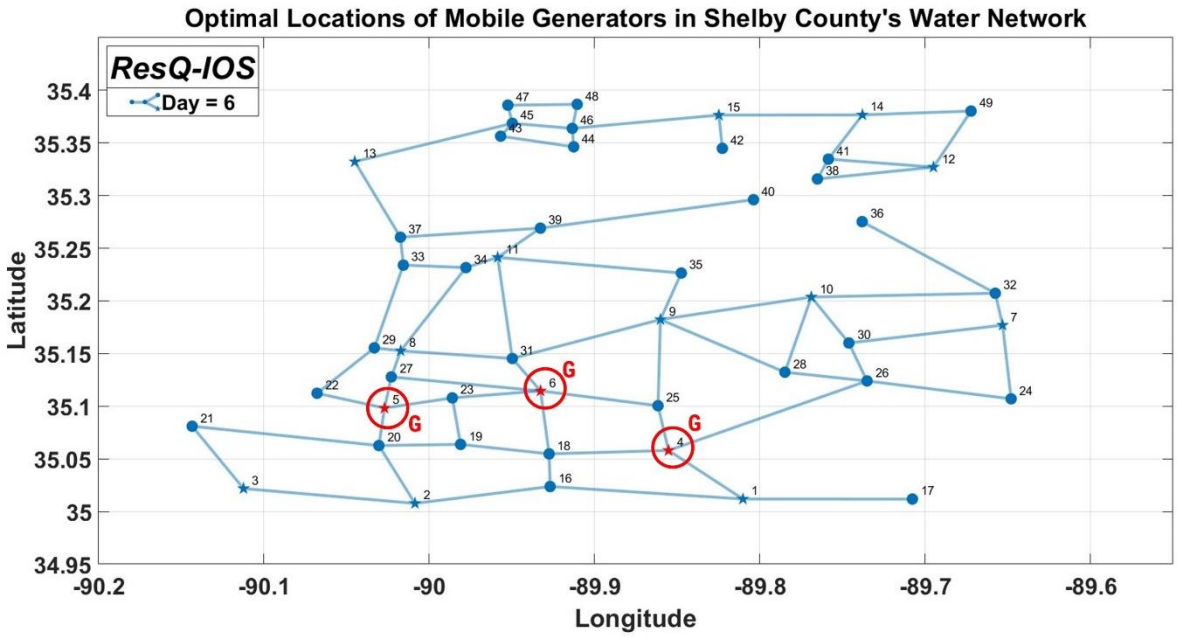

Fig. 3.10. The optimal locations (nodes 4, 5, and 6) for three truck-mounted mobile generators in the case study water network on day 6 in the magnitude 7.7 earthquake scenario.

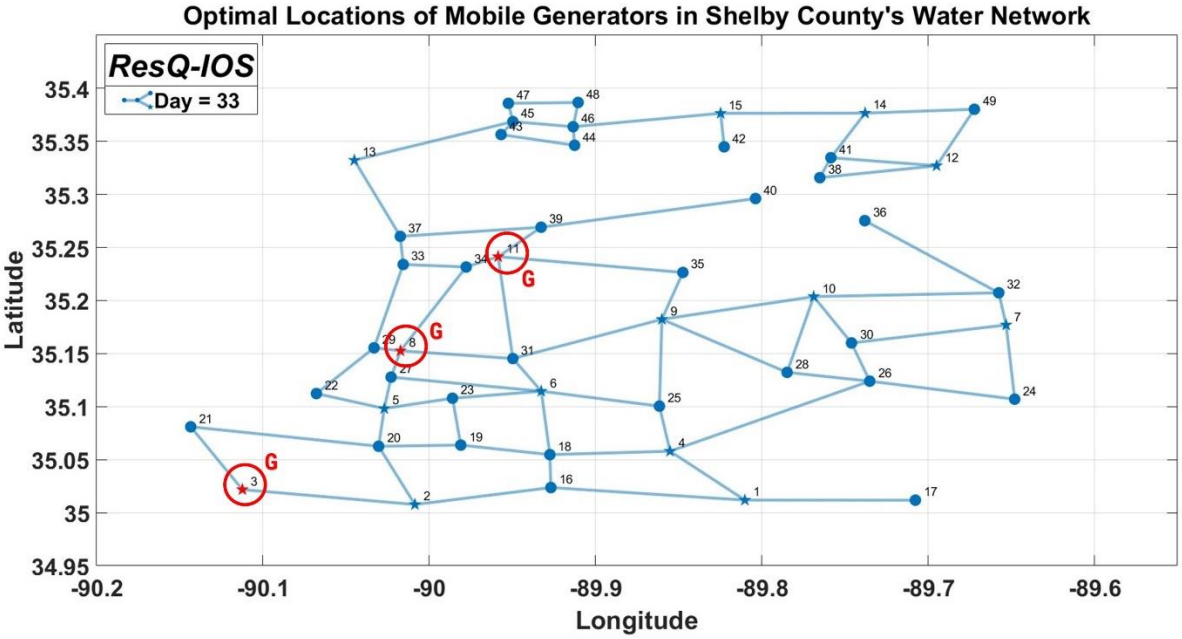

Fig. 3.11. The optimal locations (nodes 3, 8, and 11) for three truck-mounted mobile generators in the case study water network on day 33 in the magnitude 7.7 earthquake scenario.

3.4. Parametric analysis of urban disaster resilience

This section aims to investigate the role of some parameters in urban communities' disaster resilience by carrying out six parametric analyses. The considered parameters can be categorized into two groups: Internal and External. In this doctoral dissertation, internal parameters refer to factors that are manageable during post-disaster recovery. The term external parameter refers to factors that are not controllable or that require long-term CRE actions to bring under control. The six parameters whose impacts on the urban disaster resilience are analyzed are as follows:

Internal parameters

- Configuration of R&M teams
- Number of available R&M teams
- Restoration sequence of failed components

External parameters

- Housing vulnerability and housing recovery models
- Seismic hazard (Earthquake magnitude and epicenter location)

The purpose of this section is to demonstrate the capability of the ResQ-IOS framework for performing the parametric analysis of urban resilience to disruptive events. Firstly, the effect of changes in internal parameters on the Shelby County urban community resilience is explored. Then, the disaster resilience of the case study is examined in relation to the external parameters that are not directly administrable.

3.4.1. Configuration of R&M teams

To investigate the effect of R&M team configuration on the post-earthquake resilience of the Shelby County interdependent CISs, the R&M teams for repairing the water pipelines are reconfigured. The default configuration of the water pipeline R&M teams is four persons with a 16-hour workday. The water pipeline R&M teams' configuration is changed to three people with an 8-hour workday, while keeping the number for water pipeline R&M teams the same. Figure 3.12 illustrates that different R&M team configurations change the required time for repairing the damaged water

pipelines. In the default case, all damaged pipelines are repaired at an almost constant repair rate after 11 days. However, repairing the damaged pipelines with smaller R&M teams who work shorter shifts takes 19 days, as shown in Fig. 3.12. Also, this figure indicates that the required time for restoring the damaged components can take several time steps in the resilience assessment period. Although the recovery process of damaged water pipelines is affected by changing the R&M teams' configuration, the effect on the Shelby County SoCIS-ALR is negligible. As discussed earlier, due to the interdependency between water and power infrastructure systems, the full recovery of the water network is conditioned on the rate of the power network's recovery process. Reducing the effectiveness of the water pipeline R&M teams frees up the resources to strengthen the electric power R&M teams, the effect of which was illustrated in Section 3.3.2.

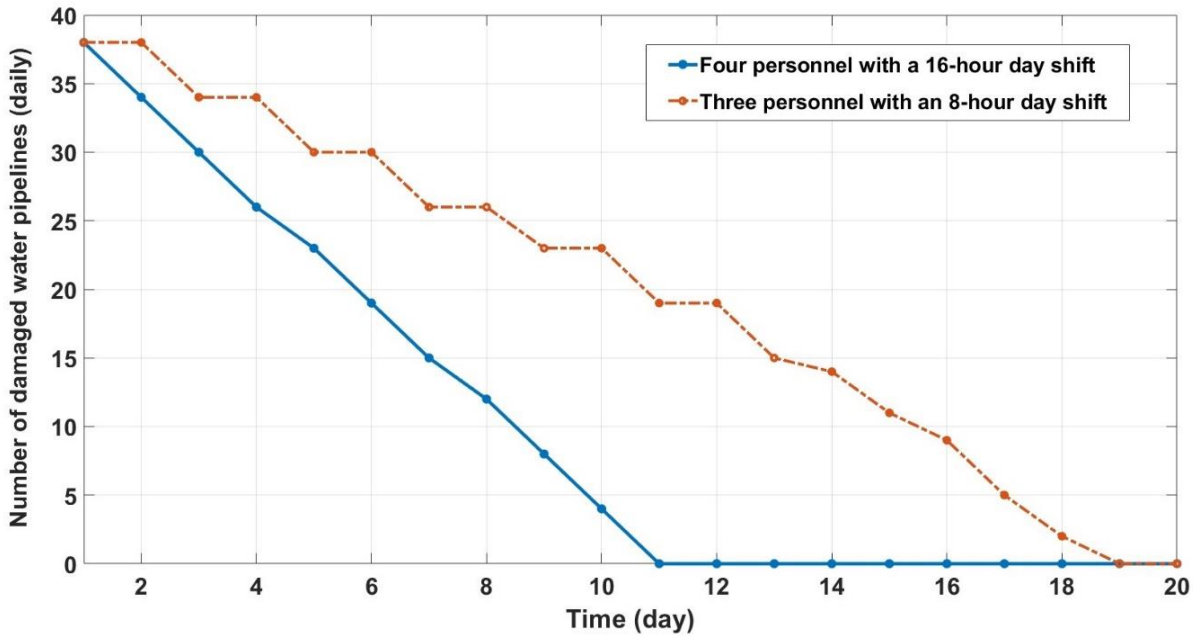

Fig. 3.12. The daily number of damaged water pipelines during the recovery of the Shelby County water network in the magnitude 8.5 earthquake scenario for two configurations of R&M teams.

3.4.2. Number of available R&M teams

The resilience of the interdependent CISs in the ResQ-IOS framework is quantified by considering constraints on the resources for the recovery process, such as limits on the number of Repair and Maintenance (R&M) teams for each type of component within the infrastructure networks. For this purpose, the ResQ-IOS framework can import the number of available R&M teams for 13 types of components belonging to three interdependent CISs in the Shelby County case study and then simulate restoring the failed components based on the restoration sequence that is determined according to the limits on the number of R&M teams and the strategy adopted for the recovery process of the Shelby County infrastructure networks.

To demonstrate the effect of the number of available R&M teams on the recovery process, a numerical experiment is designed to assess the seismic resilience of the Shelby County interdependent CISs for 540 cases. The numerical experiment considers 20 earthquake scenarios with magnitudes from 6 to 9 and 27 portfolios for various levels of repair team package availability. Firstly, it is necessary to define the term “repair package.” Each repair package comprises the R&M teams’ staff and the required machinery and resources. A portfolio consists of three elements representing the availability level of repair packages in the Shelby County interdependent CISs. For instance, the portfolio of No.12 in this numerical experiment is expressed as “12-PM,GL,WH,” which states the availability of repair packages in the power, natural gas, and water networks is medium, low, and high, respectively. The main reason for creating the repair package and 3-level availability concepts is to reduce the computational cost of carrying out the parametric analysis concerning the number of R&M teams. Each availability level (low, medium, and high) suggests that the available number of repair packages for a specific component is a percentage of the total number of that component in the infrastructure network.

The parametric analysis results for exploring how the number of available R&M teams affects the seismic resilience of the Shelby County urban community are analyzed from the SoCIS-ALR metric and recovery duration aspects. Figs. 3.13 and 3.14 represent the changes in the SoCIS-ALR metric and recovery duration for 540 resilience assessment cases, respectively. Each resilience assessment case simulates an earthquake scenario with a magnitude between 6 and 9 and considers a repair package portfolio for the recovery of interdependent CISs in Shelby County.

Those two figures (3.13 and 3.14) demonstrate that significant improvements in the value of the SoCIS-ALR metric and the duration of the case study recovery occur when more repair packages (i.e., R&M teams) are available for restoring damaged components in the power network. The parametric analysis for the number of R&M teams suggests that in the case of a fixed budget, it will be an effective and lucrative strategy if the greater part of the budget is allocated to deploying a more significant number of R&M teams in the power network. In other words, the power network has top priority for receiving repair packages. There are two reasons for this situation. First, the case study power network has a larger number of components than two other infrastructure networks. Second, the power network is more vulnerable to seismic hazards compared to water and natural gas networks in this case study.

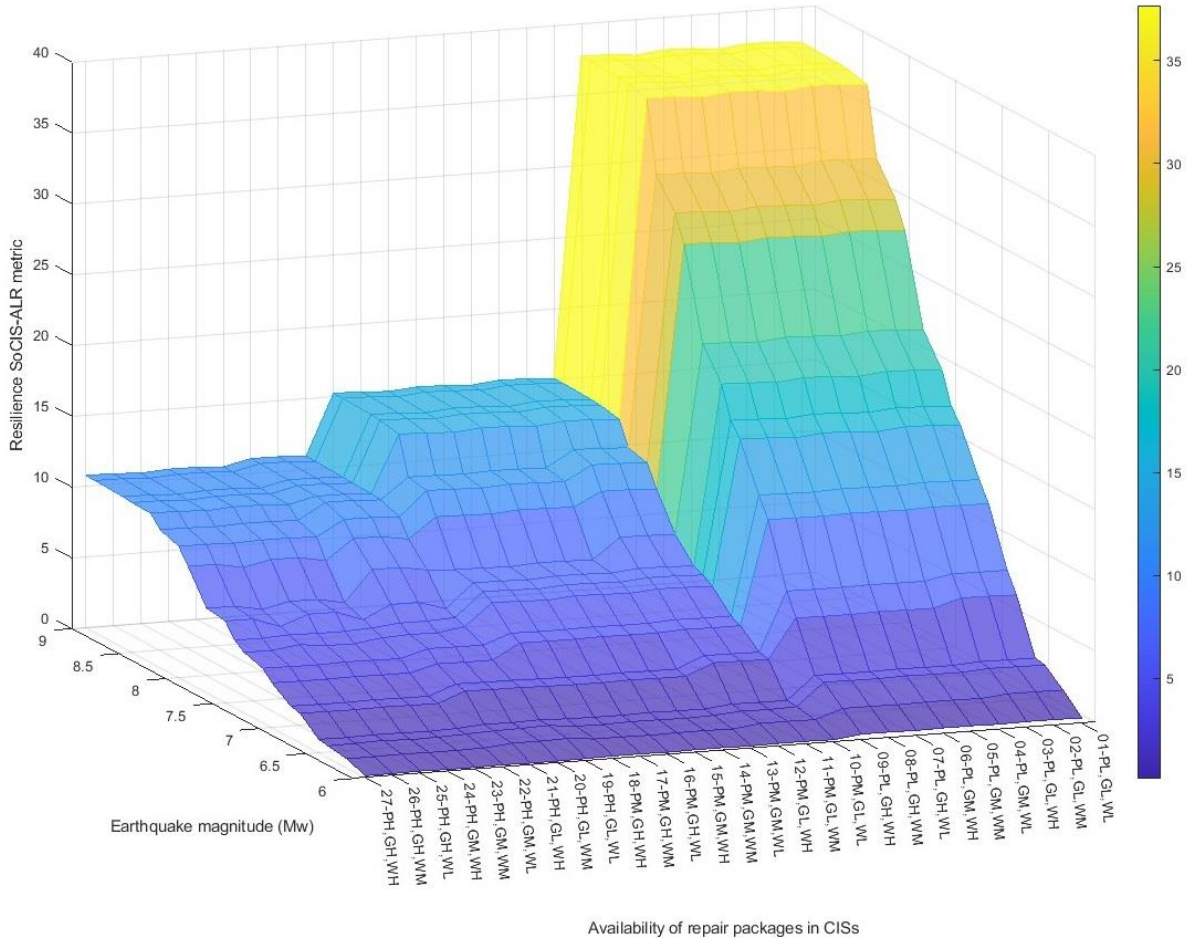

Fig. 3.13. The value of the SoCIS-ALR metric for 540 resilience assessment cases (Networks, P: Power, G: Gas, W: Water – Availability levels of repair packages, L: Low, M: Medium, H: High).

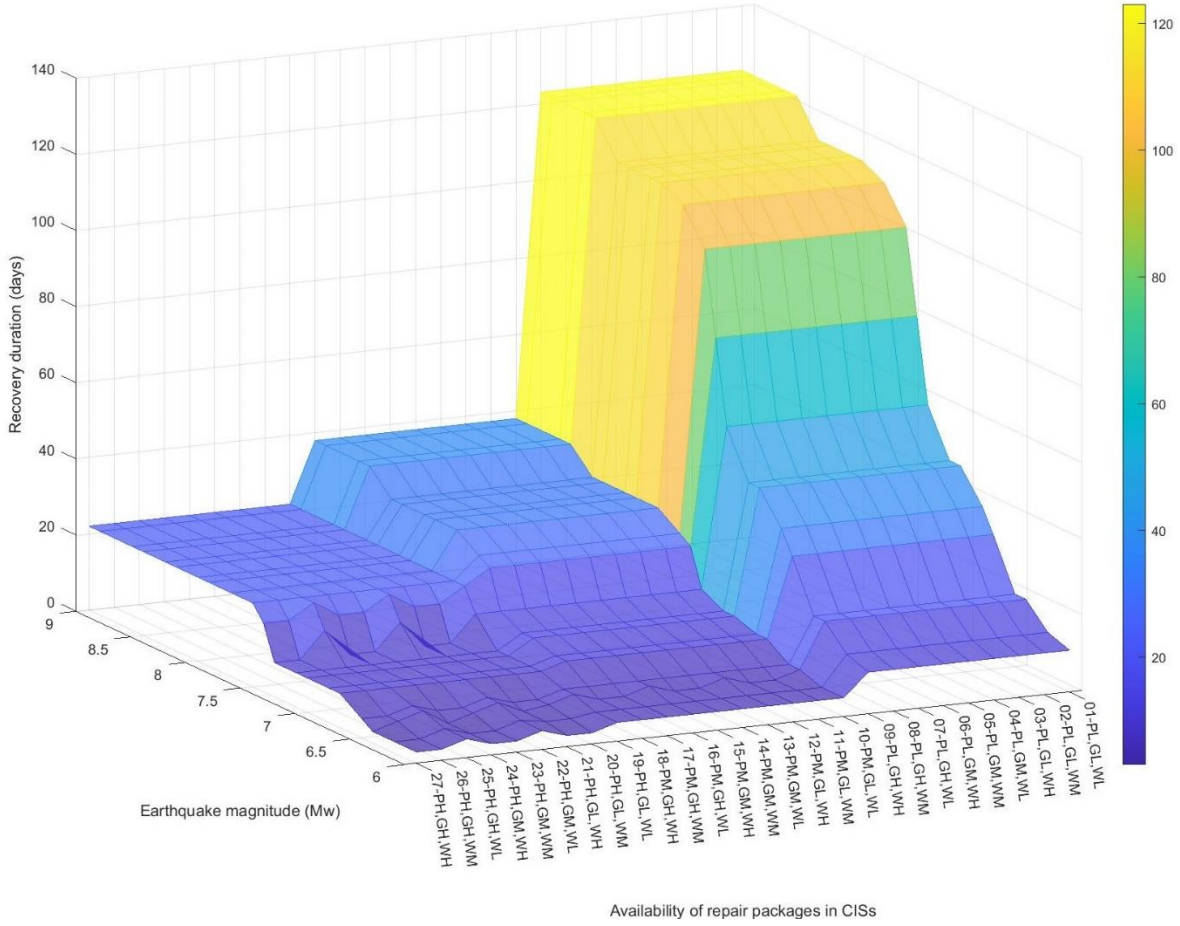

Fig. 3.14. The recovery duration of the urban community for 540 resilience assessment cases (Networks, P: Power, G: Gas, W: Water – Availability levels of repair packages, L: Low, M: Medium, H: High).

3.4.3. Restoration sequence of failed components

Due to budget constraints and the limited number of crew teams and resources, it is only feasible for a few failed components to be restored simultaneously. Hence, the availability of resources and maintenance crew teams influences the component repair start time. There are different strategies for sequencing the repairs of the damaged components. Some researchers developed optimization models to determine the optimal restoration sequence of failed components [96], [97], [98]. The main challenge of using such optimization models is the huge computational burden required for solving the optimal restoration sequence problem, particularly when the optimization

model is solved repeatedly for a set of interdependent infrastructure systems having many damaged components after the occurrence of the natural hazard [99].

The ResQ-IOS framework recovery model can adopt various restoration sequence strategies for repairing the damaged components in the network. In this doctoral dissertation, the ResQ-IOS framework utilizes a criticality-based strategy applying a performance-based (i.e., supply capacity and demand-based) importance approach to specifying the restoration sequence of damaged components located at nodes of the interdependent CISs (i.e., nodes with the greatest demand and supply capacities are repaired first), and a capacity-based method to determine the sequence of links (e.g., pipelines) to be repaired (i.e., links with the largest capacity are repaired first). Following the criticality-based strategy for restoring the damaged components does not lead to remarkable variations in the recovery of infrastructure systems compared to the optimal strategy [99].

The seismic resilience of the case study after an earthquake with a magnitude of 7.9 is quantified for two cases. In the first case, it is assumed that there is no constraint on the number of R&M teams and repair resources. Implementing the first case results in the shortest recovery duration of the case study community. The results show the SoCIS-ALR metric value is 6.94, and the urban community recovery takes 16 days. Although a 16-day period is the shortest recovery possible after the earthquake scenario, it may not be feasible due to limited recovery resources. In the second case, considering constraints on recovery resources, the damaged components in three infrastructure networks are restored according to the criticality-based repair sequence. In this case, the value of the SoCIS-ALR metric is 11.53, and the recovery duration is 31 days. The evolution of the SoCIS metric for the two cases mentioned above is shown in Fig. 3.15.

To demonstrate the criticality-based strategy is a near-optimal strategy for the restoration sequence of damaged components, 50 scenarios are defined in which the damaged components are randomly selected for restoration during the recovery process. Then, the seismic resilience of the case study is assessed for the 50 scenarios with a random selection strategy. For better illustration, the evolution of the SoCIS metric for the 50 scenarios is displayed in Fig. 3.15.

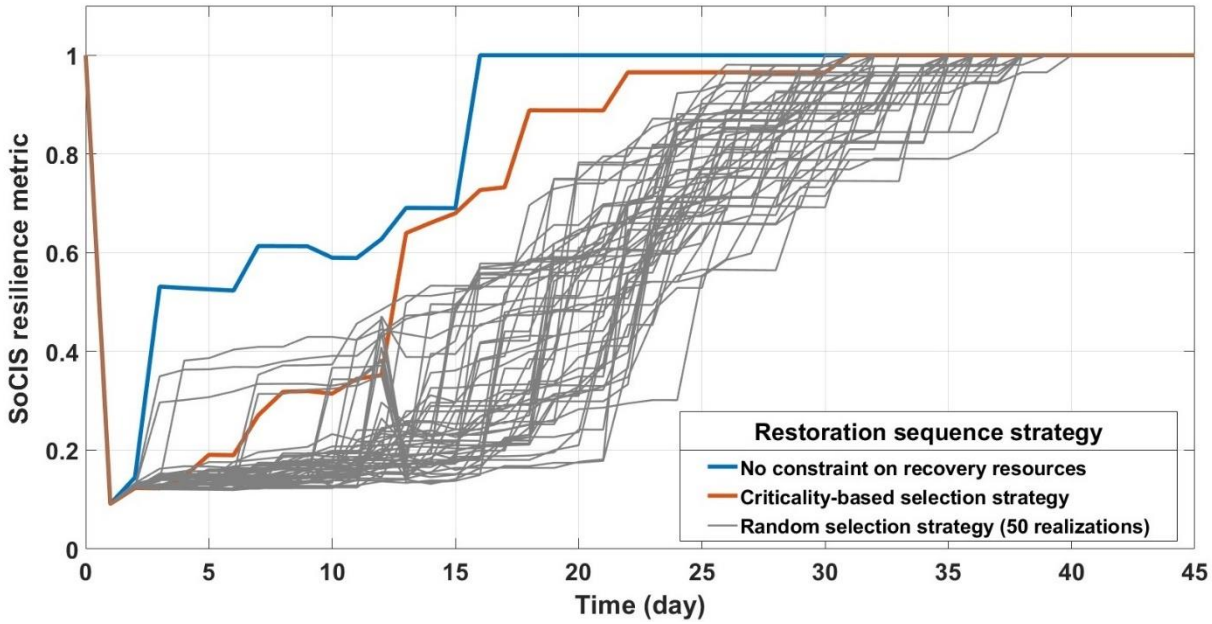

Fig. 3.15. The evolution of the SoCIS metric for different restoration sequence strategies of damaged components in the magnitude 7.9 earthquake scenario.

The minimum SoCIS-ALR metric value of the 50 scenarios with a random selection strategy is 14.12, which is still greater than 11.53, the SoCIS-ALR metric value of the criticality-based strategy. In terms of the SoCIS-ALR metric value, the criticality-based restoration sequence strategy has a better performance than all 50 realizations of the random selection strategy. Concerning the recovery duration, the minimum duration among 50 realizations is 30 days, one day shorter than the criticality-based strategy. However, the SoCIS-ALR metric related to the respective realization of the random selection strategy is 19.68, which is 70.7% greater than the criticality-based SoCIS-ALR metric value. Considering the SoCIS-ALR metric and recovery duration as two objectives simultaneously, the criticality-based strategy can serve as a near-optimal strategy for sequencing the repairs of damaged components. Nevertheless, the no-constraint case, as well as a few randomly generated scenarios, may be used to improve the start of the recovery process. A summary of the results is given in Table 3.4.

Table 3.4. The summary of results for different restoration sequence strategies of failed components in the Shelby County interdependent CISs.

Restoration sequence strategy	Constraints on recovery resources	SoCIS-ALR metric	Recovery duration (days)	Possibility	Feasibility
Relaxed on recovery constraints	No	6.94	16	Yes	No
Criticality-based selection	Yes	11.53	31	Yes	Yes
Random selection (Minimum SoCIS-ALR metric)	Yes	14.12	35	Yes	Yes
Random selection (Minimum recovery duration)	Yes	19.68	30	Yes	Yes

3.4.4. Housing vulnerability and housing recovery models

Since the Shelby County case study of this doctoral dissertation is located in the USA, the vulnerability models for the damage estimation of infrastructure components are obtained from the HAZUS Earthquake Model Technical Manual (HAZUS 5.1) published by the Federal Emergency Management Agency (FEMA) in July 2022 [77]. In the case of applying ResQ-IOS to other case studies around the world, the localized vulnerability models (i.e., damage functions) can be used in the structure of the ResQ-IOS framework.

Modeling the recovery of housing after the occurrence of a disaster is a topic of interest for researchers in the fields of urban planning, social and financial resilience, construction, infrastructure management, etc. Applying accurate housing recovery models can provide stakeholders with valuable information about how pre-disruption demands for services in the housing sector revive after an extreme event, as well as how to develop long-term CRES aimed at reducing the vulnerability and speeding up the recovery of housing. Although studying housing vulnerability and recovery models is not the objective of this doctoral dissertation, this section aims to represent the ResQ-IOS framework's ability to consider sophisticated housing and infrastructure systems demand evolution models and their effect on the community recovery process.

To this end, the resilience of the Shelby County urban community after an earthquake with a magnitude of 7.2 is quantified for two types of demand evolution models of the housing sector in Shelby County. Each model considers mathematical expressions for relating the damage level of residential buildings and demands for the services provided by the infrastructure systems. Since the damage level of residential buildings evolves during the recovery, the Shelby County residents' demands for infrastructure services evolve in time, too. The first model considers a simple linear relation between the damage level and the recovered demands for power, natural gas, and water services in the housing sector. The second model combines three types of mathematical functions: polynomial for electricity, trigonometric for natural gas, and exponential for water service. The various relations between the normalized damage level and normalized demand are shown in Fig. 3.16.

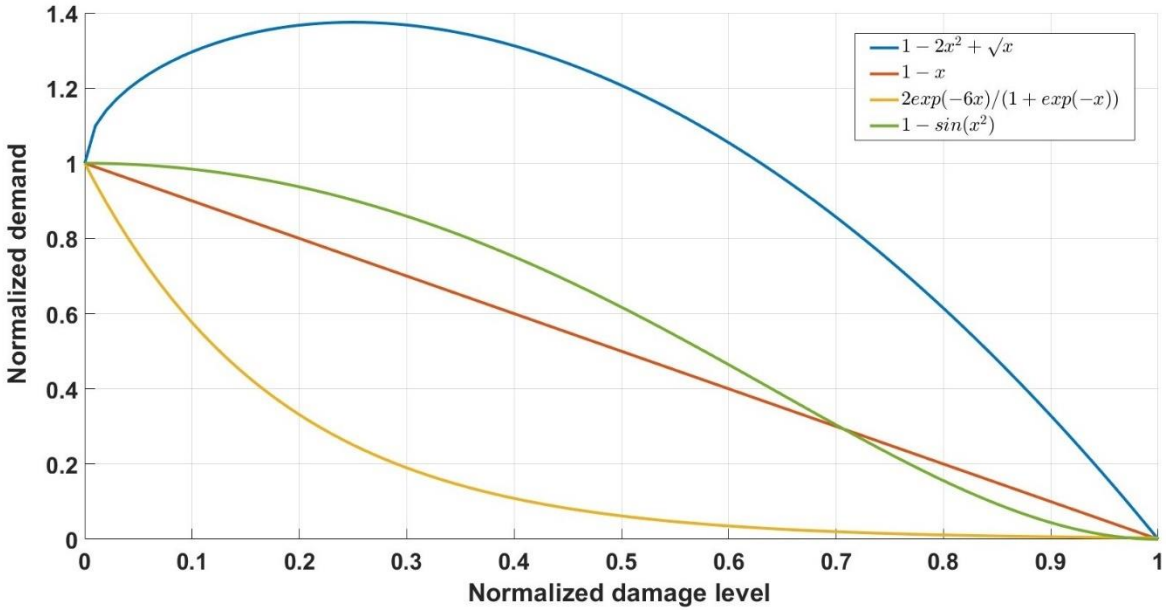

Fig. 3.16. The various relations between the normalized damage level and normalized demand for modeling demand evolution during the housing sector's recovery.

Although the relation between damage level and demand is often inverse, the mathematical expressions of the second model are defined to contain both increasing and decreasing variations of demands for infrastructure services in the housing sector. Some services, like communication, may face increased demand after an extreme event [100].

The results of the seismic resilience assessment for the case study with two different demand evolution models (linear and non-linear) are displayed in Fig. 3.17. The non-linear demand evolution model considers a polynomial function for electricity, a trigonometric function for natural gas, and an exponential function for water service demand evolution. The SoCIS-ALR metric values for linear and nonlinear models are 6.96 and 2.74, respectively. The full recovery of the Shelby County urban community for linear and nonlinear models takes 16 and 13 days, respectively. As shown in Fig. 3.17, applying two different demand evolution models for the housing sector leads to considerable changes in the recovery curve of the case study urban community while other parts of the resilience assessment model in the ResQ-IOS framework remained unchanged. After the same earthquake scenario, having two different community recovery curves indicates the importance of using accurate housing recovery models. The results of this section also reflect ResQ-IOS's capability to consider the demand evolution of various housing recovery models, including the daily basis data of housing recovery progress simulated by an external software package or derived from the usage data collected by the CIS operator during the recovery process.

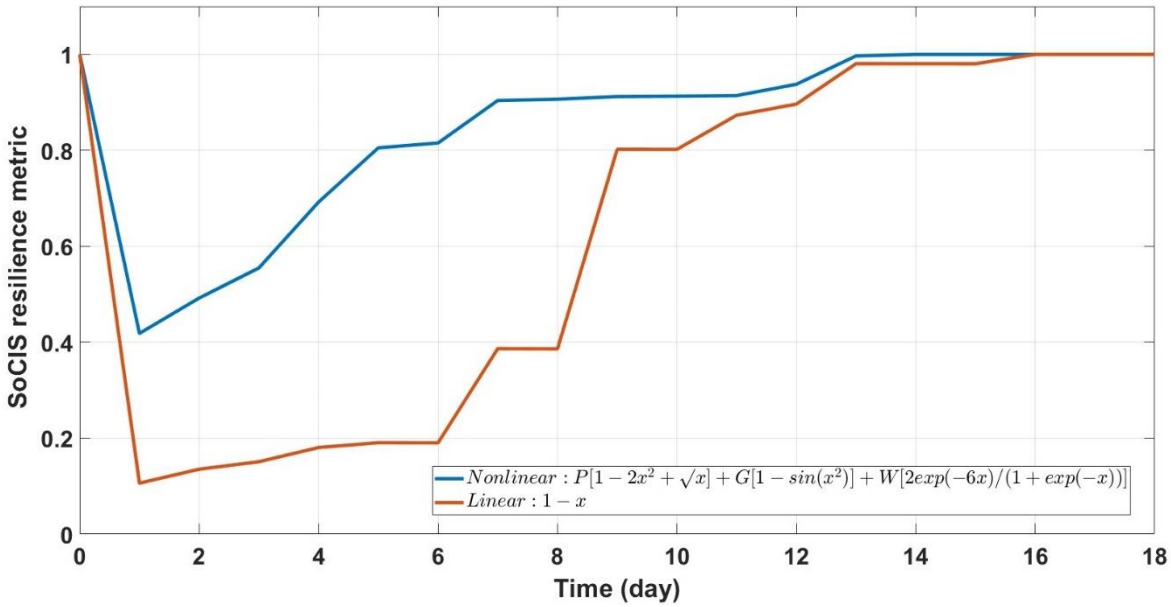

Fig. 3.17. The changes in the SoCIS metric after an earthquake with M_w=7.2 for two different demand evolution models considered for the housing sector's recovery.

3.4.5. Earthquake magnitude

To gain an insight into the relation between the seismic hazard and the seismic resilience of the Shelby County interdependent CISs, case study resilience analyses were done for earthquakes with the magnitude varying between M_w=6 and M_w=9 and the same epicenter location. In addition to SoCIS-ALR, the required time for a full recovery of all Shelby County CISs is calculated. Figure 3.18 demonstrates the relation between the magnitude of the seismic hazard and the seismic resilience of the interdependent CISs in Shelby County. As shown in Fig. 3.18, the SoCIS-ALR metric values increase monotonically from 0.279 for the M_w=6 earthquake to 23.22 for the M_w=9 earthquake, an increase of 83-fold, but not at the same rate. Furthermore, the SoCIS-ALR metric saturates at earthquake M_w=8.5. The time to fully recover the joint function of the Shelby County interdependent CISs varies from six to 62 days. Notably, the full functional recovery time saturates at M_w=8.0. The cause of such saturation is that the power network that controls the community's recovery duration reaches the maximum level of function degradation during the M_w=8.0 earthquake scenario, with the number of damaged nodes (including both total and partial damage) is 57 and 58 (out of 59 nodes) after the M_w=8.0 and M_w=8.2 earthquakes, respectively. The SoCIS-ALR metric is still sensitive to the number of damaged power CIS nodes, saturating after the M_w=8.5 earthquake.

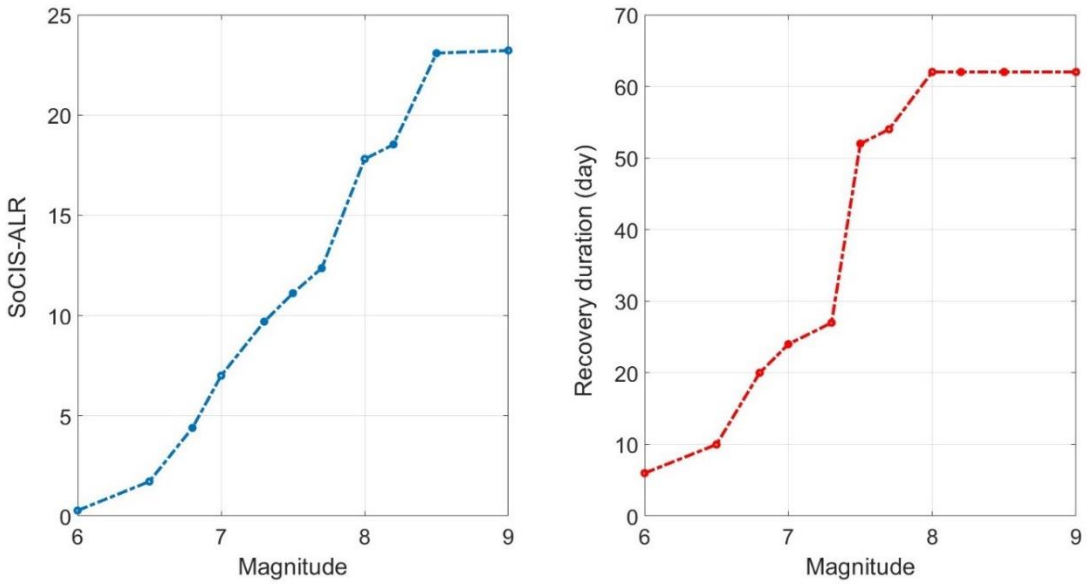

Fig. 3.18. The time to full recovery (100%) and the SoCIS-ALR metric values for the Shelby County interdependent CISs as a function of the case study earthquake magnitude.

3.4.6. Earthquake epicenter location

This section investigates the impact of the location of the earthquake epicenter on urban seismic resilience. The vulnerability of the infrastructure components is very sensitive to the distance between the earthquake epicenter and the location of the components. For this purpose, a numerical experiment is designed to quantify the resilience of the case study urban community against ten earthquake scenarios with ten different epicenter locations and the same magnitude. The locations of epicenters are selected to perform the topological vulnerability analysis of the case study interdependent infrastructure systems. The details of ten selected epicenters are given in Table 3.5 and shown in Fig. 3.2. The magnitude of all earthquake scenarios is 7.7, and it is assumed the availability of repair packages is low for the restoration of the damaged components of three interdependent networks in Shelby County. Scenario No.10 is the realistic earthquake scenario introduced in Section 3.2, called the reference scenario in this section.

Table 3.5. The geographical coordinates of selected earthquake epicenters.

Scenario No.	Location	Longitude	Latitude
1	Northwest	-90.2	35.4
2	West	-90.2	35.2
3	Southwest	-90.2	35
4	North	-89.85	35.5
5	Center	-89.85	35.2
6	South	-89.85	34.9
7	Northeast	-89.5	35.4
8	East	-89.5	35.2
9	Southeast	-89.5	35
10	Reference	-90.3	35.3

For a better understanding, the SoCIS-ALR metric values and recovery duration of the urban community for the ten earthquake epicenter location scenarios of the numerical experiment are illustrated in Figs. 3.19 and 3.20, respectively. The analysis of the results indicates that the location of the earthquake epicenter is an influential parameter in urban seismic resilience. According to Fig. 3.19, the worst scenario for

the case study occurs when the epicenter of the earthquake is in the center of Shelby County. In that case, the joint accumulated loss of resilience is about ten times that of the reference scenario. Also, the recovery of the urban community takes about six times that of the reference scenario.

Although it is expected that the earthquake with an epicenter in the center of Shelby County will have the most destructive impact on the urban community, it is noteworthy that the resilience of the case study differs substantially when the location of the earthquake epicenter changes. The second worst scenario for the urban community is an earthquake with an epicenter located in the southwest of Shelby County. In this scenario, the SoCIS-ALR metric value and the recovery duration are about 4.5 and 3.5 times those of the reference scenario, respectively. The epicenter of the third worst scenario is in the south of Shelby County. It can be concluded that the CIS components in the southwest and south parts of the case study area are less resilient to seismic hazards.

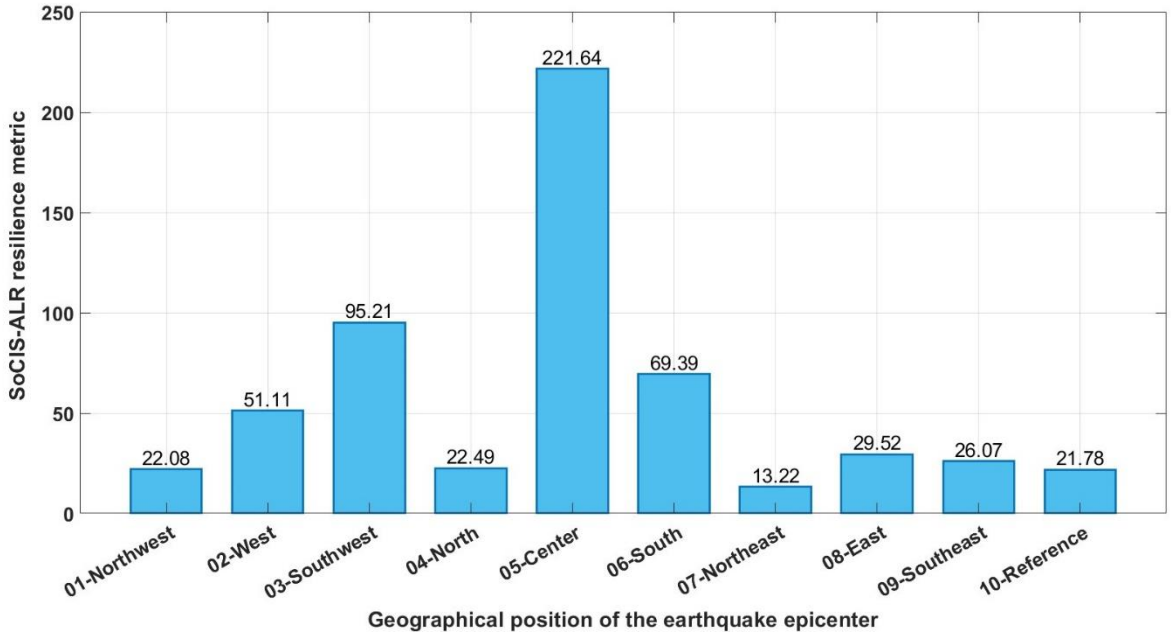

Fig. 3.19. The SoCIS-ALR metric value of the Shelby County urban community for different locations of the earthquake epicenter.

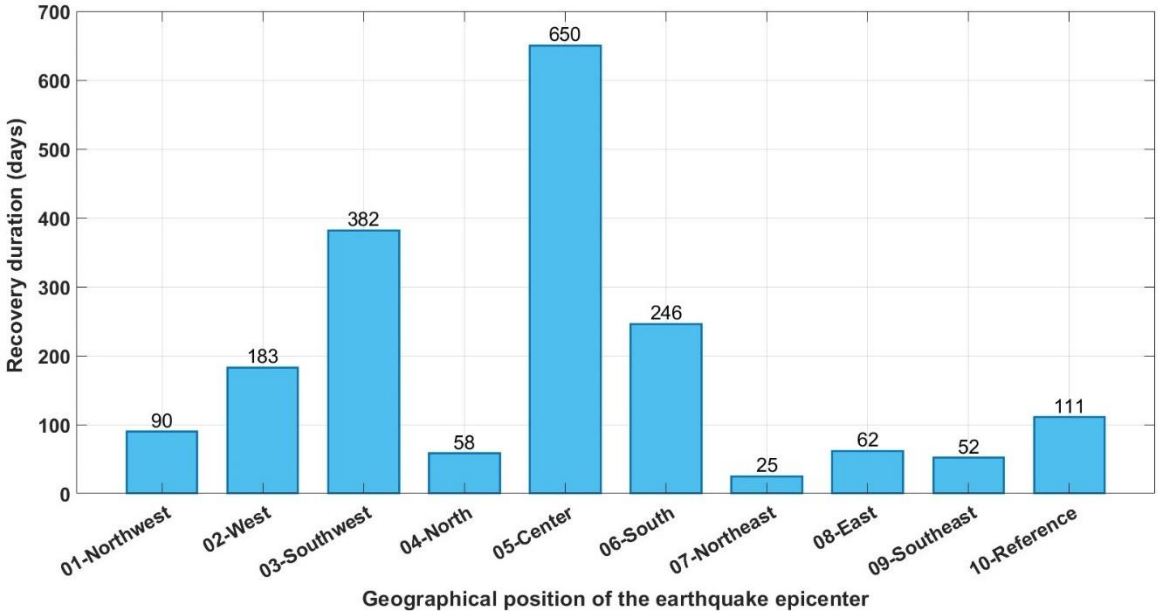

Fig. 3.20. The recovery duration of the Shelby County urban community for different locations of the earthquake epicenter.

The lowest SoCIS-ALR metric value among the numerical experiment results is related to the earthquake scenario with an epicenter in the northeast of Shelby County. This northeast earthquake scenario has the shortest duration of the urban community recovery, which is about one-fourth that of the reference scenario. It suggests that the CIS components located in the northeast part of Shelby County are the most resilient against earthquakes. As depicted in Fig. 3.21, the variations of the interdependent CISs' loss of resilience follow a similar pattern concerning the locations of the earthquake epicenter. For instance, the largest and smallest amounts of the CISs' loss of resilience are pertaining to the earthquake epicenters located in the center and northeast of Shelby County, respectively.

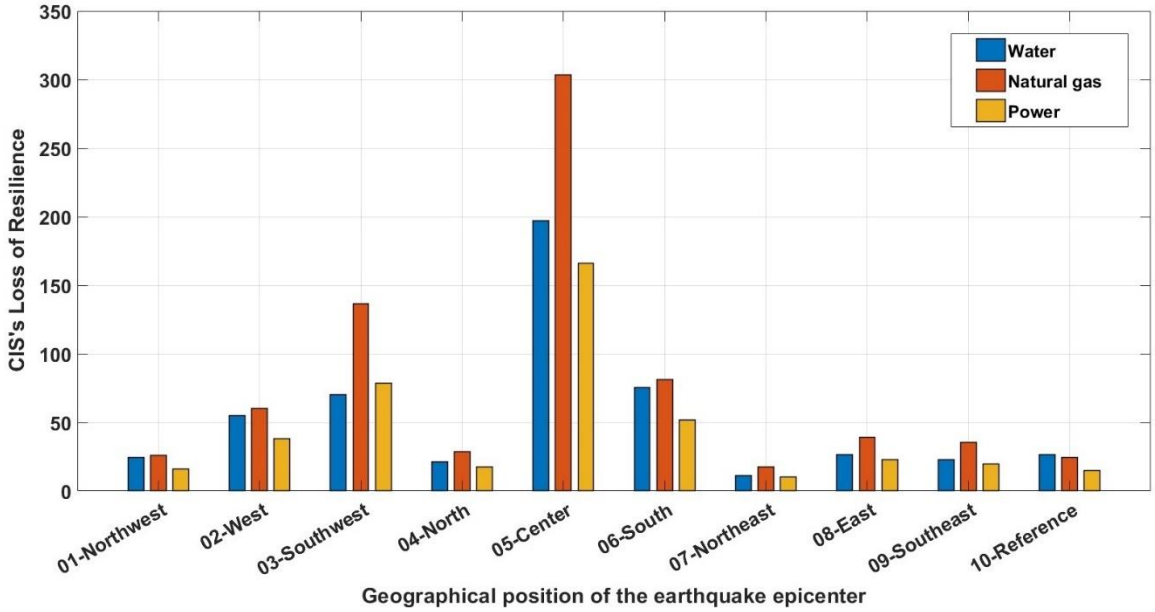

Fig. 3.21. The Shelby County CISs' loss of resilience for different locations of the earthquake epicenter.

The numerical experiment results indicate that some areas in the case study, like the south and southwest, are more vulnerable to seismic hazards compared to the northeast part of the case study. It is likely that the disparity in the geographical distribution of important components within the infrastructure networks is the reason for the discrepancies between the scenarios. Therefore, it would be a recommended policy to prioritize the areas that are less resilient to natural hazards over other parts of the Shelby County case study for implementing pre-disruption CRESs, such as increasing redundancy, improving the robustness of infrastructure components, retrofitting critical components in the infrastructure networks, or planning the peri-disruption CRES using emergency generators and water-supply trucks.

3.5. Identifying the Optimal Community Recovery Strategy

In previous sections of this chapter, the capabilities of the ResQ-IOS framework in modeling, optimizing, quantifying, and analyzing the resilience of interdependent critical infrastructure systems were demonstrated. The feasibility study of implementing several pre-disruption, peri-disruption, and post-disruption CRESs was conducted. The implementation of one of the post-disruption CRESs focusing on deploying backup systems in the water network was optimized by determining the optimal schedule and locations of backup systems. Therefore, four optimized quantities provided by ResQ-IOS were introduced. Those four quantities are as follows:

1- *SoCIS-ALR resilience metric*: considering the available recovery resources, the SoCIS-ALR metric value is the minimum loss of resilience that an urban community comprising interdependent CISs can reach after a disruptive event.
2- *Optimal daily dispatching of services within infrastructure networks*: to minimize the urban community's loss of resilience, the ResQ-IOS framework determines the optimal service dispatching (i.e., distribution) within infrastructure networks daily. In other words, the objective of optimal dispatching is to minimize the daily unmet demands for services (power, natural gas, and water) in the urban community during the recovery.
3- *Optimal locations of backup systems*: in the case of using backup systems to improve the disaster resilience of interdependent CISs, the ResQ-IOS framework can specify the optimal locations for deploying the backup systems to maximize resilience improvement.
4- *Optimal schedule for deploying backup systems*: the ResQ-IOS framework is able to determine the optimal timetable for moving and deploying backup systems within infrastructure networks during the post-disruption recovery.

This section aims to demonstrate how the ResQ-IOS framework can be utilized to identify the optimal recovery strategy, minimizing the total recovery cost. To identify the optimal recovery strategy, a numerical experiment is designed and conducted for the seismic resilience assessment of Shelby County after an earthquake with a magnitude of 7.7 and an epicenter that was introduced in Section 3.2 (reference scenario in Table 3.5). This experiment considers 27 portfolios for the availability of

repair packages and 10 cases for the availability of truck-mounted mobile generators in the water network introduced in Section 3.3.3. In order to perform the cost analysis, a function calculating the total cost of the post-disaster recovery for an urban community is defined. The total cost function comprises the community disruption cost, restoration cost of failed components, and implementation cost of CRESs. This cost function can be expressed as follows:

$$Total\ Cost\ = Disruption\ Cost + Restoration\ Cost + \ Implementation\ Cost \quad (E.96)$$

$$Disruption\ Cost = UC_{SoCIS}. \sum_{i \in CIS} \omega_i \,. \int_{t_E}^{t_R} \left(\frac{C_{sys}^{pre,i}(t)}{D_{sys}^{pre,i}(t)} - \frac{C_{sys}^{post,i}(t)}{D_{sys}^{post,i}(t)} \right) dt \quad (E.97)$$

$$Restoration\ Cost = UC_{RP}. \sum_{i \in CIS} L_i \,. \int_{t_E}^{t_R} dt \quad (E.98)$$

$$Implementation\ Cost = UC_{BS}. \sum_{i \in CIS} Nr_i^{BS} \,. \int_{t_E}^{t_R} dt \quad (E.99)$$

The total recovery cost is formulated to consider the recovery duration and joint accumulated loss of resilience simultaneously as two parameters influencing the minimum total recovery cost. These two parameters prevent finding trivial solutions for minimum recovery cost. Therefore, the total recovery cost can be computed as follows:

$$\begin{aligned} &Total\ Recovery\ Cost\ (TRC) \\ &= UC_{SoCIS}. \sum_{i \in CIS} \omega_i \,. \int_{t_E}^{t_R} \left(\frac{C_{sys}^{pre,i}(t)}{D_{sys}^{pre,i}(t)} - \frac{C_{sys}^{post,i}(t)}{D_{sys}^{post,i}(t)} \right) dt \\ &+ UC_{RP}. \sum_{i \in CIS} L_i \,. \int_{t_E}^{t_R} dt + \ UC_{BS}. \sum_{i \in CIS} Nr_i^{BS} \,. \int_{t_E}^{t_R} dt \end{aligned} \quad (E.100)$$

where UC_{SoCIS} denotes the unit cost of the SoCIS-ALR metric. UC_{RP} and UC_{BS} are the daily unit cost of the repair package and backup system, respectively. L_i represents the availability level of repair packages in the respective infrastructure network. Nr_i^{BS} denotes the number of backup systems in the respective infrastructure network. The information related to other variables and indices is given in the nomenclature section.

The cost analysis of the numerical experiment is carried out for three levels of urban density. To this end, three cost profiles are considered for low-, medium-, and high-density urban communities. The details of the cost profiles are given in Table 3.6. The unit costs for the profile of the low-, medium-, high- density urban infrastructure systems are not realistic values for the case study. They are assumed for demonstration purposes, assuming that denser urban systems are going to be costlier to recover.

Table 3.6. The cost profiles of the low-, medium-, and high-density urban communities.

Urban Community	Unit cost of the SoCIS-ALR metric UC_{SoCIS}	Daily unit cost of the repair package UC_{RP}	Daily unit cost of the backup system UC_{BS}
Low-density	USD 150,000	USD 30,000	USD 8,000
Medium-density	USD 400,000	USD 30,000	USD 8,000
High-density	USD 1,250,000	USD 30,000	USD 8,000

The results of this numerical experiment discover three optimal quantities. These three quantities are as follows:

1- Optimal portfolio for repair packages: the cost analysis of post-disruption recovery scenarios identifies the optimal repair package portfolio for minimizing the total cost of the community recovery. Consequently, the optimal portfolio determines the optimal availability level of repair packages in infrastructure systems for restoring the damaged components (e.g., the optimal number of repair teams).

2- Optimal number of backup systems: in the case of deploying backup systems, the cost analysis of recovery scenarios specifies the optimal number of backup systems (e.g., mobile generators) that can be utilized to minimize the total recovery cost.

3- *Optimal total recovery cost*: the value of this quantity is the minimum total cost for the full recovery of an urban community after an extreme event. The total recovery cost consists of the community disruption cost, restoration cost of

damaged infrastructure components (e.g., cost of providing repair packages), and implementation cost of CRESs (e.g., deploying backup systems).

According to the results of the numerical experiment considering the cost profile of low-density urban communities (Fig. 3.22), the optimal recovery strategy is to deploy three truck-mounted mobile generators in the water network and simultaneously follow the repair package portfolio No.14. The optimal portfolio (i.e., No.14) states the optimal availability level of repair packages in all power, natural gas, and water networks is medium.

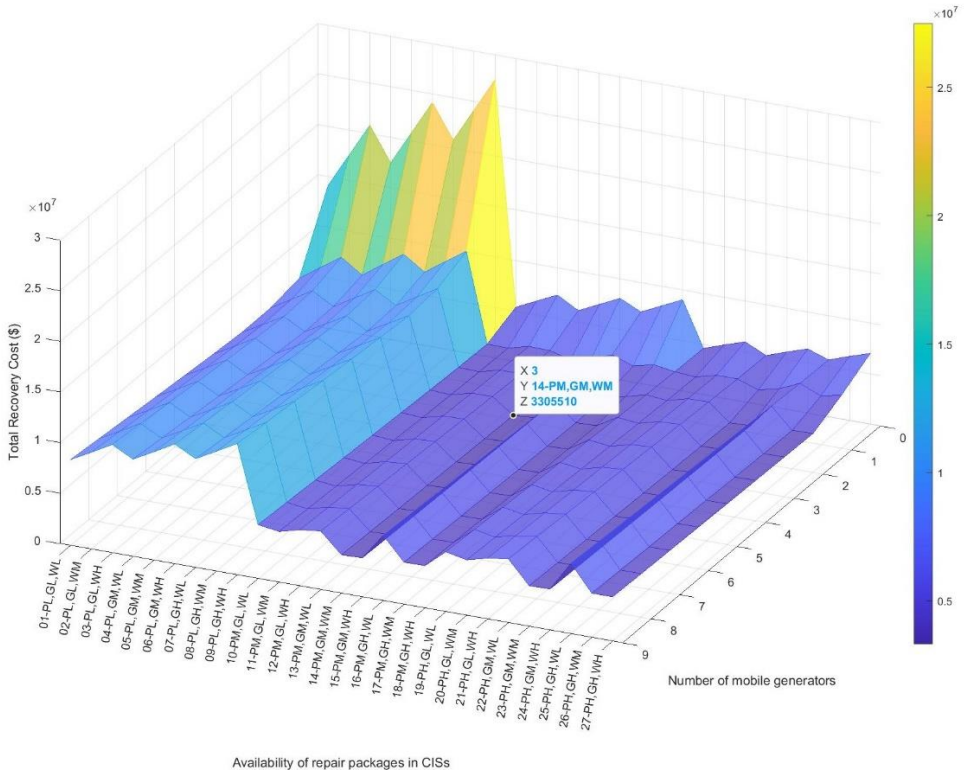

Fig. 3.22. The optimal recovery strategy in case of applying the low-density urban community cost profile to the Shelby County case study.

As shown in Fig. 3.23, performing the numerical experiment with the cost profile of medium-density urban communities indicates that the optimal strategy for the recovery of the Shelby County urban community is to employ two truck-mounted mobile generators and implement the repair package portfolio No.23, stating the optimal availability levels of repair packages in power, natural gas, and water networks are high, medium, and medium, respectively.

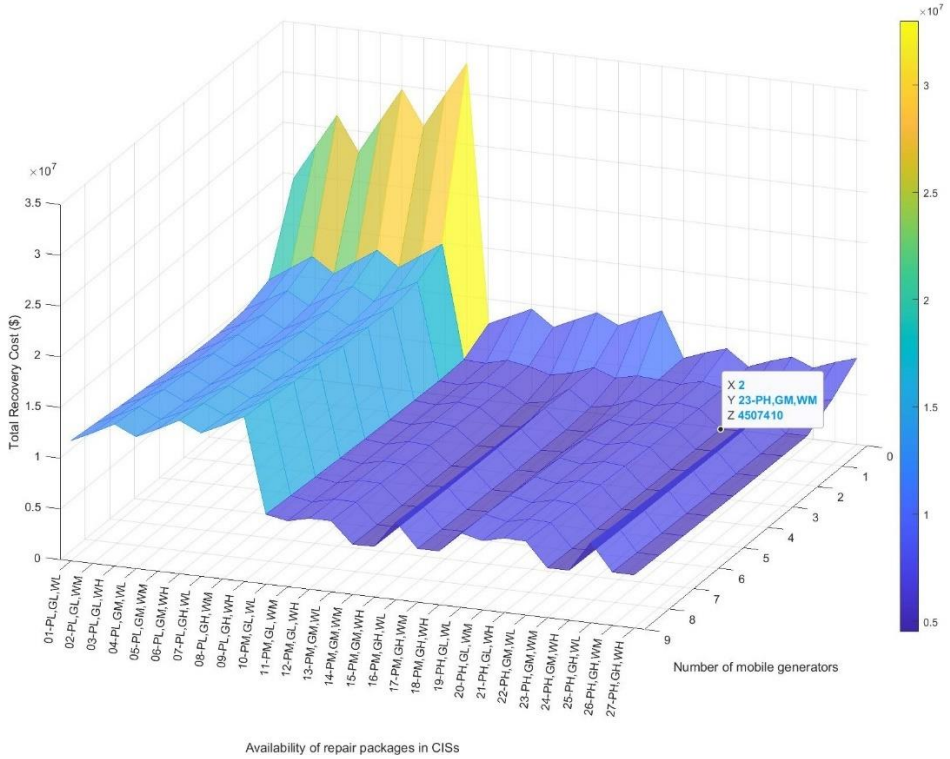

Fig. 3.23. The optimal recovery strategy in case of applying the medium-density urban community cost profile to the Shelby County case study.

The numerical experiment results for a high-density urban community are illustrated in Fig. 3.24. The recovery strategy minimizing the total cost is to deploy six truck-mounted mobile generators for water facilities and pump stations and adopt portfolio No.24, indicating the optimal availability levels of repair packages in power, natural gas, and water networks are high, medium, and high, respectively. The summary of the numerical experiment results conducted for different urban density levels is given in Table 3.7.

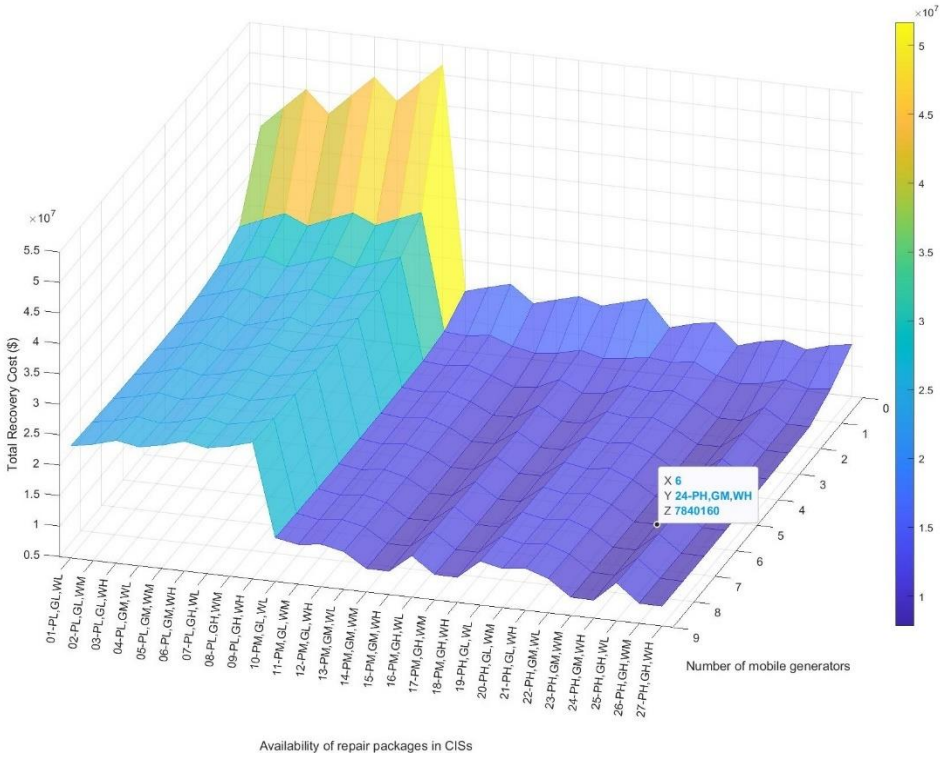

Fig. 3.24. The optimal recovery strategy in case of applying the high-density urban community cost profile to the Shelby County case study.

Table 3.7. The summary of the numerical experiment results conducted for low-, medium-, and high-density urban communities.

Urban community	Optimal portfolio	Optimal No. of mobile generators	Optimal total recovery cost (Minimum)	Recovery duration (days)
Low-density	14-PM,GM,WM	3	USD 3,305,510	12
Medium-density	23-PH,GM,WM	2	USD 4,507,410	12
High-density	24-PH,GM,WH	6	USD 7,840,160	11

The findings of this numerical experiment indicate that the density of urban communities can influence the selection of the optimal recovery strategy with the minimum total cost. Based on the experiment results, the high cost of disruption by extreme events in high-density urban communities economically justifies deploying a large number of R&M teams and implementing the CRES by using more backup systems to accelerate the post-disruption recovery of the urban community. A low-density community like a rural area can follow a less-costly CRES and deploy fewer R&M teams and backup systems for recovery after the extreme event.

3.6. Conclusion

In this chapter, the application of the ResQ-IOS framework for modeling, optimizing, and quantifying the resilience of urban communities was discussed. After introducing the Shelby County case study, the seismic resilience of the urban community in the case study was assessed and analyzed. In the next step, implementing three pre-disruption, peri-disruption, and post-disruption CRESs was investigated, and the impacts of those CRE strategies in improving the urban disaster resilience of Shelby County were appraised. The parametric analysis of Shelby County's resilience to seismic hazards was conducted to examine the role of six parameters in urban disaster resilience. In the final section of this chapter, a cost analysis was carried out for three levels of urban density to identify the optimal recovery strategy with minimum total cost. The next chapter will discuss the application of the ResQ-RDSS, the extension of the ResQ-IOS framework, for the resilience assessment of rural communities.

Chapter Four

ResQ-RDSS: An Extension of the ResQ-IOS For Rural Community Resilience Assessment

This chapter introduces the ResQ-RDSS, a Resilience Quantification-based Regional Decision Support System for formulating off-grid electrification strategies as Community Resilience Enhancement Strategies (CRESs) to enhance the availability and resilience of electricity access for rural communities. In this chapter, the structure of the ResQ-RDSS comprising four modules is described. To demonstrate the ResQ-RDSS's ability to help devise resilient regional electrification strategies, the rural settlements in Birjand County, Iran, exposed to earthquake and flood risks are selected as the case study. The material of this chapter is directly or indirectly based on the following paper:

• Hamed Hafeznia and Božidar Stojadinović, “Resilience-based decision support system for installing standalone solar energy systems to improve disaster resilience of rural communities,” submitted to Energy Strategy Reviews.

4.1. Problem statement and motivation

A considerable percentage of the world's population (about 754 million people in 2021 [101]) suffers from the lack of access to electricity, known as energy poverty [102], [103]. Most of the affected people live in rural areas of emerging economies. Access to electricity has an essential role in the socioeconomic development of rural communities and can reduce poverty locally and nationally in developing countries [104], [105], [106], [107]. The efficacy and environmental footprint of the traditional energy provision methods often used by people living in distant rural areas for activities such as cooking, heating, and illumination of their houses are not satisfactory. The primary reason is fossil fuels: they cause environmental degradation and pollution, and their prices fluctuate unpredictably [108], [109].

Electrifying rural communities is the principal policy adopted by many governments to provide a stable and reliable supply of electric energy to the people living in villages. Considering that resilience has a pivotal role in the future planning and development of Critical Infrastructure Systems (CISs), Resilient Rural Electrification (RRE) is imperative. There are two main rural electrification strategies: the first is to expand the power grid throughout the rural areas, and the second is to set up stand-alone power supply systems in the villages. In addition to the power grid's stability problems, extending the power network to rural areas often confronts financial and technical constraints [110], [111]. Considering the high costs of the power grid's extension to such distant areas, the second strategy, deploying stand-alone power systems, is often the better choice to speed up the rural electrification programs [112], [113], [114], [115]. However, utilizing fossil fuel-based stand-alone power systems may not be a resilient rural electrification strategy alternative: the operation of such autonomous power systems requires a secure and stable supply of fossil fuel, as well as continuous technical maintenance. These are subject to unpredictable price fluctuations, geopolitical tensions, natural hazards, technical issues related to the supply chain sector, as well as failures in the transmission network or road closure due to natural disasters such as extreme weather events and earthquakes. The most recent such examples (at the time of writing this doctoral dissertation) are the October 4, 2023, glacial lake outburst flood in Sikkim and West Bengal, India [116], and the October 7, 11, and 15, 2023 earthquake sequence in Herat, Afghanistan [117]. In addition to the

lack of disaster resilience, fossil fuel stand-alone power systems pollute the often-pristine rural environment.

Raising public awareness of climate change and natural disaster resilience issues gives Renewable Energy Sources (RESs) a significant role in acting as a sustainable Community Resilience Enhancement Strategy (CRES) in plans for rural energy supply in many countries. RES-based stand-alone electric power systems are an environmentally friendly option to mitigate the impact of Greenhouse Gas (GHG) emissions by the power generation sector. Renewable Energy (RE)-based autonomous power systems are more reliable and effective for electrifying regions with dispersed populations where providing fossil fuels is demanding [118], [119].

Since considering resilience in rural electrification planning can bring about longer techno-economic viability of rural power supply projects, the motivation for the work done in this chapter is to specify a resilient electrification solution most suitable for each village: installing stand-alone systems or connecting to the power grid, whichever is more resilient over the planned use period. To this end, the disaster resilience of rural areas should be quantified in the first instance. Then, the implementation of different electrification strategies is evaluated as CRESs to appraise the improvement in the resilience of rural communities. Considering the capabilities of the ResQ-IOS framework demonstrated in Chapter 3 and based on the experiences from the parametric analysis of Shelby County's urban disaster resilience, the ResQ-IOS framework, developed in Chapter 2, can be employed to quantify the resilience of rural communities against natural hazards and carry out the feasibility study of implementing CRESs. In other words, the purpose of this chapter is to develop a resilience-based framework as a regional decision support system to advise resilient electrification planning for improving electricity access in rural areas. This framework is designed based on the capabilities of the ResQ-IOS framework to conduct feasibility studies on implementing pre-disruption resilience enhancement strategies with an application to rural communities. Similar to the feasibility studies carried out by ResQ-IOS for Shelby County's urban community at the city level, the new framework aims to enhance robustness and rapidity indicators for rural communities against multi-hazards. It can be concluded that the framework of this chapter is an extension of the ResQ-IOS framework with a broader scope of application to rural settlements at the

county level. Hence, both frameworks address the dissertation's objectives that are as follows:

- Integrate optimization into the simulation-based methodology of the resilience assessment framework to benefit from simultaneous resilience quantification and improvement.
- Model and conduct the feasibility study of implementing Community Resilience Enhancement Strategies (CRESs).
- Incorporate a multi-hazard resilience assessment framework into the regional development planning.

4.2. State-of-the-art review

The number of studies about stand-alone renewable energy systems indicates the high suitability of this type of power system for scattered rural communities. After a systematic review of the literature on RE-based stand-alone systems, the published research studies can be classified into three groups as follows:

1- The first group of studies addressed the assessment of RESs for installing power systems in different countries. These studies evaluated the technical potential of utilizing RE-based power systems and, in case studies, produced maps showing the regions with higher suitability for installing such power systems. Principally, the research was carried out in Geographic Information System (GIS) environments, and in some cases, the Multi-Criteria Decision Making (MCDM) methods were used. This group of studies considered two types of RE-based power systems based on the connectivity to the power grid: stand-alone (off-grid) and utility-scale (on-grid). The representative papers in this group are [120], [121], [122], [123], [124], [125], [126], [127], [128], [129].

2- The second group includes studies that investigated national energy policies worldwide, typically in regional case studies, to identify the barriers to achieving the goals of sustainable development programs. Considering socioeconomic, technical, and cultural conditions, these studies propose strategies to enhance the utilization of RE-based power systems. Papers [130], [131], [132], [133], [134], [135], [136], [137], [138] are classified in this group.

3- The third group comprises research studies focused on the techno-economic analysis and performance optimization of RE-based stand-alone power systems. The primary purpose of these studies is to find the optimal size of the components of RE-based power systems. Aspects of the employed objective functions include maximizing system reliability, minimizing total costs, and minimizing GHG emissions. Some of the papers in this group include [139], [140], [141], [142], [143], [144], [145], [146], [147], [148].

Even though many studies investigated the deployment and use of hybrid RE-based power systems from technical, socio-economical, and environmental standpoints, the implementation of stand-alone electrification projects has not been successful in a remarkable number of cases [149]. A systematic survey of the literature indicates that such implementations did not consider the resilience of the deployed RE-based power systems, a key part of the long-term planning of infrastructure systems.

This chapter of the doctoral dissertation attempts to fill this implementation gap by presenting a Resilience Quantification-based Regional Decision Support System (ResQ-RDSS) for the electrification of rural communities. The ResQ-RDSS considers connecting to the power grid or installing off-grid Solar Energy (SE) power systems as the two main strategies for electrifying remote villages.

4.3. Structure of the ResQ-RDSS

The ResQ-RDSS consists of four modules, namely: Spatial Techno-Economic Assessment (STEA), Earthquake-induced Risk Assessment (ERA), Flood-induced Risk Assessment (FRA), and Decision Maker (DM). The task of the STEA, ERA, and FRA modules in the ResQ-RDSS is to classify the villages in a rural region into two sets with respect to two different electrification strategies, on-grid or off-grid. The ERA and FRA modules utilize ResQ-IOS to quantify the resilience of rural communities to natural hazards. The resilient electrification strategy for the first set of villages is installing stand-alone solar photovoltaic (PV) power systems, while connecting villages to the regional power grid is the better strategy for the second set. Each module carries out the village classification process according to its own criterion for selecting the resilient electrification strategy. As a result, these three modules generate

six different, possibly overlapping, sets of villages. The role of the DM module is to determine the electrification strategy for each village in the region with respect to the classification results produced by STEA, ERA, and FRA modules using set theory. In fact, the selected electrification strategy is the most suitable pre-disruption CRES to enhance the rural community's resilience against earthquake and flood hazards. The workflow of the proposed ResQ-RDSS for improving the electricity access of rural communities is shown in Fig. 4.1. The modules of ResQ-RDSS are described next.

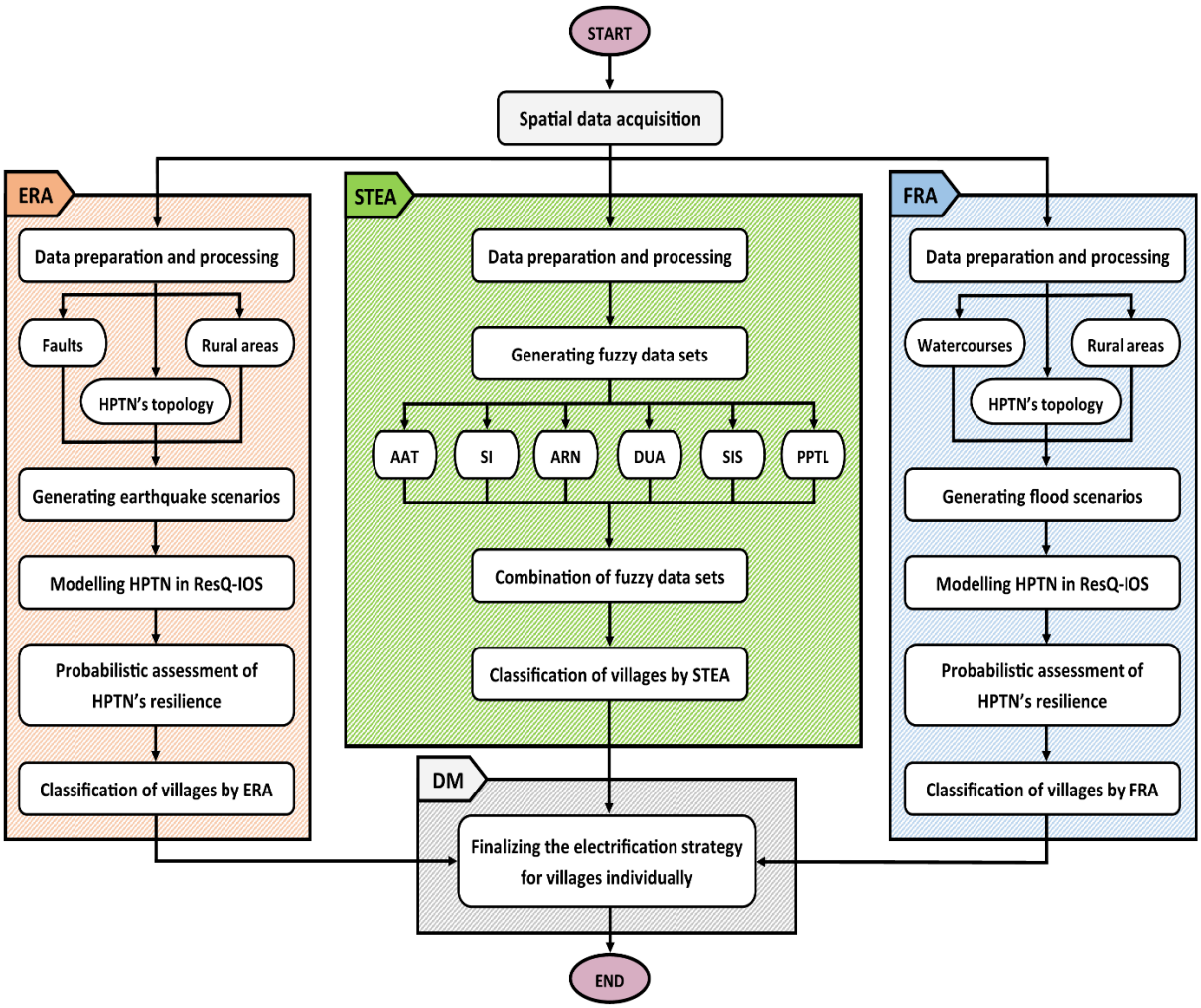

Fig. 4.1. The workflow of the ResQ-RDSS.

4.3.1. Spatial Techno-Economic Assessment (STEA)

Since the technical performance and economic viability of solar PV power systems are affected by geospatial factors, the STEA module aims to consider these factors and identify villages in rural areas suitable for installing stand-alone PV power systems by quantifying several geospatial suitability aspects. The purpose of the STEA module is to perform the techno-economic assessment of implementing two types of pre-disruption CRESs in rural settlements, aiming to improve the robustness and redundancy indicators of rural power supply (connection to the regional grid or installing stand-alone solar PV systems).

To create an accurate set of geospatial factors influencing the performance of stand-alone PV power systems, the literature on the site selection of solar power systems was surveyed. For this purpose, six criteria (i.e., geospatial factors) were selected to specify suitable villages for the deployment of autonomous solar power systems. The criteria considered for the spatial techno-economic assessment are examined next.

4.3.1.1. Average Annual Temperature (AAT)

Increased operating temperature of PV modules adversely affects the performance of photovoltaic power systems and results in lower power generation efficiency. Considering the Average Annual Temperature (AAT) as a criterion for evaluating the suitability of villages can enhance the performance efficiency of stand-alone PV systems and mitigate the investment risks of solar PV installation projects [150]. In the STEA module, villages with lower average annual temperatures are considered to be more suitable for installing solar PV systems. A decreasing linear fuzzy membership function is defined to rate the case study's areas regarding the average annual temperature. A fuzzy value of one is considered for areas with AAT less than 20 degrees Celsius. Areas with AAT above 25 degrees Celsius are given a fuzzy value of zero. The fuzzy value for other areas is linearly mapped between one and zero (Fig. 4.2-A).

4.3.1.2. Solar Irradiance (SI)

The amount of solar irradiance received by PV modules is an essential factor in the design process of photovoltaic power systems. This factor (i.e., received solar irradiance) can be influenced by parameters such as dust, humidity, cloudiness, sun angle, and geographical coordinates of the PV installation site [151], [152], [153]. Global Horizontal Irradiance (GHI) is the quantity applied to measure the solar irradiance for installing PV systems. GHI measures the total amount of shortwave radiation received from above by a horizontal surface on the ground [123]. Since the power generation of photovoltaic systems highly relies on the amount of received solar irradiance, it is more productive and reliable to set up stand-alone PV systems in rural areas with higher received GHI. To rate the rural areas regarding received GHI using a fuzzy logic-based method, an increasing linear membership function is defined, which starts at 4.9 kWh/m2/day [154] and flattens at 6 kWh/m2/day [123]. The areas with GHI values less than 4.9 and greater than 6 kWh/m2/day are assigned fuzzy values of zero and one, respectively. Other GHI values between 4.9 and 6 will linearly be transformed to a value between zero and one (Fig. 4.2-B).

4.3.1.3. Accessibility to the Road Network (ARN)

In general, the proximity of villages to the road network can accelerate the implementation of on-grid rural electrification programs due to the lower transportation cost of technical equipment and staff. Installing stand-alone solar PV power systems in villages situated in impassable locations with no or inadequate access to the regional road network is a more economical electrification strategy since expanding the power grid to such villages is costly and time-consuming. The STEA module considers the villages' distance from the road network as a criterion for spatial planning: villages farther from a road are more suitable for using off-grid PV power systems. To this end, a sigmoid function is defined to assign the degree of fuzzy membership to villages. This function gives values greater than zero to villages whose distance from the road equals or exceeds 2 km. If the distance of the village from the nearest road is 15 km or more, it will be assigned the value of one [141] (Fig. 4.2-C).

4.3.1.4. Distance to Urban Areas (DUA)

The proximity of villages to urban areas is another determining factor in rural electrification programs. Connection to the regional power grid is a more probable electrification strategy for villages near the urban areas. In fact, most cities in emerging economies have future development plans that include providing access to essential services such as electricity, clean water, and natural gas to near-by villages, while the remote villages are given lower priorities. In the STEA module, the villages that are more distant from urban areas are deemed more suitable for establishing stand-alone PV power systems. To perform the fuzzy evaluation of regions surrounding cities, an increasing sigmoid function is defined with a fuzzy value of zero for locations closer than 1 km from the boundary of the city and a fuzzy value of one for locations more than 25 km away [141] (Fig. 4.2-D).

4.3.1.5. Slope of Installation Site (SIS)

The slope of the PV system site is an economic factor considered by the STEA module. The total cost of establishing a solar power system highly depends on the slope of the installation site. A steep site increases the construction costs, including land levelling and installation costs of the solar system’s structures and equipment. Moreover, steep slopes are more prone to landslides. Flat and low-slope lands are, therefore, considered as desirable locations for installing PV power systems in the STEA module to reduce construction costs, secure the site of the solar PV system, and maintain the safety of its equipment against landslide hazards. Then, a linear function is used to evaluate the slope of the installation site such that the locations with a slope higher than 36.4%, entirely unsuitable for PV system installation, receive a fuzzy value of zero. Locations with a slope of up to 7% get a fuzzy value of one [141]. Others are linearly mapped to a value from one to zero (Fig. 4.2-E).

4.3.1.6. Proximity to Power Transmission Lines (PPTL)

Proximity to power transmission lines is another economic factor in rural communities' electrification planning. Installing stand-alone solar power systems in villages close to power transmission lines is not economically justified. Thus, installing stand-alone solar systems is the more economical strategy for supplying the power

demand of rural communities far away from the transmission network. The STEA module considers villages distant from power lines as more suitable locations for deploying off-grid solar PV systems. A sigmoid function is applied to evaluate the fuzzy membership degree of the villages with respect to this criterion. The villages located at a distance less than 800 m from the power transmission lines have a fuzzy value of zero, while 5 km or further from a power transmission line are given a value of one [141] (Fig. 4.2-F).

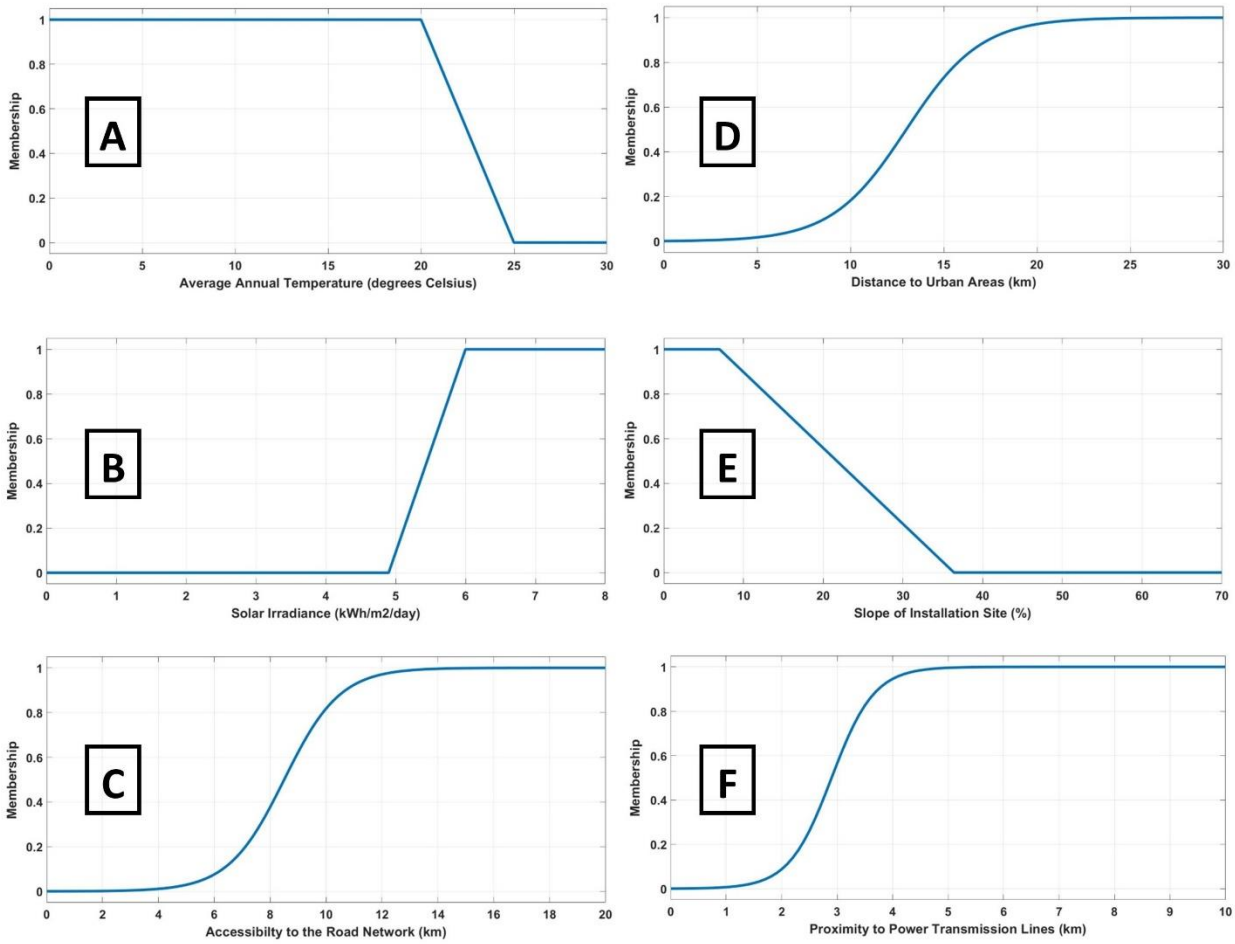

Fig. 4.2. Fuzzy membership functions used for six geospatial factors of the STEA module.

4.3.1.7. Implementing the STEA module

The first step of implementing the STEA module is to prepare the required spatial data and digital maps of rural areas considered for evaluation using the ResQ-RDSS. The second step is to produce the rasterized maps by converting the vector layers of the maps into raster data layers. The third step is to generate the fuzzy data set for

each of the six criteria considered in the STEA module, resulting in six fuzzy data sets. To create the fuzzy sets, the fuzzy membership functions defined for each criterion of the STEA are evaluated in each pixel of the rasterized map of the region. The assigned fuzzy value indicates the membership degree (or fuzzy grade) of the pixel in the fuzzy set for the concerned criterion, with zero being the lowest and one the highest membership degree. The last step of the STEA is to combine the fuzzy sets for the six criteria using the Fuzzy Gamma Operator (FGO) comprising fuzzy product and sum operators as follows:

$$\varphi_{sum} = 1 - \left(\prod_{n=1}^{6} (1 - \varphi_n) \right) \qquad (E.101)$$

$$\varphi_{product} = \prod_{n=1}^{6} \varphi_n \qquad (E.102)$$

$$\varphi_{FGO} = (\varphi_{sum})^{\tau} \times (\varphi_{product})^{1-\tau} \qquad (E.103)$$

where φ_n is the pixel's fuzzy grade (membership degree) in the fuzzy data set of the n^{th} criterion. The constant parameter τ has a value between zero and one. A τ value closer to one results in a higher combined suitability level for utilizing stand-alone solar PV systems as the electrification strategy. In other words, increasing the constant parameter τ value leads to a less conservative, more lenient, spatial techno-economic assessment of villages. Ultimately, the STEA module classifies the considered villages into two groups with different electrification strategies based on a threshold level of their Combined Fuzzy Grade (CFG) (a value between 0 and 1) and the associated value of the constant parameter τ.

4.3.2. Earthquake-induced Risk Assessment (ERA)

The occurrence of an earthquake may disrupt the well-functioning of human settlements by destroying structures and damaging the components of infrastructure systems. The purpose of the Earthquake-induced Risk Assessment (ERA) module is to evaluate the seismic resilience of the power transmission network. The ERA module considers a Hypothetical Power Transmission Network (HPTN) extended to all villages

in the case study; thus, all villages are assumed to be electrified by connecting to the regional power grid, i.e., no village is assumed to utilize an off-grid photovoltaic system for power supply.

To implement the probabilistic resilience analysis of the hypothetical power network against the earthquake hazard, the ERA module defines a set of earthquake scenarios with a varying return period between 475 and 2475 years (i.e., the scenario earthquake has an intensity with a probability of exceedance between 10% and 2% in any 50-year period) and with epicenters on various earthquake faults pertinent to the case study region. The ERA module applies the Latin Hypercube Sampling (LHS) method to reduce the computational burden of the probabilistic HPTN resilience analysis. As the ResQ-IOS's capabilities demonstrated in Chapters Two and Three, the ResQ-IOS [155] framework is utilized to model and evaluate the resilience of the regional HPTN in the selected earthquake scenarios. ResQ-IOS is a powerful and versatile computational tool for modeling, quantifying, and analyzing the resilience of interdependent critical infrastructure systems against natural disasters [155].

The output of the ERA module is the classification of villages into two groups with respect to the HPTN resilience metric. The selected resilience metric considers the required time for restoring the power supply of villages that experience a lack of access to electricity after the earthquake and is consistent with the functional recovery metrics recommended by the NIST SP-1190 report [57]. This resilience metric is computed using ResQ-IOS as explained in Chapter 2 and also shown in Chapter 3, Section 3.2. Since the ERA module conducts the probabilistic assessment of the HPTN's seismic resilience, classifying the villages considers the uncertainties in the resilience assessment process. Accordingly, if it takes N_E days since the occurrence of the earthquake to restore the power supply to a village, and this situation (lack of electricity access for at least N_E days) occurs in L_E percentage of the total number of examined earthquake scenarios, then this village is classified to be suitable for electrification by installing off-grid solar PV systems. Otherwise, connection to the regional power grid is the resilient electrification strategy for that village. Parameters N_E and L_E are determined by the earthquake vulnerability of the rural areas, characteristics of the power grid, the economic and societal conditions of the region, and stakeholders' priorities.

4.3.3. Flood-induced Risk Assessment (FRA)

Flood is a type of natural hazard that frequently occurs in rural areas. Damage to power lines and potable water pipelines and the destruction of buildings and roads, such as bridge collapses, are examples of the floods' aftermath. To mitigate the negative impacts of floods on human settlements, it is essential to improve the resilience of civil infrastructure systems against flood hazards. The task of the Flood-induced Risk Assessment (FRA) module is to assess the resilience of the Hypothetical Power Transmission Network (HPTN) to floods. The HPTN in the FRA module is the same as in the ERA module.

The FRA module creates a set of flood scenarios to carry out the probabilistic resilience analysis of the hypothetical transmission network against the flood. In each flood scenario, some watercourses are assumed to overflow and disconnect the power lines that intersect them. To reduce the computational cost of the probabilistic resilience analysis of the HPTN, the Latin Hypercube Sampling (LHS) method is used to define various flood scenarios. Modeling and resilience assessment of the hypothetical power transmission network to flood scenarios are conducted by the ResQ-IOS, developed in Chapter 2 [155].

The FRA module aims to classify the villages into two groups. The resilience metric of the FRA module is the restoration time for the power supply of the villages suffering from the lack of electricity access after the flood. This resilience metric is similar to the ERA module's metric. The details of the resilience metric are described in Chapter 2. Accordingly, if the power supply of a village has not been restored N_F days after the flood occurrence, and this situation (lack of access to electricity for at least N_F days) occurred in L_F percentage of the examined flood scenarios, then establishing an off-grid PV power system is the resilient strategy for electrifying this village. Otherwise, it is more resilient to electrify that village by connecting it to the power grid. Parameters N_F and L_F are determined by the flood vulnerability of the rural areas, characteristics of the power grid, the economic and societal conditions of the region, and stakeholders' priorities.

4.3.4. Decision Maker (DM)

The aim of the Decision Maker (DM) module is to finalize the electrification strategy decision for each village in the region of interest, considering the classification results produced by the STEA, ERA, and FRA modules. To recapitulate, the STEA module assigns a suitable electrification strategy to each village based on its fuzzy value of the combined spatial techno-economic criteria. In other words, the STEA module specifies the most effective pre-disruption CRES for each village from technical and economic aspects. In contrast, the ERA and FRA modules, applying ResQ-IOS and using its capability for computing instantaneous and cumulative resilience metrics, classify the villages into two groups based on their earthquake and flood resilience, respectively, considering the statistics of the electric power restoration time for a village in the examined earthquake and flood scenarios.

The output of the STEA, ERA, and FRA modules are three pairs of complementary sets of villages. These sets are typically different and may be overlapping because the classification in these modules is conducted independently. Hence, to choose the resilient electrification strategy for an individual village, set theory is applied to create a decision space containing all combinations of the classification decisions. Based on the union and intersection of sets, 17 possible decision sets exist for the final classification of the villages in the region of interest. The decision space of the DM module is shown in Fig. 4.3, with the convention that the STEA, ERA, and FRA sets contain the villages whose suitable and resilient electrification strategy is the off-grid installation of a solar PV system.

Although the Decision Maker module can take various approaches for choosing the resilient electrification strategy, the most stringent approach is that a village is electrified by installing an off-grid solar PV system if it has been classified as suitable and resilient for such electrification by the STEA, ERA, and FRA modules simultaneously (i.e., it is in the intersection decision set $D(STEA \cap ERA \cap FRA)$ for the three-modules strategy in Fig. 4.3). In contrast, the most lenient decision is $D(STEA \cup ERA \cup FRA)$ in Fig. 4.3, where a village is electrified using an off-grid solar PV system if it is classified as either suitable or resilient by any of the STEA, ERA or FRA modules.

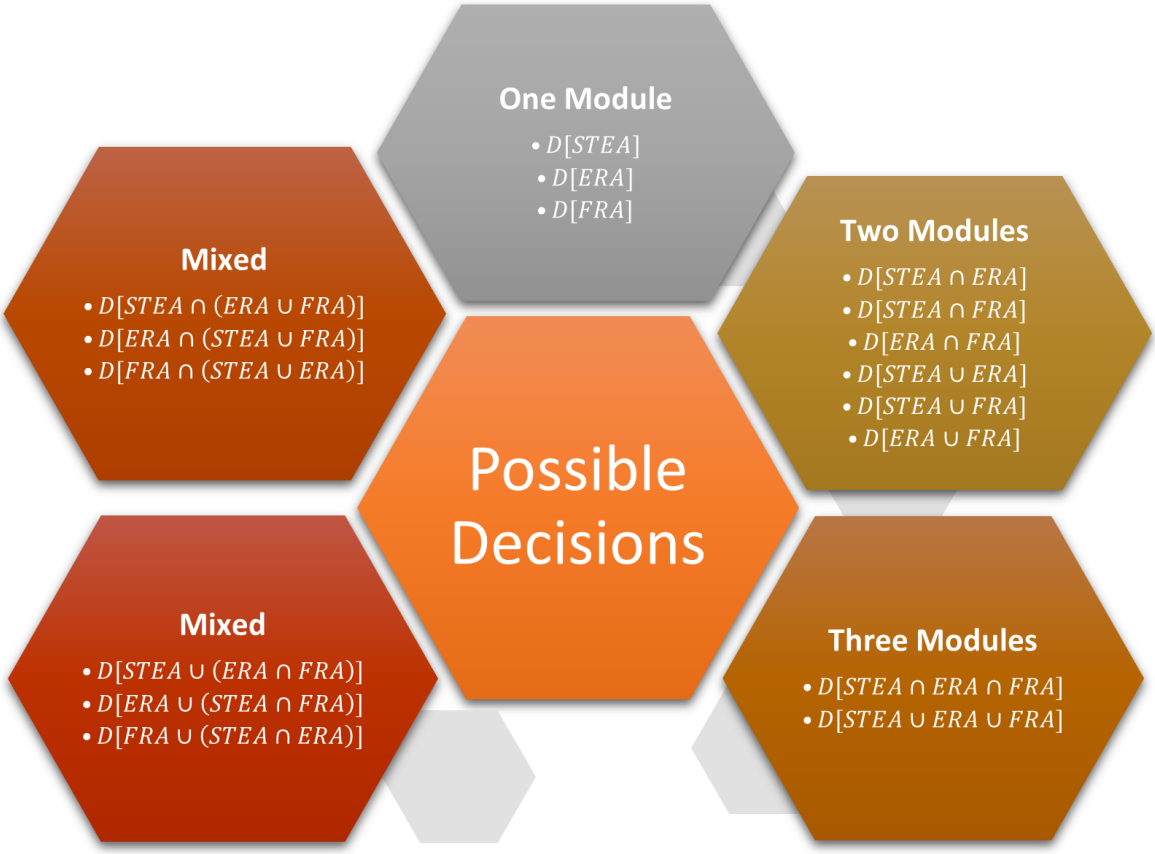

Fig. 4.3. The decision space for the Decision Maker (DM) module.

4.4. Case Study: Rural settlements in Birjand County

The rural areas of Birjand County in South Khorasan Province, located in the east of Iran (Fig. 4.4), are selected to demonstrate the ResQ-RDSS in a case study. Notably, the epicenters of the October 2023 Herat sequence earthquakes are about 300 km away, a reminder that Birjand County is in a high seismic hazard zone [156]. The residents of Birjand County's villages are also exposed to flood hazards [157], [158].

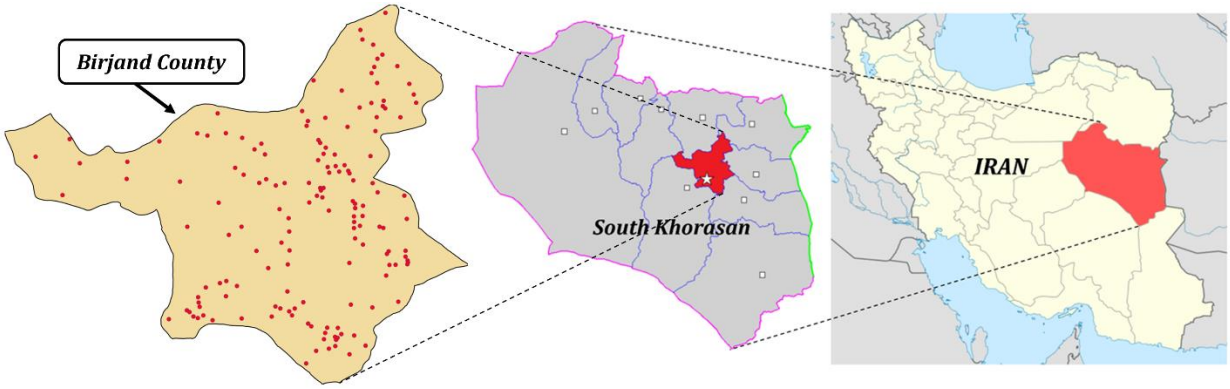

Fig. 4.4. The Birjand County case study region (the 158 villages are marked with red points).

The geographical position of Birjand County's capital is 32.9 N and 59.2 E. Because of its cold arid climate, this county often has hot summers and cool winters. The total area of the county is about 4320 square kilometers. Birjand City, the capital of the county, is situated 1491 meters above sea level [123]. As Birjand County is located in the world's Sun Belt [159], this county enjoys abundant sunshine. Its annual sunshine duration is estimated at around 3200 hours (8.8 hours per day) [123]. This makes solar power an efficient and reliable renewable energy source that can be harnessed for electricity supply in the county's rural areas. This case study considers 158 villages in Birjand County to exemplify how different ResQ-RDSS modules are used to evaluate and plan resilient rural electrification. The information about the case study data sources is provided in Table 4.1. For a better understanding of the ResQ-RDSS procedure, five villages, namely villages B1, B2, B3, B4, and B5, are selected for illustration (Fig. 4.5).

Table 4.1. The sources of the case study data used in this doctoral dissertation.

Data set	Scale (Resolution)	Final projection of the data	Source	Reference
Temperature	---	UTM Zone 40N	IRIMO	[160]
Solar irradiance	GHI Solar Map © 2017 Solargis	UTM Zone 40N	Solargis	[161]
Slope	GDEM - 30 m	UTM Zone 40N	USGS	[162]
Road network	1:25000	UTM Zone 40N	INCC	[163]
Urban areas	1:25000	UTM Zone 40N	INCC	[163]
Rural areas	1:25000	UTM Zone 40N	INCC	[163]
Power lines	1:25000	UTM Zone 40N	INCC	[163]
Faults	1:25000	UTM Zone 40N	INCC	[163]
Floodways	1:25000	UTM Zone 40N	INCC	[163]

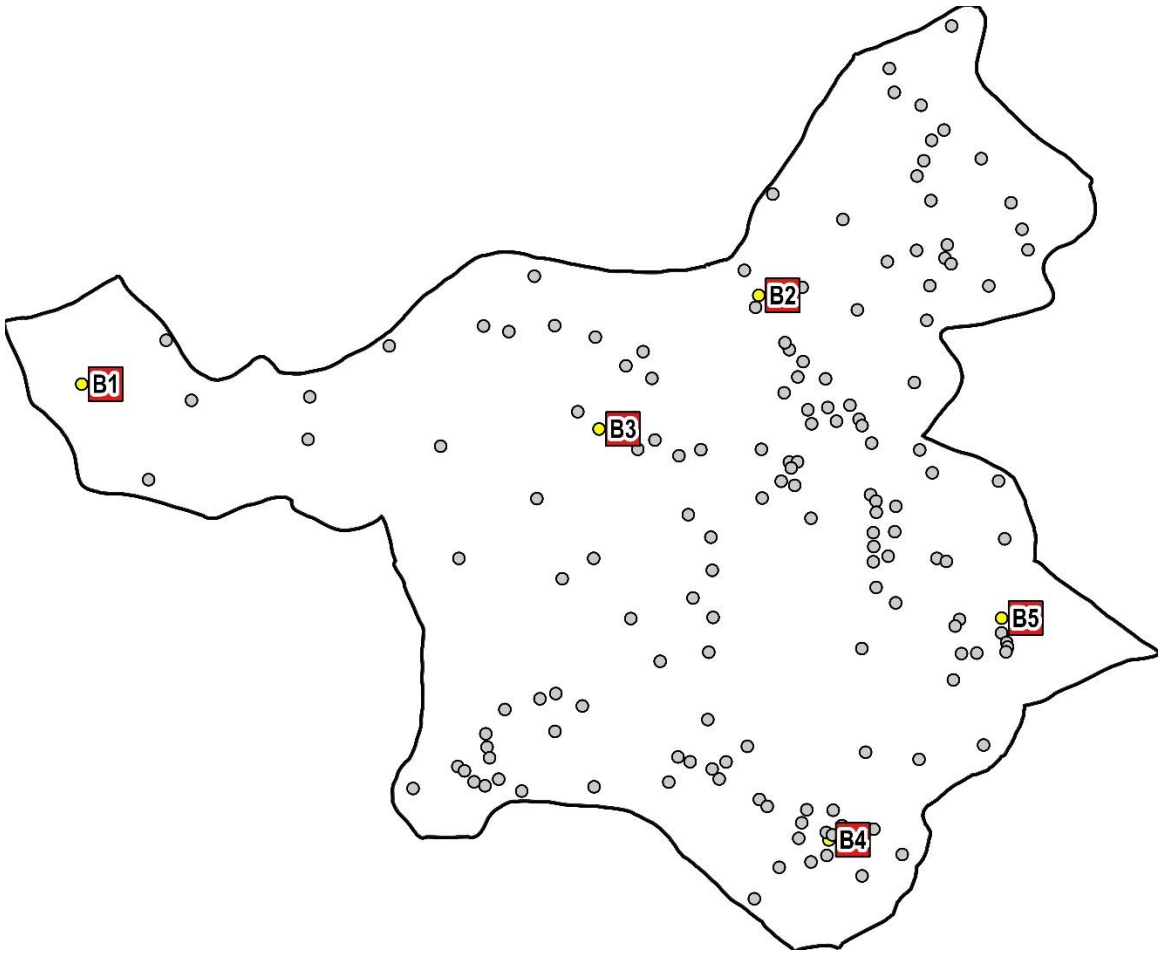

Fig. 4.5. Five selected example villages in Birjand County.

4.5. Results analysis of implementing the ResQ-RDSS

The purpose of developing the ResQ-RDSS is to enable resilient rural settlement electrification planning. To demonstrate this capability, the ResQ-RDSS is utilized to determine the resilient electrification strategy for each village in Birjand County. The STEA module spatially evaluates the techno-economic suitability of villages for installing off-grid solar PV systems. To this end, the spatial data of the case study is prepared, and then the rasterized maps are produced. In the next step, the fuzzy data set for each STEA module criterion is generated by using the respective fuzzy membership function. The output of the STEA module is the combined fuzzy data set created by the Fuzzy Gamma Operator, integrating the six fuzzy data sets of the STEA's criteria. To better understand the results of the STEA module, the combined fuzzy data set is displayed as a map, which is called the suitability map.

The suitability map for implementing the CRES, that is, the deployment of solar power systems, resulting from the spatial techno-economic assessment of the rural settlements in Birjand County, is shown in Fig. 4.6. This suitability map displays the villages that are desirable sites for establishing off-grid solar PV systems based on classification results by the STEA module. The villages identified as suitable locations for deploying stand-alone solar systems are marked with yellow points. In this map, villages have been classified according to their Combined Fuzzy Grade (CFG), computed by combining six fuzzy datasets using the Fuzzy Gamma Operator (FGO) with a constant parameter τ value of 0.8. The villages whose combined fuzzy grades are higher than 0.4 are classified to be electrified by installing off-grid solar PV systems. In contrast, connecting to the regional power grid is the resilient electrification strategy for villages with a combined fuzzy grade equal to or less than 0.4. These villages are marked with grey points on the suitability map (Fig. 4.6).

The classification by the STEA identifies 38 villages (out of 158) as suitable for installing off-grid solar PV systems to supply rural electrical demands. The combined fuzzy grade for these villages is larger than 0.4 (CFG > 0.4), indicating good geolocation suitability as well as technical and economic performance. If the constant parameter τ value is set to 0.6, a smaller number of villages would be classified as suitable for installing off-grid solar PV systems, leading to stricter decision-making. Among the five sample villages, solar PV systems installed in villages B1, B3, and B5

would have higher technical efficiency than those installed in villages B2 and B4. Higher efficiency in generating electricity from the received solar irradiance, long distances to power transmission lines, and inadequate access to the regional road network are the common characteristics of the villages B1, B3, and B5.

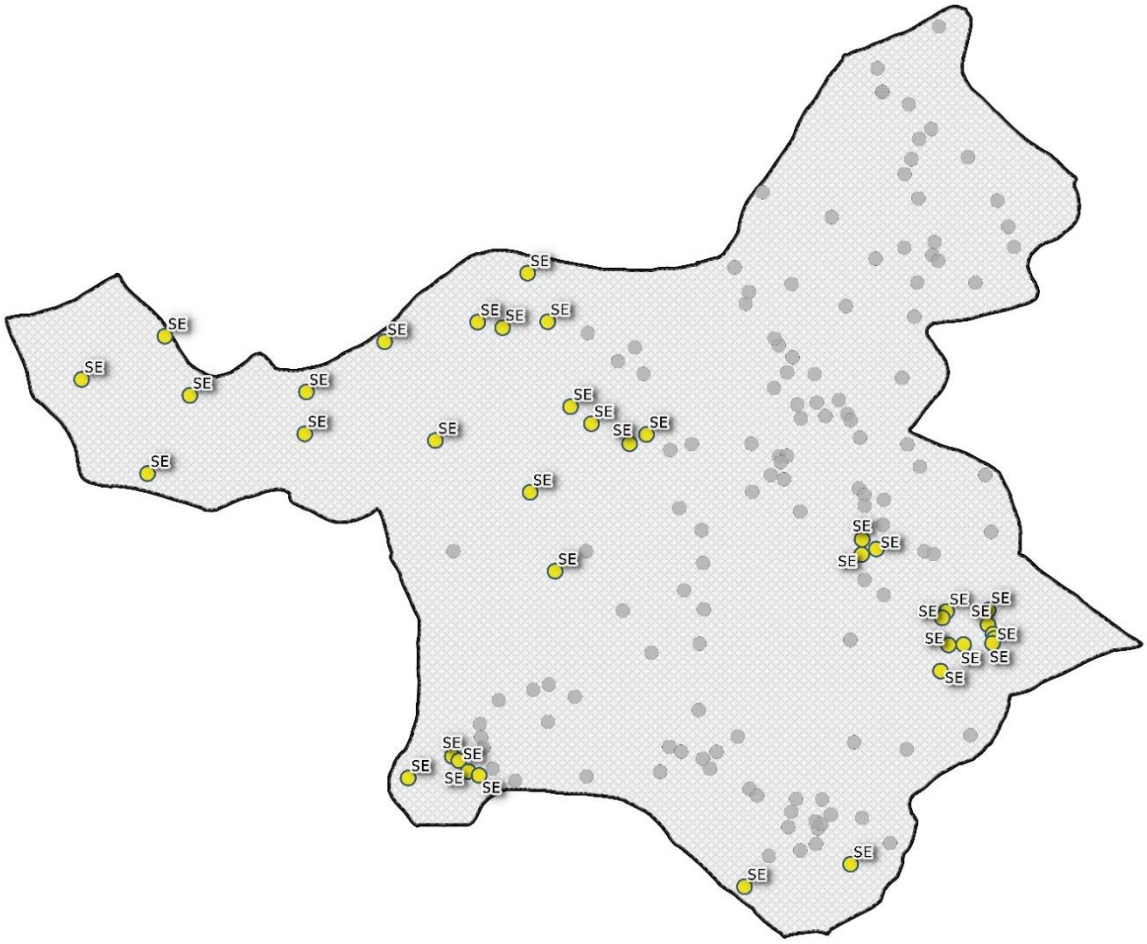

Fig. 4.6. Villages marked with yellow points are identified as suitable locations for installing off-grid Photovoltaic (PV) systems based on the classification results conducted by the Spatial Techno-Economic Assessment (STEA) module.

The second module of the ResQ-RDSS is the Earthquake-induced Risk Assessment (ERA). This module carries out the probabilistic seismic resilience analysis of the Hypothetical Power Transmission Network (HPTN), which is assumed to be extended to all 158 case study villages. In other words, the ERA module considers the scenario in which the case study villages are connected to the power grid, and no stand-alone PV system is deployed for power supply in the rural

settlements. To conduct the probabilistic seismic resilience of HPTN, the ERA module simulates 50 earthquake scenarios with a magnitude varying between 6 and 9, roughly corresponding to 475- and 2475-year return periods. The epicenters of earthquake scenarios are either within the territory of Birjand County or close to the county's borders. The procedure of simulating earthquake scenarios defined in the ERA module is the same procedure used by ResQ-IOS for quantifying the seismic resilience of the Shelby County case study in different sections of Chapter 3.

The analysis of the results of the ERA's probabilistic seismic resilience assessment considering 50 earthquake scenarios, such as the mean, standard deviation, and maximum number of villages that experience the lack of access to electricity for different time intervals after the earthquake occurrence, is given in Table 4.2. These results were obtained using ResQ-IOS [155].

Table 4.2. The results of the probabilistic seismic resilience assessment of the rural settlements in Birjand County (based on 50 earthquake scenarios).

Time interval after the earthquake occurrence	Number of villages experiencing the lack of electricity access		
	Mean	Standard deviation	Max
1 day	85.50	56.41	157
15 days	49.54	52.44	151
30 days	32.54	43.78	143
45 days	21.76	35.22	130
60 days	16.20	30.47	115
75 days	10.90	23.97	102
90 days	5.64	17.49	81
120 days	2.08	10.55	65

The ERA's resilience-based threshold for classifying the case study villages as suitable for off-grid electrification using solar PV systems is that if the power supply of the village is not restored after 45 days since the earthquake occurrence, and this situation (i.e., lack of access to electricity for 45 days) occurs in more than 20 percent of the simulated earthquake scenarios (i.e., $N_E = 45$ days and $L_E = 20\%$). Using this threshold, the ERA module identifies 53 villages in Birjand County (out of 158) where an off-grid solar PV system is the resilient electrification strategy with respect to

earthquake hazard. These villages are shown in Fig. 4.7 with red points. These villages are often the last villages whose power supply is restored after the earthquake occurrence. The ERA module classified villages B2, B3, and B5 into the off-grid electrification strategy set. Villages B1 and B4 were categorized for connecting to the power grid.

The number of villages identified by the ERA module to deploy off-grid solar PV systems for different values of N_E and L_E thresholds is given in Table 4.3. Setting higher N_E thresholds means that longer electric power restoration times are acceptable. Similarly, a higher L_E threshold means that more villages in the region will be without power. Combined high N_E and L_E thresholds indicate that a regional HPTN is not seismically resilient, as a large number of villages will be without electric power for a long time: if such a situation is acceptable, then no off-grid electrification strategy will be deemed as justified. The opposite, a highly seismically resilient electric power supply in the region, would require that practically all (146 out of 158) villages be electrified using off-grid solar PV systems. A practical decision for implementing the CRES of deploying off-grid solar PV systems is somewhere in between these two extremes. The ResQ-RDSS enables considering a variety of such practical options.

Table 4.3. The number of villages identified by the ERA module for utilizing off-grid solar PV systems as the seismically more resilient electrification strategy.

Number of villages		N_E (days)			
		15	30	45	60
L_E (%)	10	146	117	95	75
	20	130	78	53	6
	30	95	32	1	0
	40	31	0	0	0

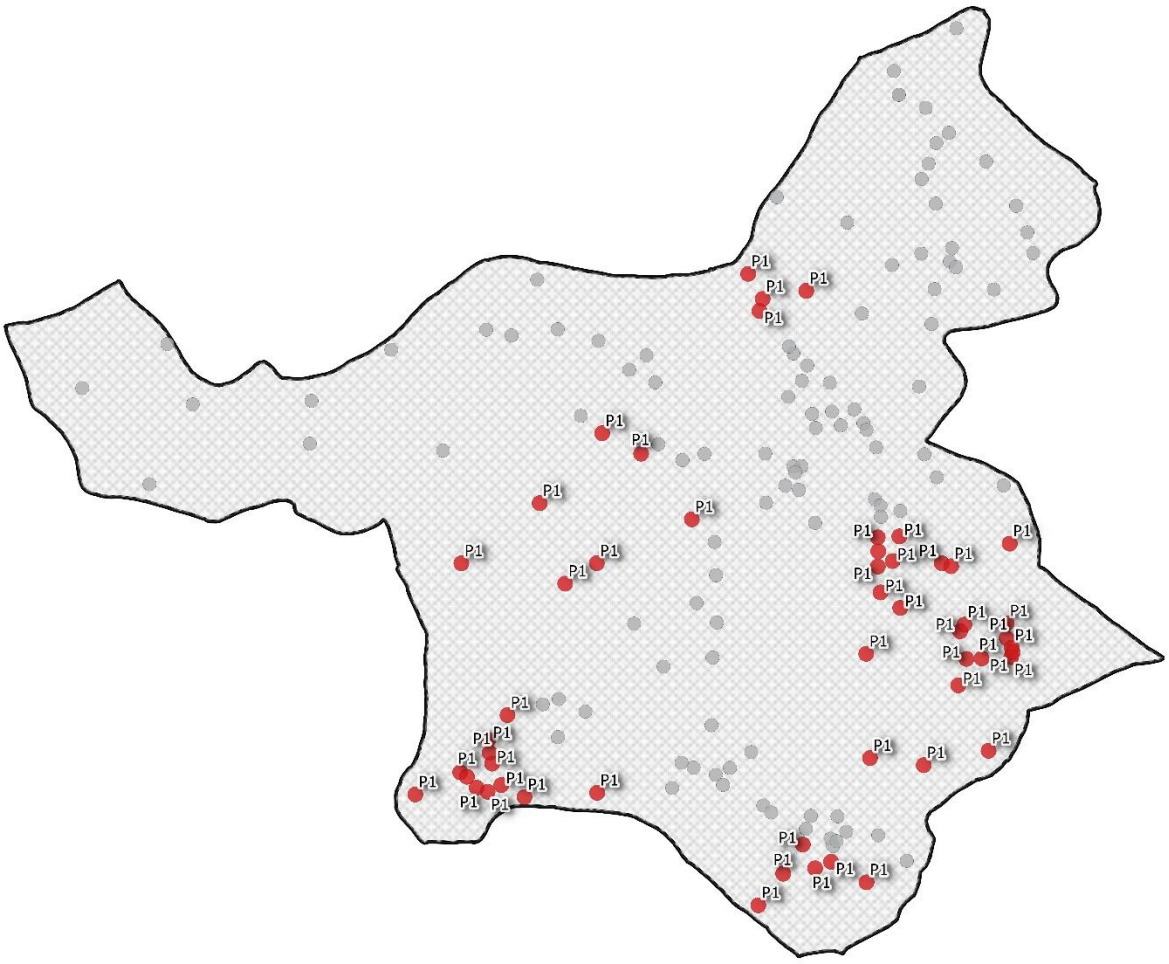

Fig. 4.7. Villages marked with red points are identified as suitable locations for installing off-grid Photovoltaic (PV) systems based on the classification results conducted by the Earthquake-induced Risk Assessment (ERA) module.

Flood-induced Risk Assessment (FRA) is the third module of the ResQ-RDSS. The FRA module implements the probabilistic resilience analysis of the HPTN against flood hazards in a manner similar to the ERA module, also using ResQ-IOS [155]. Since floods are usually pluvial in the case study (i.e., caused by localized intensive rainfall), each flood scenario randomly considers the overflow in a number of the case study watercourses and then simulates disconnects of the power lines intersecting these watercourses. Considering flood return periods (e.g., 100 or 500 years) can lead to a more accurate risk assessment. The analysis of the results of the FRA's probabilistic resilience assessment considering 50 flood scenarios is given in Table 4.4.

Table 4.4. The results of the probabilistic resilience assessment of rural settlements in the case study against 50 flood scenarios.

Time interval after the flood occurrence	Number of villages experiencing the lack of electricity access		
	Mean	Standard deviation	Max
1 day	108.52	34.92	139
15 days	52.78	35.38	96
30 days	20.58	26.20	68
45 days	3.30	8.99	31
60 days	0	0	0

The FRA module classifies a village into the off-grid PV power systems set if the power supply of the village is not restored after 30 days since the flood occurrence and the situation of lack of electricity access (for 30 days) occurs in more than 20 percent of the simulated flood scenarios (i.e., $N_F = 30$ days and $L_F = 20\%$). The FRA module identifies 55 villages in Birjand County (out of 158) that will be more flood-resilient if an off-grid PV power system is installed. These villages are marked with blue points in Fig. 4.8. Based on the FRA module's results, villages B2 and B5 would be more flood-resilient if off-grid solar PV systems are installed, while connecting to the regional power grid is a more flood-resilient strategy for villages B1, B3, and B4.

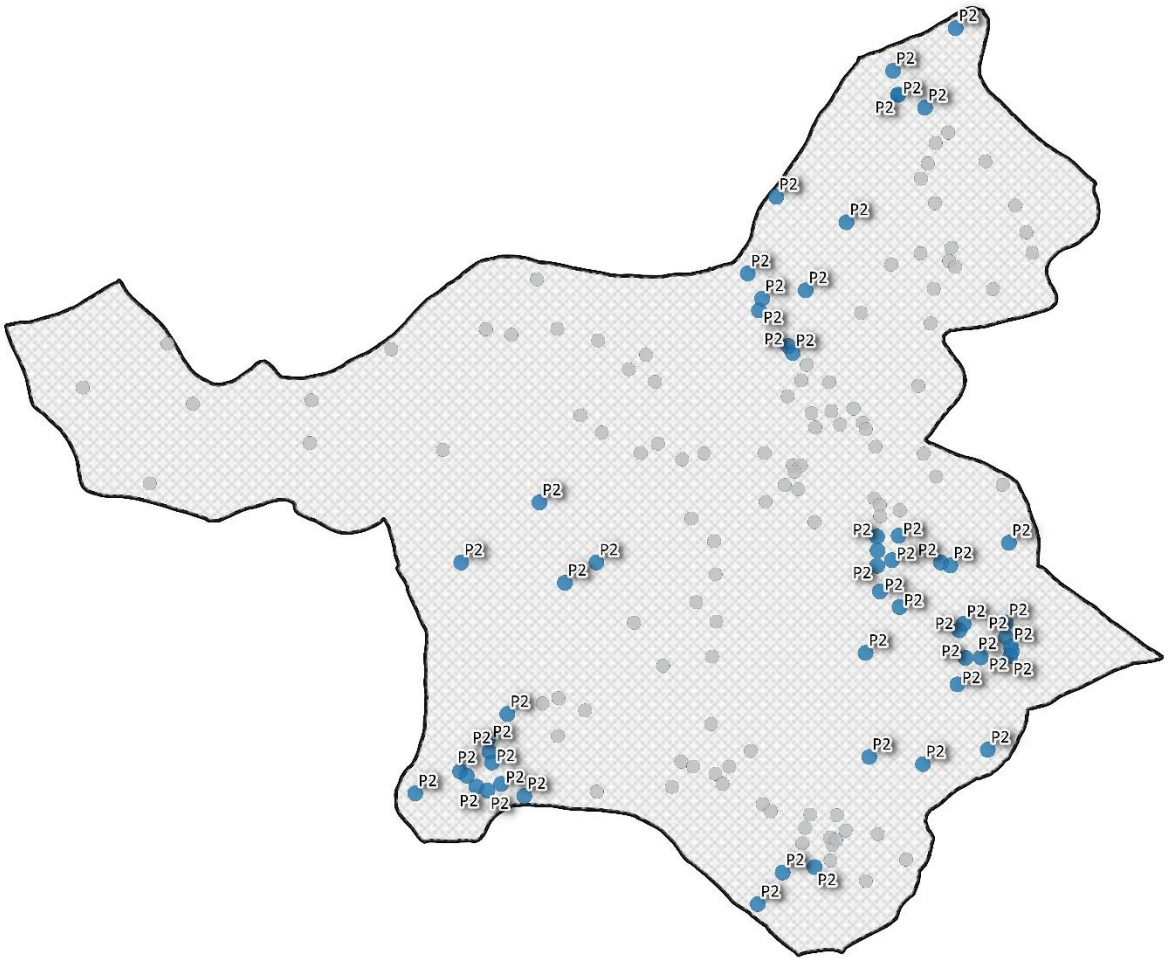

Fig. 4.8. Villages marked with blue points are identified as suitable locations for installing off-grid Photovoltaic (PV) systems based on the classification results conducted by the Flood-induced Risk Assessment (FRA) module.

The number of villages identified by the FRA module to utilize off-grid solar PV systems for different values of N_F and L_F is given in Table 4.5. As in the seismic resilience case, high N_F and L_F values indicate a region that is not very resilient to floods. Improving flood resilience by installing off-grid solar PV systems is possible. The range of practical, economic, and societally acceptable solutions is uncovered by ResQ-RDSS and shown in Table 4.5.

Table 4.5. The number of villages identified by the FRA module for deploying off-grid solar PV systems as the more resilient electrification strategy with respect to the flood hazard.

Number of villages		N_F (days)		
		15	30	45
L_F (%)	10	94	67	10
	20	93	55	0
	30	84	22	0
	40	81	4	0

As shown in Figures 4.5, 4.6, and 4.7, different sets of villages have been identified by the STEA, ERA, and FRA modules. Hence, it is possible that a village is classified into different electrification strategy sets by different ResQ-RDSS modules. For instance, the ERA and FRA modules classified village B2 into the set with the off-grid electrification strategy, whereas the STEA module selected village B2 for on-grid electrification because this village has a low combined fuzzy grade (CFG) with respect to the six STEA module criteria. Another example is village B3, where the STEA and ERA modules recommended using off-grid solar systems in that village. However, the FRA module suggested connecting to the power grid would be a more resilient strategy for village B3.

The role of the Decision Maker (DM) module is to resolve the probable disagreement between the results of three ResQ-RDSS modules. The DM module aims to finalize the resilient electrification strategy, the pre-disruption CRES, for the case study villages by combining the classification results carried out by three ResQ-RDSS modules. As stated earlier, the DM module constructs the entire decision space by firming all possible unions and intersections of the STEA, ERA, and FRA village sets. The results of different decisions made by the DM module for finalizing the resilient electrification strategy (CRES) are given in Table 4.6.

Table 4.6. The results of different decisions made by the DM module for finalizing the resilient electrification strategy for CFG = 0.4, τ = 0.8, $N_E = 45$ days, $L_E = 20\%$, $N_F = 30$ days, and $L_F = 20\%$.

Decision [D]		Number of the case study villages with	
		Off-grid solar PV electrification	On-grid electrification
1	$D[STEA \cap ERA \cap FRA]$ (Most stringent)	21	137
2	$D[STEA]$	38	120
3	$D[ERA]$	53	105
4	$D[FRA]$	55	103
5	$D[STEA \cap ERA]$	24	134
6	$D[STEA \cap FRA]$	21	137
7	$D[ERA \cap FRA]$	46	112
8	$D[STEA \cup ERA]$	67	91
9	$D[STEA \cup FRA]$	72	86
10	$D[ERA \cup FRA]$	62	96
11	$D[STEA \cap (ERA \cup FRA)]$	24	134
12	$D[ERA \cap (STEA \cup FRA)]$	49	109
13	$D[FRA \cap (STEA \cup ERA)]$	46	112
14	$D[STEA \cup (ERA \cap FRA)]$	63	95
15	$D[ERA \cup (STEA \cap FRA)]$	53	105
16	$D[FRA \cup (STEA \cap ERA)]$	58	100
17	$D[STEA \cup ERA \cup FRA]$ (Most lenient)	76	82

The STEA module appraised the techno-economic suitability level of the case study villages for installing stand-alone PV systems. The STEA module identified about 24% of the villages as desirable sites for establishing off-grid solar PV systems. The results of the ERA and FRA modules suggest deploying off-grid power systems is the resilient electrification strategy for about 34% of the case study villages. However, the ERA and FRA modules rendered different geographical distributions of suitable villages for utilizing the off-grid power systems. The remaining case study villages (66%) would have a more resilient power supply if connected to the regional power grid.

Various approaches can be taken to finalize each village's resilient electrification strategy in the case study based on the classification results of the STEA, ERA, and FRA modules. The most stringent (i.e., most conservative) approach that can be pursued to select a village as suitable for installing off-grid solar PV systems is that none of the STEA, ERA, and FRA modules has recommended the strategy of connecting to the regional power grid for that village. In other words, all three ResQ-RDSS modules have classified 21 villages into the group with the off-grid electrification strategy. Following this approach, ResQ-RDSS identifies these 21 villages (13.3%) in Birjand County for deploying off-grid solar PV systems. The identified case study villages (21 out of 158) marked with green points are displayed in Fig. 4.9.

In contrast, the most lenient approach that can be followed to identify a village as desirable for off-grid PV systems is that at least one of the STEA, ERA, and FRA modules has recommended the off-grid electrification strategy for that village. Applying the least conservative (i.e., most lenient) approach identifies 76 villages (48.1%) in Birjand County as suitable for off-grid solar PV systems.

The DM module of ResQ-RDSS provides 17 possible decisions for improving the disaster resilience of rural communities in Birjand County by either connecting them to a regional power grid or electrifying them using off-grid solar PV systems. Each possible decision in Table 4.6 specifies a particular set of desirable villages for utilizing off-grid solar energy systems to improve the resilience of rural settlements against multi-hazard risks. Local governments can make the final decision for implementing the resilient electrification strategy by considering many criteria such as the local conditions of rural areas, characteristics of the regional power grid, policymakers'

opinions, future development plans of the region of interest, budget constraints, stakeholders' interests, regional hazard risk assessments reports, etc.

In the DM module's decision space, the most stringent and the most lenient approaches (decisions No.1 and 17, respectively) are the marginal decisions in that decision space. To illustrate that the ResQ-RDSS can improve the multi-hazard resilience of rural settlements, the resilience of rural power supply is quantified against an earthquake with a magnitude of M_w = 7.2 for four cases. In the first case, it is assumed that all villages in Birjand County are connected to the power grid, and no village is equipped with an off-grid solar system (the HPTN case). The second and third cases consider that villages in Birjand County are electrified using off-grid solar PV systems according to the ResQ-RDSS decisions No. 1 and No. 17, respectively.

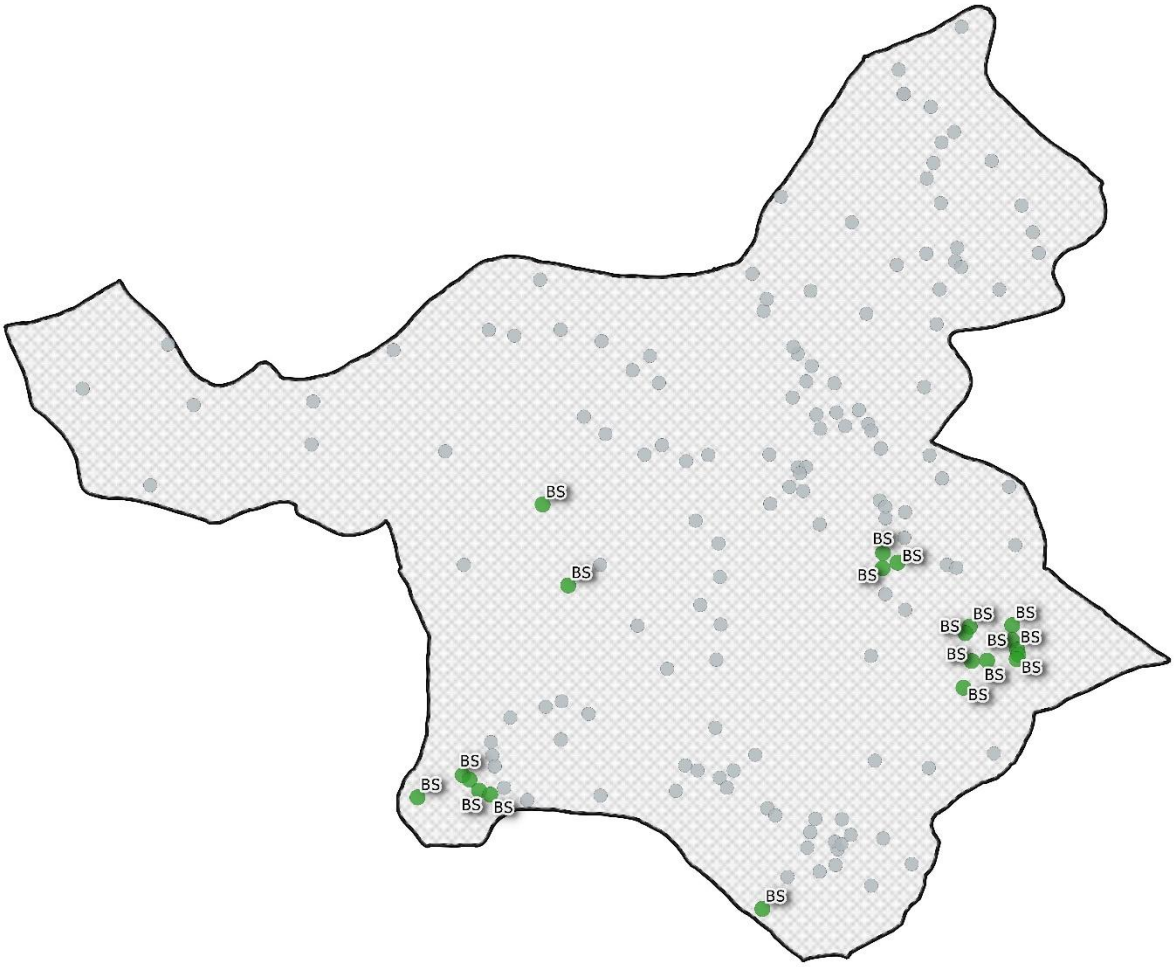

Fig. 4.9. Villages marked with green points are identified as suitable locations for installing off-grid Photovoltaic (PV) systems based on the most stringent combination of classification results conducted by the STEA, ERA, and FRA modules.

The metric for assessing the rural power supply resilience is the ratio of the consumption to the demand for electric power in the rural settlements of the case study tracked over time from the occurrence of the disaster to the end of the recovery process. More information on this metric for the resilience assessment of infrastructure systems can be found in Chapter 2 and in [155]. The results of ResQ-IOS [155] resilience quantification for rural power supply in Birjand County are depicted in Fig. 4.10. This figure indicates the evolution of rural power supply after an earthquake scenario for different CRES implementations to illustrate how various CRESs improve the rural communities' resilience indicators described in Sections 1.4.6 and 3.3.

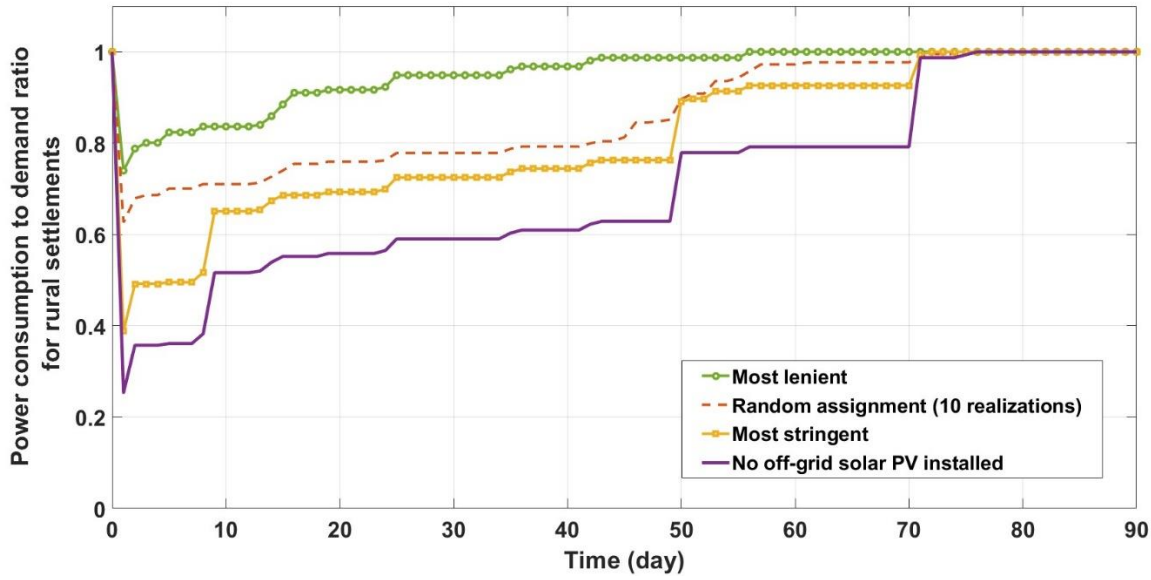

Fig. 4.10. The seismic resilience assessment of the case study rural power supply after an earthquake with M_w =7.2 for four cases.

The most lenient approach (decision No. 17, with 76 villages equipped with standalone PV systems) is the most costly decision for enhancing the resilience of rural power supply in Birjand County. However, taking this most lenient approach leads to the maximum improvement of multi-hazard resilience of Birjand County, as shown in Fig. 4.10. On the contrary, the most stringent approach (decision No. 1, with 21 villages equipped with standalone PV systems) requires the lowest budget for implementing resilient rural electrification. As expected, following this most stringent approach results in the minimum improvement of disaster resilience in the rural districts of the case study. The recovery durations for the two extreme approaches are 56 and 71 days. Notably, opting to connect all villages to the power grid (no off-grid

solar PV systems installed) leads to the least resilient solution (Fig. 4.10). Thus, even the most stringent and the least costly deployment of off-grid solar PV systems improves the electric power system resilience in Birjand County.

To demonstrate that the ResQ-RDSS can be used to find an optimal resilient electrification strategy for rural communities, the seismic resilience of rural power supply for the third and fourth cases is evaluated considering the $M_w = 7.2$ scenario. The third case follows the most lenient approach suggested by the ResQ-RDSS. This case assumes that 76 villages selected earlier by the DM module's decision No.17 are equipped with off-grid solar PV systems. In the fourth case, 76 villages are selected randomly to be equipped with off-grid solar PV systems. To minimize bias, ten realizations of the 76-village set are created, and an average of ten ResQ-IOS resilience quantifications is computed. As indicated in Fig. 4.10, the ResQ-RDSS's most lenient approach made it possible to enhance the rural power supply resilience more than the random scenario did. Notably, both selections are better than the on-grid scenario, in which no village is equipped with standalone PV systems.

4.6. Conclusion

After describing the problem statement and motivation for improving electricity access in rural areas, a systematic review of the literature on rural electrification was conducted. The identified research gap was the lack of resilience in electrification planning. To this end, ResQ-RDSS, a resilience-based regional decision support system, was introduced for resilient rural electrification.

The ResQ-RDSS was developed based on the capabilities of the ResQ-IOS framework demonstrated in Chapter 3 by conducting the resilience analysis of Shelby County. The experiences from the parametric analysis of seismic urban resilience of Shelby County and, subsequently, the feasibility study of implementing various CRESs to improve the resilience of Shelby County to earthquake hazards in Chapter 3 illuminated the necessity of developing a decision support system to select the most effective CRES among many options for implementation.

The structure of ResQ-RDSS is composed of four modules: Spatial Techno-Economic Assessment (STEA), Earthquake-induced Risk Assessment (ERA), Flood-

induced Risk Assessment (FRA), and Decision Maker (DM). The ResQ-RDSS can specify the resilient electrification strategy as a pre-disruption CRES for each village in rural areas. The ResQ-RDSS framework advises each village to either install stand-alone solar PV systems or connect to the power network to improve the disaster resilience of rural communities. The ResQ-RDSS achieved the objectives of this doctoral dissertation by incorporating multi-hazard resilience assessment into regional development planning. The rural settlements of Birjand County were selected as the case study to demonstrate the ResQ-RDSS's capability of devising resilient electrification strategies for rural areas.

Chapter Five

Conclusion

The material of this chapter is directly or indirectly based on the following papers:

• Hamed Hafeznia and Božidar Stojadinović. “ResQ-IOS: An iterative optimization-based simulation framework for quantifying the resilience of interdependent critical infrastructure systems to natural hazards,” *Applied Energy*, vol. 349, p. 121558, Nov. 2023, doi: 10.1016/j.apenergy.2023.121558.

• Hamed Hafeznia and Božidar Stojadinović, “Resilience-based decision support system for installing standalone solar energy systems to improve disaster resilience of rural communities,” submitted to Energy Strategy Reviews.

5.1. Conclusions

Interdependent and complex relations between critical infrastructure systems, along with inevitable exposure to disruptive events, have increased the risk of cascading failures, resulting in a prolonged lack of service delivery in urban communities. The resilience analysis of interdependent critical infrastructure systems can be an efficient and practicable solution to mitigate the adverse impacts of extreme events on urban communities. For this purpose, this doctoral dissertation presented the ResQ-IOS framework, an Iterative Optimization-based Simulation (IOS) framework to analyze the resilience of interdependent CISs against natural hazards. This framework consists of five modules: Risk Assessment, Simulation, Database, Optimization, and Controller. Those five modules work together to model and simulate critical infrastructure systems and their interdependencies, optimize the post-disruption performance of interdependent CISs during the recovery process, quantify individually the resilience of infrastructure systems, and jointly assess the disaster resilience of the urban community.

Conducting the resilience analysis of the Shelby County case study demonstrated the capabilities of the ResQ-IOS framework to allow for real-world conditions of infrastructure components in quantifying the disaster resilience of interdependent CISs. Based on the results from the resilience assessment of the Shelby County case study, the time required for the full recovery of an urban community depends on how fast the functioning of interdependent CISs evolves. Due to interdependencies between the infrastructure systems, the urban community recovery may be conditioned on the performance evolution of one infrastructure system. For instance, the recovery rate of damaged components in the power network controls the recovery duration of the Shelby County case study.

Utilizing the ResQ-IOS framework enables stakeholders to conduct the feasibility study of implementing Community Resilience Enhancement Strategies (CRESs) for urban and rural communities. This doctoral dissertation investigated the impacts of implementing three strategies to improve the urban community’s resilience evaluation indicators. The pre-disruption CRES considers the enhancement of redundancy and robustness indicators of the urban community, the post-disruption CRES aims to improve the rapidity and resourcefulness, and the peri-disruption CRES mitigates the

adverse effects of interdependencies during the urban community's recovery. This capability of the ResQ-IOS framework assists policymakers, local governments, urban planners, and infrastructure managers in efficiently implementing the resilience enhancement strategy, for instance, by determining the optimal schedule and locations for deploying truck-mounted mobile generators in the water network. For instance, the case study results indicated that among the Shelby County interdependent CISs, implementing the strategy of increasing the infrastructure networks' supply capacity for the water network has the best resilience improvement. This finding was not evident since the recovery of the Shelby County urban community is controlled by the power network.

Performing the parametric analysis of urban disaster resilience using ResQ-IOS provides stakeholders with an insight into the parameters influencing the recovery of urban communities. This doctoral dissertation explored the impacts of six parameters on the urban resilience of the case study to extreme events, such as the number and configuration of R&M teams, the restoration sequence of damaged components, housing recovery models, earthquake magnitude, and earthquake epicenter location. For example, the parametric analysis of the number of available R&M teams suggested that in case of a constraint on the budget, the local government can remarkably shorten the recovery duration of the urban community in the case study by allocating the greater part of the budget for employing a larger number of R&M teams in the power network. The parametric analysis of earthquake epicenters revealed that some areas of the Shelby County case study are more vulnerable to seismic hazards, like the south and southwest parts of the case study. In light of this finding, the local government and infrastructure managers can prioritize the urban areas that are less resilient to disruptions over other parts of the case study for the implementation of CRESs, such as pre-disruption retrofitting important components in the infrastructure networks, increasing redundancy, and improving the robustness of infrastructure components, or peri-disruption optimal dispatch and structure of repair crews, or post-disruption planning of the recovery process.

In addition to optimizing the service dispatching during the post-disaster recovery of the community to minimize the interdependent CISs' joint accumulated loss of resilience, the ResQ-IOS framework can be utilized to identify the optimal recovery strategy with the minimum total recovery cost. Accordingly, ResQ-IOS determines the

optimal number of backup systems and the optimal portfolio for the availability levels of repair teams and resources in each infrastructure network. Since the SoCIS resilience metric of the ResQ-IOS framework is normalized and unitless, it would be possible to apply economic models to the resilience assessment results carried out by ResQ-IOS. As an example, this doctoral dissertation investigated the effect of the urban density parameter on the optimal recovery strategy by considering three cost profiles for low-, medium-, and high-density urban communities. The capabilities of the ResQ-IOS framework reflect the contributions of this doctoral dissertation mentioned earlier in Chapter 1. The ResQ-IOS framework is developed to be compatible with various types of case studies, from high-density cities like Singapore, New York, Tehran, and Tokyo to medium-density cities like Zurich, Geneva, and Basel in Switzerland and low-density regions like the Birjand County of Iran.

People who live in rural settlements and have no access to electricity constitute a considerable percentage of the world's population. Considering the importance of access to electricity for the socioeconomic development of rural communities, many research studies have been conducted to investigate the feasibility of electrifying rural areas by utilizing renewable energy-based stand-alone power systems. The systematic review of respective research studies indicated that although those studies have considered the social, techno-economic, and environmental aspects of renewable energy-based rural electrification, the resilience concept has rarely been considered as an essential factor in the long-term planning and development of rural electrification. That was the strong motivation for developing ResQ-RDSS, the extension of the ResQ-IOS framework, to incorporate the resilience concept and enable resilience enhancement by deploying off-grid solar power systems (as a pre-disruption CRES) in the strategic planning of rural electrification. The objective of the ResQ-RDSS framework in this doctoral dissertation is to devise resilient electrification strategies to improve electricity access in rural communities.

The ResQ-RDSS is a Resilience Quantification-based Regional Decision Support System. The structure of ResQ-RDSS comprises four modules: Spatial Techno-Economic Assessment (STEA), Earthquake-induced Risk Assessment (ERA), Flood-induced Risk Assessment (FRA), and Decision Maker (DM). The task of the STEA, ERA, and FRA modules is to classify the villages in the region of interest into two sets based on their specific classification methods and thresholds. The STEA module aims

to investigate the suitability of implementing two types of pre-disruption CRESs (on-grid and off-grid electrification) in rural areas by performing a techno-economic assessment. The ERA and FRA modules employ ResQ-IOS to quantify the resilience of rural power supply against earthquake and flood hazards, respectively. Due to probable discrepancy between the classification results, the role of the DM module is to create the entire decision space by applying set theory to the classification results carried out by the STEA, ERA, and FRA modules. The DM module contains 17 possible decisions for selecting the electrification strategy. The decision-maker can use MCDM techniques to opt for the resilient electrification strategy for implementation. The final decision, made based on the ResQ-RDSS results, classifies the villages in the region of interest into two sets, one for connection to the regional power network (on-grid) and the other for installing solar PV systems (off-grid).

Although the ResQ-RDSS framework is developed to devise strategies for resilient rural electrification with the purpose of enhancing electricity access, this framework can also be employed to improve the resilience of the rural power network against disruptive events. For instance, if all rural settlements in the case study region are currently connected to the power network, the ERA and FRA modules can be implemented to determine which areas in the current rural power network are less resilient to seismic and flood hazards. Accordingly, power infrastructure managers can adopt resilience enhancement strategies for implementation in the villages that are more vulnerable to earthquakes and floods. Also, the STEA module of the ResQ-RDSS can be applied to specify the villages that are more desirable locations for installing solar PV systems in terms of higher techno-economic viability and lower investment risks.

The workflow of the ResQ-RDSS can be utilized by stakeholders, such as local governments, infrastructure managers, hazard risk management agencies, etc., for devising resilient rural electrification strategies in developing countries around the world like Cambodia, Laos, India, Afghanistan, countries in Africa, and countries with numerous islands like Indonesia, Philippines, etc. as well as for improving the multi-hazard resilience of rural power networks in developed countries.

There are two recommendations to plan resilient rural electrification precisely and successfully implement strategies. First, it is imperative to have accurate and detailed

data regarding the local conditions of rural settlements, technical characteristics of the rural power network, development plans of rural districts, etc. In this doctoral dissertation, the need for such data concerning the case study was challenging for implementing the ResQ-RDSS framework. Second, the ResQ-RDSS framework can be combined with MCDM methods and project economic analysis models to build an all-in-one tool for evaluating the resilience of rural communities to multi-hazard scenarios.

The ResQ-RDSS is built on the capabilities of the ResQ-IOS framework (methodology and code). The experiences from the parametric analysis of seismic urban resilience of Shelby County and, subsequently, the feasibility study of implementing various CRESs to enhance the resilience of Shelby County to earthquake hazards illuminated the necessity of developing a decision support system to select the most effective pre-disruption, peri-disruption or post-disruption CRES among many options for implementation. The resulting tools, ResQ-IOS and ResQ-RDSS, are versatile, and their capabilities are demonstrated in very different case studies, from prosperous, advanced, and dense urban communities to less developed and sparse rural communities.

5.2. Potential extensions of the present research

This doctoral dissertation developed the ResQ-IOS framework to function as a robust and versatile tool for modeling, quantifying, optimizing, and analyzing the disaster resilience of urban communities by considering interdependencies between critical urban infrastructure systems. Since critical infrastructure systems act as the backbone of urban communities and resilience has a fundamental role in planning for the future development of infrastructure systems, the ResQ-IOS computational tool can be utilized for the resilience-oriented planning of developments in urban areas. Investigating the impacts of implementing different Community Resilience Enhancement Strategies (CRESs) on improving the resilience of urban and rural communities suggests that ResQ-IOS can be utilized to conceptualize, plan, and implement resilience enhancement actions in communities. Hence, ResQ-IOS can be incorporated into urban planning procedures to evaluate the disaster resilience of urban regions for various future development plans. Accordingly, the resilience

assessment results of different urban development plans can serve as a decision-making criterion for selecting the resilient-oriented development plan for the urban community. The application of the ResQ-IOS framework can be extended to social and financial resilience assessments. The economic and social models can be integrated into the ResQ-IOS framework to fill the gap between technical and social resilience models. Establishing relations between these two fields of resilience can provide more precise forecasting of service demand evolution during the housing recovery and population movements in urban areas. Optimizing the restoration sequence of failed components to achieve a shorter recovery duration can be an interesting topic for the future extension of the ResQ-IOS framework.

The current version of the ResQ-RDSS framework developed in this doctoral dissertation considers earthquake and flood hazards for the risk assessment of rural areas. The extension of the ResQ-RDSS framework can be developed to include other types of natural hazards like landslides, windstorms, typhoons, etc. In addition to solar PV systems as an off-grid power supply option for rural electrification, the procedure of the STEA module for desirability-based site selection can be extended for other renewable energy-based power supply systems, such as mini hydroelectric generators, wind turbines, and biomass installations. The ResQ-RDSS framework has been developed with a focus on the power infrastructure system. This framework can be expanded to consider other types of critical infrastructure systems in rural districts, like the potable water supply network and cellular communication and internet connectivity systems.

Bibliography

[1] Y. Zhou, J. Li, G. Wang, S. Chen, W. Xing, and T. Li, “Assessing the short-to medium-term supply risks of clean energy minerals for China,” *J Clean Prod*, vol. 215, pp. 217–225, Apr. 2019, doi: 10.1016/j.jclepro.2019.01.064.

[2] S. Mirkhani and Y. Saboohi, “Stochastic modeling of the energy supply system with uncertain fuel price - A case of emerging technologies for distributed power generation,” *Appl Energy*, vol. 93, pp. 668–674, 2012, doi: 10.1016/j.apenergy.2011.12.099.

[3] S. Ahmadi, Y. Saboohi, and A. Vakili, “Frameworks, quantitative indicators, characters, and modeling approaches to analysis of energy system resilience: A review,” *Renewable and Sustainable Energy Reviews*, vol. 144. Elsevier Ltd, Jul. 01, 2021. doi: 10.1016/j.rser.2021.110988.

[4] S. M. Rinaldi, J. P. Peerenboom, and T. K. Kelly, “Identifying, understanding, and analyzing critical infrastructure interdependencies,” *IEEE Control Systems Magazine*, vol. 21, no. 6, pp. 11–25, 2001, doi: 10.1109/37.969131.

[5] M. Ouyang, “Review on modeling and simulation of interdependent critical infrastructure systems,” *Reliability Engineering and System Safety*, vol. 121. Elsevier Ltd, pp. 43–60, 2014. doi: 10.1016/j.ress.2013.06.040.

[6] J. Kong, C. Zhang, and S. P. Simonovic, “Optimizing the resilience of interdependent infrastructures to regional natural hazards with combined improvement measures,” *Reliab Eng Syst Saf*, vol. 210, Jun. 2021, doi: 10.1016/j.ress.2021.107538.

[7] F. H. Jufri, V. Widiputra, and J. Jung, “State-of-the-art review on power grid resilience to extreme weather events: Definitions, frameworks, quantitative assessment methodologies, and enhancement strategies,” *Applied Energy*, vol. 239. Elsevier Ltd, pp. 1049–1065, Apr. 01, 2019. doi: 10.1016/j.apenergy.2019.02.017.

[8] Z. Zeng, Y. P. Fang, Q. Zhai, and S. Du, “A Markov reward process-based framework for resilience analysis of multistate energy systems under the threat

of extreme events," *Reliab Eng Syst Saf*, vol. 209, May 2021, doi: 10.1016/j.ress.2021.107443.

[9] M. Panteli and P. Mancarella, "Influence of extreme weather and climate change on the resilience of power systems: Impacts and possible mitigation strategies," *Electric Power Systems Research*, vol. 127. Elsevier Ltd, pp. 259–270, Jun. 29, 2015. doi: 10.1016/j.epsr.2015.06.012.

[10] M. Ouyang and Z. Wang, "Resilience assessment of interdependent infrastructure systems: With a focus on joint restoration modeling and analysis," *Reliab Eng Syst Saf*, vol. 141, pp. 74–82, Jul. 2015, doi: 10.1016/j.ress.2015.03.011.

[11] H. Zakernezhad, M. S. Nazar, M. Shafie-khah, and J. P. S. Catalão, "Optimal resilient operation of multi-carrier energy systems in electricity markets considering distributed energy resource aggregators," *Appl Energy*, vol. 299, Oct. 2021, doi: 10.1016/j.apenergy.2021.117271.

[12] A. Barnes, H. Nagarajan, E. Yamangil, R. Bent, and S. Backhaus, "Resilient design of large-scale distribution feeders with networked microgrids," *Electric Power Systems Research*, vol. 171, pp. 150–157, Jun. 2019, doi: 10.1016/j.epsr.2019.02.012.

[13] A. Younesi, H. Shayeghi, A. Safari, and P. Siano, "Assessing the resilience of multi microgrid based widespread power systems against natural disasters using Monte Carlo Simulation," *Energy*, vol. 207, Sep. 2020, doi: 10.1016/j.energy.2020.118220.

[14] A. R. Sayed, C. Wang, and T. Bi, "Resilient operational strategies for power systems considering the interactions with natural gas systems," *Appl Energy*, vol. 241, pp. 548–566, May 2019, doi: 10.1016/j.apenergy.2019.03.053.

[15] H. Hafeznia, H. Yousefi, and F. Razi Astaraei, "A novel framework for the potential assessment of utility-scale photovoltaic solar energy, application to eastern Iran," *Energy Convers Manag*, vol. 151, pp. 240–258, Nov. 2017, doi: 10.1016/j.enconman.2017.08.076.

[16] B. Gillessen, H. Heinrichs, J. F. Hake, and H. J. Allelein, “Natural gas as a bridge to sustainability: Infrastructure expansion regarding energy security and system transition,” *Appl Energy*, vol. 251, Oct. 2019, doi: 10.1016/j.apenergy.2019.113377.

[17] C. Peng, M. Yuan, C. Gu, Z. Peng, and T. Ming, “A review of the theory and practice of regional resilience,” *Sustainable Cities and Society*, vol. 29. Elsevier Ltd, pp. 86–96, Feb. 01, 2017. doi: 10.1016/j.scs.2016.12.003.

[18] M. Yoo, T. Kim, J. T. Yoon, Y. Kim, S. Kim, and B. D. Youn, “A resilience measure formulation that considers sensor faults,” *Reliab Eng Syst Saf*, vol. 199, Jul. 2020, doi: 10.1016/j.ress.2019.02.025.

[19] R. Francis and B. Bekera, “A metric and frameworks for resilience analysis of engineered and infrastructure systems,” *Reliability Engineering and System Safety*, vol. 121. Elsevier Ltd, pp. 90–103, 2014. doi: 10.1016/j.ress.2013.07.004.

[20] E. Zio, “Challenges in the vulnerability and risk analysis of critical infrastructures,” *Reliab Eng Syst Saf*, vol. 152, pp. 137–150, Aug. 2016, doi: 10.1016/j.ress.2016.02.009.

[21] B. Pickering and R. Choudhary, “Quantifying resilience in energy systems with out-of-sample testing,” *Appl Energy*, vol. 285, Mar. 2021, doi: 10.1016/j.apenergy.2021.116465.

[22] V. Proag, “The Concept of Vulnerability and Resilience,” *Procedia Economics and Finance*, vol. 18, pp. 369–376, 2014, doi: 10.1016/s2212-5671(14)00952-6.

[23] M. J. Garcia-Dia, J. M. DiNapoli, L. Garcia-Ona, R. Jakubowski, and D. O’Flaherty, “Concept Analysis: Resilience,” *Archives of Psychiatric Nursing*, vol. 27, no. 6. pp. 264–270, Dec. 2013. doi: 10.1016/j.apnu.2013.07.003.

[24] M. Peciłło, “The resilience engineering concept in enterprises with and without occupational safety and health management systems,” *Saf Sci*, vol. 82, pp. 190–198, Feb. 2016, doi: 10.1016/j.ssci.2015.09.017.

[25] M. Sang, Y. Ding, M. Bao, S. Li, C. Ye, and Y. Fang, “Resilience-based restoration strategy optimization for interdependent gas and power networks,” *Appl Energy*, vol. 302, Nov. 2021, doi: 10.1016/j.apenergy.2021.117560.

[26] J. Zhou, D. W. Coit, F. A. Felder, and S. Tsianikas, “Combined optimization of system reliability improvement and resilience with mixed cascading failures in dependent network systems,” *Reliab Eng Syst Saf*, vol. 237, Sep. 2023, doi: 10.1016/j.ress.2023.109376.

[27] X. Liu, Y. P. Fang, and E. Zio, “A Hierarchical Resilience Enhancement Framework for Interdependent Critical Infrastructures,” *Reliab Eng Syst Saf*, vol. 215, Nov. 2021, doi: 10.1016/j.ress.2021.107868.

[28] Y. Almoghathawi, K. Barker, and L. A. Albert, “Resilience-driven restoration model for interdependent infrastructure networks,” *Reliab Eng Syst Saf*, vol. 185, pp. 12–23, May 2019, doi: 10.1016/j.ress.2018.12.006.

[29] Y. Almoghathawi, S. Selim, and K. Barker, “Community structure recovery optimization for partial disruption, functionality, and restoration in interdependent networks,” *Reliab Eng Syst Saf*, vol. 229, Jan. 2023, doi: 10.1016/j.ress.2022.108853.

[30] M. Panteli and P. Mancarella, “Modeling and evaluating the resilience of critical electrical power infrastructure to extreme weather events,” *IEEE Syst J*, vol. 11, no. 3, pp. 1733–1742, Sep. 2017, doi: 10.1109/JSYST.2015.2389272.

[31] G. Li *et al.*, “Risk analysis for distribution systems in the northeast U.S. under wind storms,” *IEEE Transactions on Power Systems*, vol. 29, no. 2, pp. 889–898, Mar. 2014, doi: 10.1109/TPWRS.2013.2286171.

[32] R. Rocchetta, E. Zio, and E. Patelli, “A power-flow emulator approach for resilience assessment of repairable power grids subject to weather-induced failures and data deficiency,” *Appl Energy*, vol. 210, pp. 339–350, Jan. 2018, doi: 10.1016/j.apenergy.2017.10.126.

[33] S. Balakrishnan and B. Cassottana, “InfraRisk: An open-source simulation platform for resilience analysis in interconnected power–water–transport

networks," *Sustain Cities Soc*, vol. 83, Aug. 2022, doi: 10.1016/j.scs.2022.103963.

[34] N. Blagojević, J. Kipfer, M. Didier, and B. Stojadinovic, "Probability-based Resilience Assessment of Communities with Interdependent Civil Infrastructure Systems," pp. 7d–0020, 2020, doi: 10.3929/ETHZ-B-000463549.

[35] N. Blagojević, M. Didier, and B. Stojadinović, "Quantifying component importance for disaster resilience of communities with interdependent civil infrastructure systems," *Reliab Eng Syst Saf*, vol. 228, Dec. 2022, doi: 10.1016/j.ress.2022.108747.

[36] L. Sun, D. D'Ayala, R. Fayjaloun, and P. Gehl, "Agent-based model on resilience-oriented rapid responses of road networks under seismic hazard," *Reliab Eng Syst Saf*, vol. 216, p. 108030, Dec. 2021, doi: 10.1016/J.RESS.2021.108030.

[37] T. Zhao and L. Sun, "Seismic resilience assessment of critical infrastructure-community systems considering looped interdependences," *International Journal of Disaster Risk Reduction*, vol. 59, p. 102246, Jun. 2021, doi: 10.1016/J.IJDRR.2021.102246.

[38] M. I. Dubaniowski and H. R. Heinimann, "A framework for modeling interdependencies among households, businesses, and infrastructure systems; and their response to disruptions," *Reliab Eng Syst Saf*, vol. 203, p. 107063, Nov. 2020, doi: 10.1016/J.RESS.2020.107063.

[39] M. I. Dubaniowski and H. R. Heinimann, "Framework for modeling interdependencies between households, businesses, and infrastructure system, and their response to disruptions—application," *Reliab Eng Syst Saf*, vol. 212, p. 107590, Aug. 2021, doi: 10.1016/J.RESS.2021.107590.

[40] L. Sun, B. Stojadinovic, and G. Sansavini, "Agent-Based Recovery Model for Seismic Resilience Evaluation of Electrified Communities," *Risk Analysis*, vol. 39, no. 7, pp. 1597–1614, Jul. 2019, doi: 10.1111/RISA.13277.

[41] L. Sun, B. Stojadinovic, and G. Sansavini, "Resilience Evaluation Framework for Integrated Civil Infrastructure–Community Systems under Seismic Hazard,"

Journal of Infrastructure Systems, vol. 25, no. 2, p. 04019016, Apr. 2019, doi: 10.1061/(ASCE)IS.1943-555X.0000492.

[42] M. Yazdi, E. Zarei, R. G. Pirbalouti, and H. Li, “A comprehensive resilience assessment framework for hydrogen energy infrastructure development,” *Int J Hydrogen Energy*, 2023, doi: 10.1016/j.ijhydene.2023.06.271.

[43] P. Gasser *et al.*, “Comprehensive resilience assessment of electricity supply security for 140 countries,” *Ecol Indic*, vol. 110, Mar. 2020, doi: 10.1016/j.ecolind.2019.105731.

[44] M. Arvin, P. Beiki, S. J. Hejazi, A. Sharifi, and N. Atashafrooz, “Assessment of infrastructure resilience in multi-hazard regions: A case study of Khuzestan Province,” *International Journal of Disaster Risk Reduction*, vol. 88, Apr. 2023, doi: 10.1016/j.ijdrr.2023.103601.

[45] Y. Almoghathawi and K. Barker, “Restoring Community Structures in Interdependent Infrastructure Networks,” *IEEE Trans Netw Sci Eng*, vol. 7, no. 3, pp. 1355–1367, Jul. 2020, doi: 10.1109/TNSE.2019.2927883.

[46] S. Hosseini, K. Barker, and J. E. Ramirez-Marquez, “A review of definitions and measures of system resilience,” *Reliab Eng Syst Saf*, vol. 145, pp. 47–61, Jan. 2016, doi: 10.1016/j.ress.2015.08.006.

[47] M. Bruneau *et al.*, “A Framework to Quantitatively Assess and Enhance the Seismic Resilience of Communities,” *Earthquake Spectra*, vol. 19, no. 4. Earthquake Engineering Research Institute, pp. 733–752, 2003. doi: 10.1193/1.1623497.

[48] J. Wang, W. Zuo, L. Rhode-Barbarigos, X. Lu, J. Wang, and Y. Lin, “Literature review on modeling and simulation of energy infrastructures from a resilience perspective,” *Reliability Engineering and System Safety*, vol. 183. Elsevier Ltd, pp. 360–373, Mar. 01, 2019. doi: 10.1016/j.ress.2018.11.029.

[49] G. Chen, Z. Y. Dong, D. J. Hill, G. H. Zhang, and K. Q. Hua, “Attack structural vulnerability of power grids: A hybrid approach based on complex networks,” *Physica A: Statistical Mechanics and its Applications*, vol. 389, no. 3, pp. 595–603, Feb. 2010, doi: 10.1016/j.physa.2009.09.039.

[50] X. Liu, E. Ferrario, and E. Zio, “Resilience Analysis Framework for Interconnected Critical Infrastructures,” *ASCE-ASME J Risk and Uncert in Engrg Sys Part B Mech Engrg*, vol. 3, no. 2, Feb. 2017, doi: 10.1115/1.4035728.

[51] S. Wang, Z. Guo, X. Huang, and J. Zhang, “A three-stage model of quantifying and analyzing power network resilience based on network theory,” *Reliab Eng Syst Saf*, vol. 241, Jan. 2024, doi: 10.1016/j.ress.2023.109681.

[52] Y. Fang and G. Sansavini, “Emergence of Antifragility by Optimum Postdisruption Restoration Planning of Infrastructure Networks,” *Journal of Infrastructure Systems*, vol. 23, no. 4, p. 04017024, Dec. 2017, doi: 10.1061/(asce)is.1943-555x.0000380.

[53] M. Ouyang and L. Dueñas-Osorio, “Multi-dimensional hurricane resilience assessment of electric power systems,” *Structural Safety*, vol. 48, pp. 15–24, May 2014, doi: 10.1016/j.strusafe.2014.01.001.

[54] L. Shen, B. Cassottana, H. R. Heinimann, and L. C. Tang, “Large-scale systems resilience: A survey and unifying framework,” *Qual Reliab Eng Int*, vol. 36, no. 4, pp. 1386–1401, Jun. 2020, doi: 10.1002/qre.2634.

[55] M. Ouyang and L. Dueñas-Osorio, “Time-dependent resilience assessment and improvement of urban infrastructure systems,” *Chaos: An Interdisciplinary Journal of Nonlinear Science*, vol. 22, no. 3, p. 033122, Sep. 2012, doi: 10.1063/1.4737204.

[56] N. Blagojević, F. Hefti, J. Henken, M. Didier, and B. Stojadinović, “Quantifying disaster resilience of a community with interdependent civil infrastructure systems,” *Structure and Infrastructure Engineering*, 2022, doi: 10.1080/15732479.2022.2052912.

[57] NIST, “Community resilience planning guide for buildings and infrastructure systems : volume I,” Gaithersburg, MD, Oct. 2015. doi: 10.6028/NIST.SP.1190v1.

[58] M. H. Oboudi and M. Mohammadi, “Two-Stage Seismic Resilience Enhancement of Electrical Distribution Systems,” *Reliab Eng Syst Saf*, vol. 241, p. 109635, Jan. 2024, doi: 10.1016/J.RESS.2023.109635.

[59] Y. Zhang, W. Weng, and Q. Qi, “Resilience assessment and enhancement methods of large-scale gas distribution networks against disruptions due to earthquakes,” *Reliab Eng Syst Saf*, vol. 240, p. 109583, Dec. 2023, doi: 10.1016/J.RESS.2023.109583.

[60] F. Ma *et al.*, “Assessing and enhancing urban road network resilience under rainstorm waterlogging disasters,” *Transp Res D Transp Environ*, vol. 123, p. 103928, Oct. 2023, doi: 10.1016/J.TRD.2023.103928.

[61] A. Noutash and M. Kalantar, “Resilience Enhancement with Transportable Storage Systems and Repair Crews in Coupled Transportation and Distribution Networks,” *Sustain Cities Soc*, vol. 99, p. 104922, Dec. 2023, doi: 10.1016/J.SCS.2023.104922.

[62] A. S. Kiran, “Simulation and Scheduling,” in *Handbook of Simulation*, John Wiley & Sons, Ltd, 1998, pp. 677–717. doi: https://doi.org/10.1002/9780470172445.ch21.

[63] M. Dehghanimohammadabadi, “Iterative optimization-based simulation (IOS) with predictable and unpredictable trigger events in simulated time,” Western New England University, 2016.

[64] J. April, M. Better, F. Glover, J. Kelly, and M. Laguna, “Enhancing Business Process Management with Simulation Optimization,” in *Proceedings of the 2006 Winter Simulation Conference*, 2006, pp. 642–649. doi: 10.1109/WSC.2006.323141.

[65] M. Dehghanimohammadabadi, T. K. Keyser, and S. H. Cheraghi, “A novel Iterative Optimization-based Simulation (IOS) framework: An effective tool to optimize system’s performance,” *Comput Ind Eng*, vol. 111, pp. 1–17, Sep. 2017, doi: 10.1016/j.cie.2017.06.037.

[66] A. Syberfeldt, I. Karlsson, A. Ng, J. Svantesson, and T. Almgren, “A web-based platform for the simulation–optimization of industrial problems,” *Comput Ind Eng*, vol. 64, no. 4, pp. 987–998, Apr. 2013, doi: 10.1016/J.CIE.2013.01.008.

[67] M. Göçken, A. T. Dosdoğru, A. Boru, and F. Geyik, “Characterizing continuous (s, S) policy with supplier selection using Simulation Optimization,” *Simulation*, vol. 93, no. 5, pp. 379–396, 2017, doi: 10.1177/0037549716687044.

[68] A. Klemmt, S. Horn, G. Weigert, and K. J. Wolter, “Simulation-based optimization vs. mathematical programming: A hybrid approach for optimizing scheduling problems,” *Robot Comput Integr Manuf*, vol. 25, no. 6, pp. 917–925, Dec. 2009, doi: 10.1016/J.RCIM.2009.04.012.

[69] T. Chai, S. J. Qin, and H. Wang, “Optimal operational control for complex industrial processes,” *Annu Rev Control*, vol. 38, no. 1, pp. 81–92, Jan. 2014, doi: 10.1016/J.ARCONTROL.2014.03.005.

[70] G. Figueira and B. Almada-Lobo, “Hybrid simulation–optimization methods: A taxonomy and discussion,” *Simul Model Pract Theory*, vol. 46, pp. 118–134, Aug. 2014, doi: 10.1016/J.SIMPAT.2014.03.007.

[71] R. C. Lin, M. Y. Sir, and K. S. Pasupathy, “Multi-objective simulation optimization using data envelopment analysis and genetic algorithm: Specific application to determining optimal resource levels in surgical services,” *Omega (Westport)*, vol. 41, no. 5, pp. 881–892, Oct. 2013, doi: 10.1016/J.OMEGA.2012.11.003.

[72] J. T. Lin and C. M. Chen, “Simulation optimization approach for hybrid flow shop scheduling problem in semiconductor back-end manufacturing,” *Simul Model Pract Theory*, vol. 51, pp. 100–114, Feb. 2015, doi: 10.1016/J.SIMPAT.2014.10.008.

[73] T. Wang, J. Xu, J. Q. Hu, and C. H. Chen, “Efficient estimation of a risk measure requiring two-stage simulation optimization,” *Eur J Oper Res*, Jun. 2022, doi: 10.1016/J.EJOR.2022.06.028.

[74] C. Klanke and S. Engell, “Scheduling and batching with evolutionary algorithms in simulation-optimization of an industrial formulation plant,” *Comput Ind Eng*, p. 108760, Oct. 2022, doi: 10.1016/J.CIE.2022.108760.

[75] Y. Xiao and R. Yoogalingam, “A simulation optimization approach for planning and scheduling in operating rooms for elective and urgent surgeries,” *Oper Res Health Care*, vol. 35, p. 100366, Dec. 2022, doi: 10.1016/J.ORHC.2022.100366.

[76] M. A. Ahmed and T. M. Alkhamis, “Simulation optimization for an emergency department healthcare unit in Kuwait,” *Eur J Oper Res*, vol. 198, no. 3, pp. 936–942, Nov. 2009, doi: 10.1016/J.EJOR.2008.10.025.

[77] Federal Emergency Management Agency (FEMA), *Hazus Earthquake Model Technical Manual*, Hazus 5.1. Washington, DC: FEMA, 2022.

[78] Porter Keith A., “An Overview of PEER’s Performance-Based Earthquake Engineering Methodology,” in *Ninth International Conference on Applications of Statistics and Probability in Civil Engineering (ICASP9)*, San Francisco, Jul. 2003.

[79] M. Didier, M. Broccardo, S. Esposito, and B. Stojadinovic, “A compositional demand/supply framework to quantify the resilience of civil infrastructure systems (Re-CoDeS),” *https://doi.org/10.1080/23789689.2017.1364560*, vol. 3, no. 2, pp. 86–102, Apr. 2017, doi: 10.1080/23789689.2017.1364560.

[80] Y. P. Fang and E. Zio, “An adaptive robust framework for the optimization of the resilience of interdependent infrastructures under natural hazards,” *Eur J Oper Res*, vol. 276, no. 3, pp. 1119–1136, Aug. 2019, doi: 10.1016/j.ejor.2019.01.052.

[81] J. Kong, S. P. Simonovic, and C. Zhang, “Sequential Hazards Resilience of Interdependent Infrastructure System: A Case Study of Greater Toronto Area Energy Infrastructure System,” *Risk Analysis*, vol. 39, no. 5, pp. 1141–1168, May 2019, doi: 10.1111/risa.13222.

[82] E. E. Lee, J. E. Mitchell, and W. A. Wallace, “Restoration of services in interdependent infrastructure systems: A network flows approach,” *IEEE*

Transactions on Systems, Man and Cybernetics Part C: Applications and Reviews, vol. 37, no. 6, pp. 1303–1317, Nov. 2007, doi: 10.1109/TSMCC.2007.905859.

[83] Y. Y. Haimes *et al.*, “Inoperability Input-Output Model for Interdependent Infrastructure Sectors. I: Theory and Methodology”, doi: 10.1061/ASCE1076-0342200511:267.

[84] B. A. Carreras, V. E. Lynch, I. Dobson, and D. E. Newman, “Critical points and transitions in an electric power transmission model for cascading failure blackouts,” *Chaos*, vol. 12, no. 4, pp. 985–994, 2002, doi: 10.1063/1.1505810.

[85] R. Kinney, P. Crucitti, R. Albert, and V. Latora, “Modeling cascading failures in the North American power grid,” *European Physical Journal B*, vol. 46, no. 1, pp. 101–107, Jul. 2005, doi: 10.1140/epjb/e2005-00237-9.

[86] M. Ouyang, “A mathematical framework to optimize resilience of interdependent critical infrastructure systems under spatially localized attacks,” *Eur J Oper Res*, vol. 262, no. 3, pp. 1072–1084, Nov. 2017, doi: 10.1016/j.ejor.2017.04.022.

[87] S. G. Nurre, B. Cavdaroglu, J. E. Mitchell, T. C. Sharkey, and W. A. Wallace, “Restoring infrastructure systems: An integrated network design and scheduling (INDS) problem,” *Eur J Oper Res*, vol. 223, no. 3, pp. 794–806, Dec. 2012, doi: 10.1016/j.ejor.2012.07.010.

[88] M. Ouyang and Y. Fang, “A Mathematical Framework to Optimize Critical Infrastructure Resilience against Intentional Attacks,” *Computer-Aided Civil and Infrastructure Engineering*, vol. 32, no. 11, pp. 909–929, 2017, doi: 10.1111/mice.12252.

[89] A. D. González, L. Dueñas-Osorio, M. Sánchez-Silva, and A. L. Medaglia, “The Interdependent Network Design Problem for Optimal Infrastructure System Restoration,” *Computer-Aided Civil and Infrastructure Engineering*, vol. 31, no. 5, pp. 334–350, May 2016, doi: 10.1111/mice.12171.

[90] The MathWorks Inc., “MATLAB (R2022a).” The MathWorks Inc., Natick, Massachusetts, United States, 2022.

[91] Johan Löfberg, “YALMIP : A Toolbox for Modeling and Optimization in MATLAB,” in *In Proceedings of the CACSD Conference*, Taipei, Taiwan, 2004.

[92] IBM ILOG, *IBM ILOG CPLEX 12.10 user’s manual*. IBM ILOG, 2019.

[93] A. D. González, L. Dueñas-Osorio, M. Sánchez-Silva, and A. L. Medaglia, “The Interdependent Network Design Problem for Optimal Infrastructure System Restoration,” *Computer-Aided Civil and Infrastructure Engineering*, vol. 31, no. 5, pp. 334–350, May 2016, doi: 10.1111/mice.12171.

[94] W. Zhang, P. Lin, N. Wang, C. Nicholson, and X. Xue, “Probabilistic Prediction of Postdisaster Functionality Loss of Community Building Portfolios Considering Utility Disruptions,” *Journal of Structural Engineering*, vol. 144, no. 4, Apr. 2018, doi: 10.1061/(asce)st.1943-541x.0001984.

[95] T. Adachi and B. R. Ellingwood, “Serviceability assessment of a municipal water system under spatially correlated seismic intensities,” *Computer-Aided Civil and Infrastructure Engineering*, vol. 24, no. 4, pp. 237–248, 2009, doi: 10.1111/j.1467-8667.2008.00583.x.

[96] Y. Ge, L. Du, and H. Ye, “Co-optimization approach to post-storm recovery for interdependent power and transportation systems,” *Journal of Modern Power Systems and Clean Energy*, vol. 7, no. 4, pp. 688–695, Jul. 2019, doi: 10.1007/s40565-019-0524-7.

[97] T. C. Sharkey, B. Cavdaroglu, H. Nguyen, J. Holman, J. E. Mitchell, and W. A. Wallace, “Interdependent network restoration: On the value of information-sharing,” in *European Journal of Operational Research*, Elsevier B.V., Jul. 2015, pp. 309–321. doi: 10.1016/j.ejor.2014.12.051.

[98] S. G. Nurre, B. Cavdaroglu, J. E. Mitchell, T. C. Sharkey, and W. A. Wallace, “Restoring infrastructure systems: An integrated network design and scheduling (INDS) problem,” *Eur J Oper Res*, vol. 223, no. 3, pp. 794–806, Dec. 2012, doi: 10.1016/j.ejor.2012.07.010.

[99] W. Liu, Z. Song, M. Ouyang, and J. Li, “Recovery-based seismic resilience enhancement strategies of water distribution networks,” *Reliab Eng Syst Saf*, vol. 203, Nov. 2020, doi: 10.1016/j.ress.2020.107088.

[100] M. Didier, S. Baumberger, R. Tobler, S. Esposito, S. Ghosh, and B. Stojadinovic, “Seismic Resilience of Water Distribution and Cellular Communication Systems after the 2015 Gorkha Earthquake,” *Journal of Structural Engineering*, vol. 144, no. 6, p. 04018043, Mar. 2018, doi: 10.1061/(ASCE)ST.1943-541X.0002007.

[101] IEA, “World Energy Outlook 2022,” Paris, 2022.

[102] C. W. Njiru and S. C. Letema, “Energy Poverty and Its Implication on Standard of Living in Kirinyaga, Kenya,” *Journal of Energy*, vol. 2018, pp. 1–12, Nov. 2018, doi: 10.1155/2018/3196567.

[103] W. Li *et al.*, “Nexus between energy poverty and energy efficiency: Estimating the long-run dynamics,” *Resources Policy*, vol. 72, p. 102063, Aug. 2021, doi: 10.1016/J.RESOURPOL.2021.102063.

[104] T. Fujii, A. S. Shonchoy, and S. Xu, “Impact of Electrification on Children’s Nutritional Status in Rural Bangladesh,” *World Dev*, vol. 102, pp. 315–330, Feb. 2018, doi: 10.1016/J.WORLDDEV.2017.07.016.

[105] L. Romero Rodríguez, J. Sánchez Ramos, Mc. Guerrero Delgado, J. L. Molina Félix, and S. Álvarez Domínguez, “Mitigating energy poverty: Potential contributions of combining PV and building thermal mass storage in low-income households,” *Energy Convers Manag*, vol. 173, pp. 65–80, Oct. 2018, doi: 10.1016/J.ENCONMAN.2018.07.058.

[106] C. L. Azimoh, P. Klintenberg, F. Wallin, B. Karlsson, and C. Mbohwa, “Electricity for development: Mini-grid solution for rural electrification in South Africa,” *Energy Convers Manag*, vol. 110, pp. 268–277, Feb. 2016, doi: 10.1016/J.ENCONMAN.2015.12.015.

[107] N. Asghar, M. A. Amjad, H. ur Rehman, M. Munir, and R. Alhajj, “Achieving sustainable development resilience: Poverty reduction through affordable access to electricity in developing economies,” *J Clean Prod*, vol. 376, Nov. 2022, doi: 10.1016/j.jclepro.2022.134040.

[108] I. M. Bugaje, “Renewable energy for sustainable development in Africa: a review,” *Renewable and Sustainable Energy Reviews*, vol. 10, no. 6, pp. 603–612, Dec. 2006, doi: 10.1016/J.RSER.2004.11.002.

[109] S. Karekezi, “Renewables in Africa—meeting the energy needs of the poor,” *Energy Policy*, vol. 30, no. 11–12, pp. 1059–1069, Sep. 2002, doi: 10.1016/S0301-4215(02)00058-7.

[110] S. Karekezi and W. Kithyoma, “Renewable energy strategies for rural Africa: is a PV-led renewable energy strategy the right approach for providing modern energy to the rural poor of sub-Saharan Africa?,” *Energy Policy*, vol. 30, no. 11–12, pp. 1071–1086, Sep. 2002, doi: 10.1016/S0301-4215(02)00059-9.

[111] C. Mazur *et al.*, “A holistic resilience framework development for rural power systems in emerging economies,” *Applied Energy*, vol. 235. Elsevier Ltd, pp. 219–232, Feb. 01, 2019. doi: 10.1016/j.apenergy.2018.10.129.

[112] S. C. Bhattacharyya, “Review of alternative methodologies for analysing off-grid electricity supply,” *Renewable and Sustainable Energy Reviews*, vol. 16, no. 1, pp. 677–694, Jan. 2012, doi: 10.1016/J.RSER.2011.08.033.

[113] M. Welsch *et al.*, “Smart and Just Grids for sub-Saharan Africa: Exploring options,” *Renewable and Sustainable Energy Reviews*, vol. 20, pp. 336–352, Apr. 2013, doi: 10.1016/J.RSER.2012.11.004.

[114] S. Mandelli, J. Barbieri, R. Mereu, and E. Colombo, “Off-grid systems for rural electrification in developing countries: Definitions, classification and a comprehensive literature review,” *Renewable and Sustainable Energy Reviews*, vol. 58, pp. 1621–1646, May 2016, doi: 10.1016/J.RSER.2015.12.338.

[115] P. Pandiyan *et al.*, “A comprehensive review of the prospects for rural electrification using stand-alone and hybrid energy technologies,” *Sustainable Energy Technologies and Assessments*, vol. 52, p. 102155, Aug. 2022, doi: 10.1016/J.SETA.2022.102155.

[116] “India - Flash floods (NDMIndia, India Meteorological Department) (ECHO Daily Flash of 16 October 2023),” *reliefweb.int.*

https://reliefweb.int/report/india/india-flash-floods-ndmindia-india-meteorological-department-echo-daily-flash-16-october-2023 (accessed October 25, 2023).

[117] "2023 Herat earthquakes," *en.wikipedia.org. https://en.wikipedia.org/wiki/2023_Herat_earthquakes (accessed October 25, 2023)*.

[118] N. Ramchandran, R. Pai, and A. K. S. Parihar, "Feasibility assessment of Anchor-Business-Community model for off-grid rural electrification in India," *Renew Energy*, vol. 97, pp. 197–209, Nov. 2016, doi: 10.1016/J.RENENE.2016.05.036.

[119] M. K. Shahzad, A. Zahid, T. Rashid, M. A. Rehan, M. Ali, and M. Ahmad, "Techno-economic feasibility analysis of a solar-biomass off grid system for the electrification of remote rural areas in Pakistan using HOMER software," *Renew Energy*, vol. 106, pp. 264–273, Jun. 2017, doi: 10.1016/J.RENENE.2017.01.033.

[120] D. Mentis *et al.*, "A GIS-based approach for electrification planning—A case study on Nigeria," *Energy for Sustainable Development*, vol. 29, pp. 142–150, Dec. 2015, doi: 10.1016/J.ESD.2015.09.007.

[121] B. Pillot, M. Muselli, P. Poggi, P. Haurant, and I. Hared, "Solar energy potential atlas for planning energy system off-grid electrification in the Republic of Djibouti," *Energy Convers Manag*, vol. 69, pp. 131–147, May 2013, doi: 10.1016/J.ENCONMAN.2013.01.035.

[122] A. Almasad, G. Pavlak, T. Alquthami, and S. Kumara, "Site suitability analysis for implementing solar PV power plants using GIS and fuzzy MCDM based approach," *Solar Energy*, vol. 249, pp. 642–650, Jan. 2023, doi: 10.1016/J.SOLENER.2022.11.046.

[123] H. Hafeznia, H. Yousefi, and F. Razi Astaraei, "A novel framework for the potential assessment of utility-scale photovoltaic solar energy, application to eastern Iran," *Energy Convers Manag*, vol. 151, pp. 240–258, Nov. 2017, doi: 10.1016/J.ENCONMAN.2017.08.076.

[124] N. Y. Aydin, E. Kentel, and H. Sebnem Duzgun, “GIS-based site selection methodology for hybrid renewable energy systems: A case study from western Turkey,” *Energy Convers Manag*, vol. 70, pp. 90–106, Jun. 2013, doi: 10.1016/J.ENCONMAN.2013.02.004.

[125] M. L. Sabo, N. Mariun, H. Hizam, M. A. Mohd Radzi, and A. Zakaria, “Spatial energy predictions from large-scale photovoltaic power plants located in optimal sites and connected to a smart grid in Peninsular Malaysia,” *Renewable and Sustainable Energy Reviews*, vol. 66, pp. 79–94, Dec. 2016, doi: 10.1016/J.RSER.2016.07.045.

[126] K. Aghaloo, T. Ali, Y. R. Chiu, and A. Sharifi, “Optimal site selection for the solar-wind hybrid renewable energy systems in Bangladesh using an integrated GIS-based BWM-fuzzy logic method,” *Energy Convers Manag*, vol. 283, p. 116899, May 2023, doi: 10.1016/J.ENCONMAN.2023.116899.

[127] D. Groppi, L. de Santoli, F. Cumo, and D. Astiaso Garcia, “A GIS-based model to assess buildings energy consumption and usable solar energy potential in urban areas,” *Sustain Cities Soc*, vol. 40, pp. 546–558, Jul. 2018, doi: 10.1016/J.SCS.2018.05.005.

[128] Y. An, T. Chen, L. Shi, C. K. Heng, and J. Fan, “Solar energy potential using GIS-based urban residential environmental data: A case study of Shenzhen, China,” *Sustain Cities Soc*, vol. 93, p. 104547, Jun. 2023, doi: 10.1016/J.SCS.2023.104547.

[129] I. Cuesta-Fernández, C. Vargas-Salgado, D. Alfonso-Solar, and T. Gómez-Navarro, “The contribution of metropolitan areas to decarbonize the residential stock in Mediterranean cities: A GIS-based assessment of rooftop PV potential in Valencia, Spain,” *Sustain Cities Soc*, vol. 97, p. 104727, Oct. 2023, doi: 10.1016/J.SCS.2023.104727.

[130] K. Singh, “Business innovation and diffusion of off-grid solar technologies in India,” *Energy for Sustainable Development*, vol. 30, pp. 1–13, Feb. 2016, doi: 10.1016/J.ESD.2015.10.011.

[131] M. R. Quitoras, P. Cabrera, P. E. Campana, P. Rowley, and C. Crawford, “Towards robust investment decisions and policies in integrated energy

systems planning: Evaluating trade-offs and risk hedging strategies for remote communities," *Energy Convers Manag*, vol. 229, p. 113748, Feb. 2021, doi: 10.1016/J.ENCONMAN.2020.113748.

[132] S. C. Bhattacharyya, "To regulate or not to regulate off-grid electricity access in developing countries," *Energy Policy*, vol. 63, pp. 494–503, Dec. 2013, doi: 10.1016/J.ENPOL.2013.08.028.

[133] H. Hafeznia, A. Aslani, S. Anwar, and M. Yousefjamali, "Analysis of the effectiveness of national renewable energy policies: A case of photovoltaic policies," *Renewable and Sustainable Energy Reviews*, vol. 79, pp. 669–680, Nov. 2017, doi: 10.1016/J.RSER.2017.05.033.

[134] M. T. Castro, J. D. A. Pascasio, L. L. Delina, P. H. M. Balite, and J. D. Ocon, "Techno-economic and financial analyses of hybrid renewable energy system microgrids in 634 Philippine off-grid islands: Policy implications on public subsidies and private investments," *Energy*, vol. 257, p. 124599, Oct. 2022, doi: 10.1016/J.ENERGY.2022.124599.

[135] X. Shi, X. Liu, and L. Yao, "Assessment of instruments in facilitating investment in off-grid renewable energy projects," *Energy Policy*, vol. 95, pp. 437–446, Aug. 2016, doi: 10.1016/J.ENPOL.2016.02.001.

[136] T. Urmee and A. Md, "Social, cultural and political dimensions of off-grid renewable energy programs in developing countries," *Renew Energy*, vol. 93, pp. 159–167, Aug. 2016, doi: 10.1016/J.RENENE.2016.02.040.

[137] M. C. G. Hart and M. H. Breitner, "Fostering Energy Resilience in the Rural Thai Power System—A Case Study in Nakhon Phanom," *Energies (Basel)*, vol. 15, no. 19, Oct. 2022, doi: 10.3390/en15197374.

[138] H. Lan, B. Cheng, Z. Gou, and R. Yu, "An evaluation of feed-in tariffs for promoting household solar energy adoption in Southeast Queensland, Australia," *Sustain Cities Soc*, vol. 53, p. 101942, Feb. 2020, doi: 10.1016/J.SCS.2019.101942.

[139] J. Li, P. Liu, and Z. Li, "Optimal design and techno-economic analysis of a solar-wind-biomass off-grid hybrid power system for remote rural electrification:

A case study of west China," *Energy*, vol. 208, p. 118387, Oct. 2020, doi: 10.1016/J.ENERGY.2020.118387.

[140] P. Kumar, N. Pal, and H. Sharma, "Optimization and techno-economic analysis of a solar photo-voltaic/biomass/diesel/battery hybrid off-grid power generation system for rural remote electrification in eastern India," *Energy*, vol. 247, p. 123560, May 2022, doi: 10.1016/J.ENERGY.2022.123560.

[141] A. Maleki, F. Pourfayaz, H. Hafeznia, and M. A. Rosen, "A novel framework for optimal photovoltaic size and location in remote areas using a hybrid method: A case study of eastern Iran," *Energy Convers Manag*, vol. 153, pp. 129–143, Dec. 2017, doi: 10.1016/J.ENCONMAN.2017.09.061.

[142] L. K. Gan, J. K. H. Shek, and M. A. Mueller, "Optimised operation of an off-grid hybrid wind-diesel-battery system using genetic algorithm," *Energy Convers Manag*, vol. 126, pp. 446–462, Oct. 2016, doi: 10.1016/J.ENCONMAN.2016.07.062.

[143] M. Chennaif, M. Maaouane, H. Zahboune, M. Elhafyani, and S. Zouggar, "Tri-objective techno-economic sizing optimization of Off-grid and On-grid renewable energy systems using Electric system Cascade Extended analysis and system Advisor Model," *Appl Energy*, vol. 305, p. 117844, Jan. 2022, doi: 10.1016/J.APENERGY.2021.117844.

[144] M. Guezgouz, J. Jurasz, B. Bekkouche, T. Ma, M. S. Javed, and A. Kies, "Optimal hybrid pumped hydro-battery storage scheme for off-grid renewable energy systems," *Energy Convers Manag*, vol. 199, p. 112046, Nov. 2019, doi: 10.1016/J.ENCONMAN.2019.112046.

[145] C. Mokhtara, B. Negrou, A. Bouferrouk, Y. Yao, N. Settou, and M. Ramadan, "Integrated supply–demand energy management for optimal design of off-grid hybrid renewable energy systems for residential electrification in arid climates," *Energy Convers Manag*, vol. 221, p. 113192, Oct. 2020, doi: 10.1016/J.ENCONMAN.2020.113192.

[146] M. B. Eteiba, S. Barakat, M. M. Samy, and W. I. Wahba, "Optimization of an off-grid PV/Biomass hybrid system with different battery technologies," *Sustain Cities Soc*, vol. 40, pp. 713–727, Jul. 2018, doi: 10.1016/j.scs.2018.01.012.

[147] M. M. Kamal, I. Ashraf, and E. Fernandez, “Optimal sizing of standalone rural microgrid for sustainable electrification with renewable energy resources,” *Sustain Cities Soc*, vol. 88, Jan. 2023, doi: 10.1016/j.scs.2022.104298.

[148] G. K. Suman, J. M. Guerrero, and O. P. Roy, “Optimisation of solar/wind/bio-generator/diesel/battery based microgrids for rural areas: A PSO-GWO approach,” *Sustain Cities Soc*, vol. 67, Apr. 2021, doi: 10.1016/j.scs.2021.102723.

[149] A. Kumar, P. Mohanty, D. Palit, and A. Chaurey, “Approach for standardization of off-grid electrification projects,” *Renewable and Sustainable Energy Reviews*, vol. 13, no. 8, pp. 1946–1956, Oct. 2009, doi: 10.1016/J.RSER.2009.03.008.

[150] Y. Charabi and A. Gastli, “Integration of temperature and dust effects in siting large PV power plant in hot arid area,” *Renew Energy*, vol. 57, pp. 635–644, Sep. 2013, doi: 10.1016/J.RENENE.2013.02.031.

[151] M. Mani and R. Pillai, “Impact of dust on solar photovoltaic (PV) performance: Research status, challenges and recommendations,” *Renewable and Sustainable Energy Reviews*, vol. 14, no. 9, pp. 3124–3131, Dec. 2010, doi: 10.1016/J.RSER.2010.07.065.

[152] A. A. Sabziparvar and H. Shetaee, “Estimation of global solar radiation in arid and semi-arid climates of East and West Iran,” *Energy*, vol. 32, no. 5, pp. 649–655, May 2007, doi: 10.1016/J.ENERGY.2006.05.005.

[153] C. P. Jacovides, F. S. Tymvios, V. D. Assimakopoulos, and N. A. Kaltsounides, “Comparative study of various correlations in estimating hourly diffuse fraction of global solar radiation,” *Renew Energy*, vol. 31, no. 15, pp. 2492–2504, Dec. 2006, doi: 10.1016/J.RENENE.2005.11.009.

[154] M. Ahmad, M. Zeeshan, and J. A. Khan, “Life cycle multi-objective (geospatial, techno-economic, and environmental) feasibility and potential assessment of utility scale photovoltaic power plants,” *Energy Convers Manag*, vol. 291, Sep. 2023, doi: 10.1016/j.enconman.2023.117260.

[155] H. Hafeznia and B. Stojadinović, “ResQ-IOS: An iterative optimization-based simulation framework for quantifying the resilience of interdependent critical infrastructure systems to natural hazards,” *Appl Energy*, vol. 349, p. 121558, Nov. 2023, doi: 10.1016/j.apenergy.2023.121558.

[156] R. T. Walker and M. M. Khatib, “Active faulting in the Birjand region of NE Iran,” *Tectonics*, vol. 25, no. 4, Aug. 2006, doi: 10.1029/2005TC001871.

[157] S. S. Beyraghi, V. Riahi, and S. Mostafavi Saheb, “Analysis of physical resilience of rural settlements against floods (Case study: Bagheran Dehestan in Birjand County),” *Village and Space Sustainable Development*, vol. 3, no. 3, pp. 35–57, 2022, doi: 10.22077/vssd.2022.5095.1078.

[158] R. Saberifar and H. Shokri, “Zoning the Risk of Flood in Birjand,” *Town and Country Planning*, vol. 11, no. 1, pp. 159–178, 2019, doi: 10.22059/jtcp.2019.277972.669978.

[159] H. Khorasanizadeh and K. Mohammadi, “Prediction of daily global solar radiation by day of the year in four cities located in the sunny regions of Iran,” *Energy Convers Manag*, vol. 76, pp. 385–392, Dec. 2013, doi: 10.1016/J.ENCONMAN.2013.07.073.

[160] IRIMO, “(Islamic republic of Iran meteorological organization),” *URL: https://www.irimo.ir/ (last accessed: February 2017)*.

[161] Solargis (URL: https://solargis.com/), “Global Horizontal Irradiation (GHI) solar map of Iran,” 2017.

[162] United States Geological Survey (USGS), “ASTER GDEM and Sentinel-2A satellite images,” *URL: https://earthexplorer.usgs.gov/ (last accessed: December 2016)*.

[163] INCC (Iran National Cartographic Center), “The digitized maps of Birjand,” 2016.